

Strongly Coupled Lattice Gauge Theories and Antiferromagnetic Spin Systems

Tesi presentata da
Federico Berruto
per il titolo di
Dottore di Ricerca



Dottorato di Ricerca, X Ciclo - Dicembre 1998

Strongly Coupled Lattice Gauge Theories and Antiferromagnetic Spin Systems

Federico Berruto
Dipartimento di Fisica, Università di Perugia

Abstract

In this thesis, I use the strong coupling expansion to investigate the multiflavor lattice Schwinger models in the hamiltonian formalism using staggered fermions. In particular, I am interested in analysing the mapping of these gauge theories onto quantum spin-1/2 antiferromagnetic Heisenberg chains. Exploiting this mapping, the chiral symmetry breaking patterns are studied and the spectra are computed. The extrapolation to zero lattice spacing of the results compare favorably qualitatively and quantitatively with the weak coupling studies of the gauge models in the continuum.

I studied the one-flavor lattice Schwinger model, in the strong coupling limit, showing that it is equivalent to an Ising model with long-range Coulomb interaction. Even though the continuous chiral symmetry is explicitly broken by the staggered fermions, a discrete chiral symmetry remains and appears in the lattice theory as a translation by one lattice site which forbids fermion mass and must be broken in order for the lattice model to exhibit the features of the spectrum of the continuum theory. The effects of the anomaly in the continuum appear on the lattice through spontaneous symmetry breaking: indeed I show that the ground state spontaneously breaks translations by one lattice site. The discrete symmetries are carefully defined on the lattice. The masses of the low lying bosonic excitations as well as the chiral condensate of the model are computed up to the fourth order in the strong coupling expansion. Very good agreement between lattice calculations and continuum values is found.

The two-flavor lattice Schwinger model is analysed using the same computational scheme adopted in the one-flavor case. The problem of finding the low lying excitations is showed to be equivalent to solving the spin-1/2 antiferromagnetic Heisenberg chain. In fact the Heisenberg Hamiltonian is the effective Hamiltonian of the gauge model at the second order in the strong coupling expansion. The ground state of the spin model represents the vacuum of the gauge theory in the strong coupling limit. Two kinds of excitations can be created from the ground state; one kind involves only spin flipping and has lower energy since no electric flux is created, the other involves fermion transport besides spin flipping and thus has higher energy. The massless excitations of the gauge model are the spinons of the antiferromagnetic chain. The excitation masses can be expressed in terms of spin-spin correlators evaluated on the ground state. Either the massless or the massive excitations have identical P - and G -parity to the low lying excitations of the continuum two flavor gauge model. Good agreement between lattice and continuum results is found. The ground state is translationally invariant: both the isoscalar or the isovector chiral condensates are zero to every order in the strong coupling expansion as it happens in the continuum theory as a consequence of the Coleman theorem. In addition the vacuum expectation value of the umklapp operator is non zero as it happens for the corresponding operator in the continuum and this is the only relic of the chiral anomaly on the lattice.

The \mathcal{N} -flavor lattice Schwinger models are analysed generalizing the $\mathcal{N} = 2$ case and at the second order in the strong coupling expansion are effectively described by spin-1/2 $SU(\mathcal{N})$ antiferromagnetic Heisenberg chains. The generalization is quite straightforward, even if the theory is much different depending on if \mathcal{N} is even or odd.

Tesi presentata per il titolo di Dottore di Ricerca

Preface

This thesis analyses the strong coupling limit of the multiflavor lattice Schwinger models and their relationship with generalized quantum spin-1/2 $SU(\mathcal{N})$ antiferromagnetic Heisenberg chains. My original contributions are summarized in chapters 4, 5 and 6. In chapter 4 the issues of chiral symmetry breaking and the mass spectrum are studied for the one-flavor lattice Schwinger model. Part of this work appears in the publication

- F. Berruto, G. Grignani, G. W. Semenoff and P. Sodano, Phys. Rev. **D57**, 5070 (1998).

In chapter 5 the two-flavor lattice Schwinger model and its mapping onto the quantum spin-1/2 antiferromagnetic Heisenberg chain are analysed in detail. At variance with the one-flavor theory, the chiral symmetry breaking is now explicit and the spectrum of the gauge model is derived starting from the ground state of the Heisenberg model. Many of the results concerning the analysis of this model can be found in

- F. Berruto, G. Grignani, G. W. Semenoff and P. Sodano, Phys. Rev. **D59**, 034504 (1999).
- F. Berruto, G. Grignani, G. W. Semenoff and P. Sodano, hep-th/9901142.

Chapter 6 is devoted to a generalization to the \mathcal{N} -flavor lattice Schwinger models and their mapping onto quantum spin-1/2 $SU(\mathcal{N})$ antiferromagnetic Heisenberg chains.

Acknowledgements

I am very grateful to Prof. P. Sodano for stimulating my research interests with enlightening discussions, for the huge amount of time he dedicated to our research project and for providing me with the chance to attend several meetings dealing with the topics addressed in my thesis. I thank Dr. G. Grignani for his constant guidance when problems arose, for the many suggestions and for the many pleasant working hours spent together. I thank also Prof. G. W. Semenoff for many discussions and for the kind hospitality extended to me at the University of British Columbia. Prof. R. B. Laughlin is acknowledged for a very interesting discussion concerning low dimensional quantum antiferromagnets and quantum disorder in spin chains.

Contents

1	Introduction	1
2	Lattice gauge theories	6
2.1	Bosons and fermions on the lattice	7
2.1.1	Bose fields on the lattice: scalar fields	8
2.1.2	Fermi fields on the lattice	10
2.1.3	Gauge fields on the lattice	13
2.2	Staggered fermions	18
2.3	Strong coupling lattice gauge theory	21
2.3.1	Hamiltonian formulation of lattice gauge theory	22
2.3.2	Strong coupling	23
2.4	Chiral anomaly on the lattice	27
2.4.1	The Nielsen-Ninomiya no-go theorem	28
3	Antiferromagnetic spin chains	35
3.1	Failure of spin wave theory in $D=1$	36
3.1.1	Spin-spin correlators in spin wave theory	39
3.2	The Haldane-Shastry spin model	40
3.3	The Bethe Ansatz solution of the antiferromagnetic Heisenberg chain	44
3.3.1	Finite size antiferromagnetic Heisenberg chains	51
3.3.2	Spin-spin correlators	57

3.4	$SU(\mathcal{N})$ quantum antiferromagnetic chains	60
4	The one-flavor lattice Schwinger model	63
4.1	Definition of the model	64
4.2	The low-lying excitation spectrum	67
4.2.1	Unperturbed energies of the dimer states	73
4.2.2	Perturbative matrix elements	74
4.3	The chiral condensate	76
4.4	Lattice versus continuum	77
4.5	Summary	80
5	The two-flavor lattice Schwinger model	82
5.1	Definition of the model	83
5.2	The strong coupling limit and the antiferromagnetic Heisenberg Hamiltonian	86
5.2.1	The low lying spectrum of QCD_2	89
5.3	The meson masses	89
5.4	Chiral condensate	92
5.5	Lattice versus continuum	94
5.6	Summary	96
6	The multiflavor lattice Schwinger models	98
6.1	The continuum \mathcal{N} -flavor Schwinger models	99
6.2	The lattice \mathcal{N} -flavor Schwinger models	101
	Summary and conclusions	105
	Padé approximants	107
	Bibliography	109

Chapter 1

Introduction

Quantum field theory and condensed matter physics had an amazing development in this century and each one borrowed from the other new ideas. For instance the concept of spontaneous symmetry breaking was originally introduced to study ferromagnetism and the Higgs phenomenon appears studying the Meissner effect in the theory of superconductivity [1]. Mathematical analogies between the two disciplines were pointed out by Wilson [2] who joined the concepts of renormalization, typical of particle physics, with the concepts of universality and scaling, originally introduced to describe second order phase transitions. Later Wilson [3] introduced a lattice formulation of gauge theories. Once an euclidean field theory is defined on the lattice it becomes a statistical mechanics problem. In general a quantum theory in d dimensions is equivalent to a classical statistical mechanical system in $d + 1$ dimensions. The phase diagram of a statistical system determines its physical properties. Landau introduced the general description of all phase transitions as changes of symmetry [4]. Fluctuations grow in a substance as its critical point is approached and they interact very strongly with each other so that the system is strongly correlated. The order of a phase transition is crucial: only if the phase transition is continuous, it is possible to obtain from a lattice field theory a relativistic continuous theory. The lattice approach to gauge theories provides a powerful tool to study non-perturbative properties.

One of the most important properties of non-Abelian gauge theories, such as Quantum Chromodynamics (*QCD*), is asymptotic freedom [5]. At short distances or high momenta quarks are weakly interacting and it is possible to perform a perturbative expansion. At large distances or small momenta the coupling constant increases indefinitely confining quarks. Confinement is an observed property of the strong interactions and it is an unproven, but widely believed feature of most non-Abelian gauge theories in four and lower space-time dimensions. The theoretical mechanism behind confinement is difficult to analyze since it escapes the weak coupling analysis: it is intrinsically a strong coupling and non-perturbative phenomenon.

Wilson [3] proposed on the lattice a mechanism for quark confinement. Gauge theories have been analysed in the strong coupling limit on a (3+1)-dimensional space-time lattice. In the weak coupling limit the gauge field behaves like a normal free massless field and quarks are unbound. In the strong coupling limit the gauge field is massive and the quarks are bound. There should be a confinement-deconfinement phase transition at some intermediate value of the coupling constant.

In the continuum, closely related to confinement there is dynamical chiral symmetry breaking, which creates the π mesons and keep their masses light. Chiral symmetry [6] is only an approximate symmetry of particle physics since the up and down quarks are

light but not massless. Otherwise the pion, which is the Goldstone boson arising from the symmetry breaking would be strictly massless rather than being just light. The theory behind chiral symmetry breaking is only partially understood because this phenomenon occurs at strong coupling where the standard tools of perturbation theory are not reliable. There are conjectures [7] that if one could adjust the charge of the electron e in ordinary QED , there would be a critical value of e at which a phase transition would take place and the electron would become very massive. A transition to heavy electrons would break the approximate chiral symmetry of QED which is there because electrons are very light.

The strong coupling limit [8] of lattice gauge theories though far from the scaling regime is often used to study the qualitative properties of a gauge model. Two important features of the spectrum of non-abelian gauge theories appear there. The strong coupling limit exhibits confinement [3], which is related in a rather natural way to the gauge symmetry and compactness of the non-abelian gauge group. Moreover, it is straightforward to show that strongly coupled gauge theories exhibit dynamical chiral symmetry breaking. Wilson fermions [9] explicitly break chiral symmetry but for what concerns staggered fermions [10], even if the continuous chiral symmetry is broken explicitly, a discrete axial symmetry survives the lattice regularization and appears in the lattice theory as a translation by one spacing. Several quantitative investigations of gauge theories using strong coupling techniques have been performed and there have been attempts to compute the mass spectrum of realistic models such as QCD [11]. The strong coupling expansion is an expansion in the inverse of the gauge coupling constant. Due to asymptotic freedom, the continuum limit is found where the coupling constant is small, so that one should not expect a priori that the strong coupling expansion gives accurate quantitative information about the continuum gauge theory. However, the expansion does have a finite radius of convergence [12]; this indicates that its properties are shared by the model for a finite range of the coupling parameter and certain informations can be obtained by analytic continuation to regions outside the convergence radius.

It has been recognised for some time that the strong coupling limit of lattice gauge theories with dynamical fermions is related to certain quantum spin systems. The relationship between gauge and spin systems is particularly evident in the hamiltonian formalism [13] and already appeared in some of the earliest analysis of chiral symmetry breaking in the strong coupling limit [14]. In particular mesons emerge as spin waves when spontaneous chiral symmetry breaking takes place. It was noticed that there are several formal similarities between some condensed matter systems with lattice fermions – and in particular certain antiferromagnetic spin systems – and lattice gauge theories in their strong coupling limit [15]. The quantum spin-1/2 Heisenberg antiferromagnet was recognised to be equivalent to the strong coupling limit of a $U(1)$ lattice gauge theory [16] and can also be written as a kind of $SU(2)$ gauge theory [17]. Furthermore, staggered fermions resemble ordinary lattice fermions used in tight binding models in condensed matter physics at half-filling, *i.e.* when there is one electron per site, and placed in a background $U(1)$ magnetic field $\pi \pmod{2\pi} - 1/2$ of a flux quantum – through every plaquette of the lattice. In $(2 + 1)$ -dimensions the parallel between lattice fermions in condensed matter and gauge theories was already recognized in the first work [21] on the Azbel-Wannier-Hofstaeder problem and then has been discussed in the context of the so called flux phases of the Hubbard model. It is actually true for all $d \geq 2 + 1$ [22], *i.e.* the staggered lattice fermion approximation of the relativistic Dirac field with the minimal number of flavors is identical to a condensed matter fermion problem with simple nearest neighbor hopping in a background magnetic field which has $1/2$ flux quantum per plaquette. In the condensed matter context, the magnetic flux can be produced by a condensate, as in the flux phases of the Heisenberg and Hubbard models [15]. A $1/2$ flux quantum per plaquette for ordinary lattice spacing is yet an experimentally inaccessible flux density. Nonetheless it could be achieved in analog experiments where macroscopic arrays of Josephson junctions, for example, take the place of atoms at lattice sites and their ground state in two dimensions is expected to be a flux phase [23].

The analogy between Dirac and tight-binding condensed matter fermions was exploited to find an exact mapping of the strong coupling limit of a large class of lattice gauge theories with dynamical staggered fermions onto certain quantum antiferromagnets, both the conventional Heisenberg antiferromagnets with spin S and generalized antiferromagnets with spins taking values in Lie algebras other than $SU(2)$ [24]. The precise structure of the resulting antiferromagnet depends on the number of colours in the gauge group – since $S = \mathcal{N}_c/2$ – and also on the number of fermion flavors. There are four different cases. (a) An $U(\mathcal{N}_c)$ gauge theory with an even number \mathcal{N} of lattice flavors of staggered fermions is an $SU(\mathcal{N})$ antiferromagnet in the strong coupling limit. The number of colours \mathcal{N}_c determines the representation of the antiferromagnet as being the one represented by the Young tableau with \mathcal{N}_c columns and $\mathcal{N}/2$ rows. (b) An $SU(\mathcal{N}_c)$ gauge theory with $\mathcal{N}_c \geq 3$ is an $U(\mathcal{N})$ antiferromagnet. The representation of the $U(1)$ subgroup of $U(\mathcal{N})$ is not constrained as it was in the (a) case where the local $U(1)$ charge had to vanish. The representation of the $SU(\mathcal{N})$ subgroup of $U(\mathcal{N})$ can now take on any representation on a given site, subject only to the constraint that the average fermion density is $\mathcal{N}_c\mathcal{N}/2$ and the number of fermions on each site is given by the number of boxes in the corresponding Young tableau. (c) The $SU(2)$ lattice gauge theories are special. In the strong coupling limit additional terms compared to $SU(\mathcal{N}_c \geq 3)$ appear and one obtains for \mathcal{N} lattice flavors antiferromagnets associated with the symplectic group $Sp(2\mathcal{N})$ and for $\mathcal{N} = 1$ a spin-1/2 Heisenberg antiferromagnet. (d) A gauge theory with an odd number \mathcal{N} of lattice flavors of staggered fermions in the strong coupling limit is an $SU(\mathcal{N})$ antiferromagnet where the size of representations on neighboring sites differ. One has to divide the sites in two sublattices such that the nearest neighbors of all the sites of one sublattice are in the other sublattice; if this classification in two sublattices is possible, the lattice is called bipartite. On the bipartite lattice one has the representation of $SU(\mathcal{N})$ with Young tableau with $(\mathcal{N} + 1)/2$ rows and \mathcal{N}_c columns on one sublattice and with $(\mathcal{N} - 1)/2$ rows and \mathcal{N}_c columns on the other sublattice. There exist analogs in spin systems of strong interactions behavior, particularly for what concerns confinement and chiral symmetry. Laughlin [25] recently provided an appealing interpretation of confinement in quantum antiferromagnets. The physical idea is that the phase diagram of antiferromagnets consists of competing ordered phases regulated by a nearby quantum critical point. Exactly at the critical point the low lying elementary excitations of the magnet are gauge fields and particles with fractional quantum numbers analogous to the spinon and holon excitations found in spin chains. Away from the critical point, even if very close, the “fundamental constituents” bind at low energy scales to make the familiar collective modes of ordered states which one renormalizes. The existence of “fundamental constituents” in conventional materials and models may be indirectly inferred by high-energy spectroscopy and inconsistencies in sum rules exactly the way the existence of quarks is inferred in particle physics. There exist physically identifiable objects behaving like $U(1)$ quarks out of which the elementary excitations are built. In Laughlin’s scenario quark-like objects and gauge fields would be liberated at the critical point and would become the true elementary excitations.

In quantum antiferromagnets, the appearance of Néel order is the analog of chiral symmetry breaking. Exploiting the mapping existing between gauge and spin models, rigorous results about antiferromagnets can be used to prove spontaneous broken chiral symmetry in certain strong coupling gauge theories. Whenever the ground state of the antiferromagnet is not translationally invariant, the discrete chiral symmetry is spontaneously broken. The possibility of studying in detail the patterns of chiral symmetry breaking on the lattice is very important. In particular, an interesting question is how the axial anomaly [26] appears in the lattice regularization. Anomalies occur when all of the symmetries of a classical field theory cannot be realized simultaneously in the corresponding quantum field theory. The classical example is the Adler-Bell-Jackiw anomaly in a vector like gauge theory where gauge invariance and global axial symmetry are incompatible. This is a manifestation of the fact that it is impossible to find a regularization of ultraviolet divergences preserving both axial and gauge invariance. If gauge invariance is preserved, the observable manifestation of the anomaly is the failure of the conservation laws for axial vector currents and the

resulting absence of their consequences in the spectrum of the quantized theory. Nielsen and Ninomiya [27] proved that fermion theories on a lattice have an equal number of species of left- and right-handed Weyl particles in the continuum limit, thus preventing an axial anomaly. Lattice field theories are manifestly gauge invariant by construction and therefore, to produce continuum theories, they must find a way to violate axial current conservation.

In the continuum an interesting mechanism of confinement in Quantum Electrodynamics (*QED*) with massless fermions in $(1+1)$ -dimensions was discovered by Schwinger [28] which demonstrated that the “photon” acquires a mass and the spectrum of the model does not exhibit any free electron asymptotical state. The “photon” mass is proportional to the electromagnetic coupling constant if charges are totally screened by the vacuum polarization. After this investigation *QED* in $(1+1)$ -dimensions with massless fermions has been called the Schwinger model. Moreover Schwinger speculated that in four dimensions the photon mass would be zero for any electromagnetic charge e less than e_c ; for e greater than e_c the photon mass would be non-zero and vary with e . At the critical coupling constant e_c a change of phase from zero to non-zero photon mass should take place.

In this thesis it is my purpose to investigate the one-flavor and the multflavor lattice Schwinger models in the hamiltonian formalism using staggered fermions. Exploiting these toy models I will clarify the mechanisms of chiral symmetry breaking on the lattice and the vestiges of the chiral anomaly of the continuum theory. Moreover the spectra of these models will be computed in the strong coupling limit. Extrapolating the spectra to the zero lattice spacing limit by means of Padé approximants [29], I find that the lattice compare favorably – both qualitatively and quantitatively – with the weak coupling continuum studies of the multflavor Schwinger models. The success of the procedure is not completely surprising since the continuum theory of free massive mesons can be described in terms of quarks and antiquarks pairs bound by gauge strings and it is precisely this idea which is embodied in lattice methods. The \mathcal{N} -flavor lattice Schwinger models in the strong coupling limit are effectively described by generalized quantum $SU(\mathcal{N})$ spin-1/2 Heisenberg antiferromagnetic Hamiltonians. Spinons are the fundamental spin-1/2 excitations of quantum antiferromagnets. In the same way as the Schwinger models spectra do not exhibit free quarks (electrons) but just massive bosons, the “photons” or better mesons, also the Heisenberg models excitations contain an even number of spinons and so carry integer spin. One original result of my work has been to show explicitly how spinons appear in lattice gauge theories.

In chapter 2 I shall review the lattice approach to gauge theories. In particular boson, fermion and gauge fields are defined on the lattice. The “fermion doubling” problem is analysed and Wilson and staggered fermions are introduced. The hamiltonian formulation of gauge theories and the strong coupling limit are described. Furthermore the realization of the chiral anomaly on the lattice is discussed and the Nielsen and Ninomiya no-go theorem is demonstrated.

Chapter 3 is devoted to a detailed analysis of quantum antiferromagnetic spin chains with special emphasis to the topics useful to understand the connection between Schwinger and Heisenberg models. First I demonstrate that spin wave theory fails in one dimension due to strong infrared divergences. Then I introduce the Haldane-Shastry model where it is particularly easy to see the spinons and analyse the spectrum. The Bethe ansatz solution of the spin-1/2 antiferromagnetic Heisenberg Hamiltonian is then reviewed in detail. I study the complete spectrum of finite size Heisenberg antiferromagnetic chains of 4 and 6 sites and I verify that the thermodynamic limit solution provided in [30] is already very well reproduced in the finite size chains. Moreover, I write down explicitly the ground state of 4, 6 and 8 sites chains. Spin-spin correlators relevant for evaluating the mass spectrum of the two-flavor lattice Schwinger model are calculated. In the last section, generalized Heisenberg antiferromagnets with symmetry group $SU(\mathcal{N})$ are introduced.

In chapter 4 the one-flavor lattice Schwinger model is studied. The discrete chiral sym-

metry on the lattice is broken explicitly and this mechanism reproduces the effects that in the continuum are generated by the axial anomaly. The discrete symmetries of the model are analysed in detail and the vacuum of the model is found to be the ground state of the antiferromagnetic Ising spin chain with long range Coulomb interaction. The spectrum of the continuum theory is very well reproduced when the lattice results are extrapolated using the Padé approximants.

In chapter 5 I analyse the two-flavor lattice Schwinger model. In the strong coupling limit the gauge model is effectively described by the quantum spin-1/2 antiferromagnetic Heisenberg model. The vacuum of the gauge theory in the strong coupling limit is the ground state of the spin model: a quantum disordered state very different from the classical Néel state. It is not possible to write down explicitly this ground state in the thermodynamic limit, but its energy can be computed using the Bethe ansatz as explained in chapter 3. The massless excitations of the gauge model are the spinons of the Heisenberg antiferromagnet, while the massive excitations are created by acting on the ground state with pertinent operators that have the right quantum numbers of the continuum theory and generate charge transport. The excitation masses of the gauge model are completely expressed in terms of vacuum expectation values (VEV's) of spin-spin correlation functions. The chiral symmetry breaking pattern is explicit in this case, due to the staggered fermions coupled by the gauge field. The isoscalar and isovector chiral condensates, that in the continuum are zero due to the Coleman theorem, are zero also on the lattice. The vacuum expectation value of the umklapp operator is non-zero due to the explicit breaking of $U_A(1)$; this can be viewed as a manifestation of the anomaly on the lattice.

In chapter 6 the analysis of chapter 5 is generalized to the Schwinger models with $SU(\mathcal{N})$ flavor group. In the strong coupling limit the gauge models are equivalent to generalized $SU(\mathcal{N})$ quantum Heisenberg antiferromagnets. Even if most of the analysis is a straightforward generalization of the $\mathcal{N} = 2$ case, some surprising difference arises between the \mathcal{N} even and odd models. Some concluding remarks and a short summary of results is provided.

The appendix aims at elucidating some features of Padé approximants relevant for a better understanding of chapters 4 and 5.

Chapter 2

Lattice gauge theories

It is my purpose to review in this chapter the lattice approach to gauge theories. I do not pretend to be exhaustive, but I want to illustrate the topics used in my approach to the lattice Schwinger model. The reader interested in knowing more about lattice gauge theories could usefully look up Refs.[8, 31].

Quantum field theory is so far the most appropriate scheme for describing the strong, electromagnetic and weak interactions between elementary particles. It has been known for long time that electromagnetic interactions are described by a quantum gauge field theory, but the fundamental role played by the principle of gauge invariance in the construction of a theory for the strong and weak interactions has been recognized only much later.

QCD, the theory of strong interactions, is a gauge theory based on the unbroken non-abelian $SU(3)$ group. The group $SU(3)$ has eight generators and so there are eight “massless” gluons carrying a colour charge which mediate the strong interactions between the fundamental constituents of matter, the quarks. *QCD* is an asymptotically free theory [5]. Asymptotic freedom allowed to carry out quantitative perturbative calculations of observables which are sensitive to the short distance structure of *QCD*. Quarks have never been seen free in nature and only colour neutral baryons are observed: quarks are confined. A demonstration that *QCD* accounts for quark confinement can only come from a non-perturbative treatment of the theory; confinement is indeed a consequence of the dynamics at large distances where perturbation theory breaks down.

Wilson [3] showed ¹ that in the strong coupling limit *QCD* confines quarks, however this is not a justified approximation when studying the continuum limit. There are numerical simulations which strongly suggest that *QCD* accounts for quark confinement [31]. Moreover, there are other fascinating questions that one would like to answer: does *QCD* account for the observed spectrum? Are there other particles allowed by *QCD* but not yet experimentally observed? Does *QCD* account for chiral symmetry spontaneous breaking? In order to answer the above questions it is necessary a non perturbative treatment of *QCD* which at the moment is only provided by the lattice formulation.

The lattice formulation of *QCD* by Wilson opened the way to the study of non-perturbative phenomena using numerical methods. His purpose was to study the long distance properties of *QCD* in a format where the short distance properties which lead to ultraviolet divergences are regulated by the lattice cutoff. The space-time discretization provides a natural cut-off

¹Independently, gauge theories were discussed on a lattice by Wegner [32], who elevated the global up \leftrightarrow down symmetry of the ordinary Ising to a local symmetry and in an unpublished work, which deals mostly with Abelian gauge theories, by Polyakov in 1974.

scheme as wave-lengths shorter than twice the lattice spacing, a , have no meaning and the momentum domain is restricted to a region bounded by π/a . The lattice provides then a non-perturbative regularization of ultraviolet divergences. Once a lattice field theory has been formulated, the original field theory problem becomes one of statistical mechanics. With a finite lattice there are a finite number of variables. It is then possible to study various physical interesting quantities: energy spectrum, correlation functions, critical exponents etc., for example by computer simulations based on the Monte Carlo method [31]. By now lattice gauge theories have become a branch of particle physics in its own right, and their intimate connection to statistical mechanics raised the interest of elementary particle physicists as well as of condensed matter physicists.

Since the beginning of lattice gauge theory, chiral symmetries have been perplexing. The issues revolve around anomalies and fermion doubling. For vector-like theories such as QCD the problems are largely resolved. The Wilson approach [9] breaks chiral symmetry explicitly by adding a symmetry breaking term to give all the doublers a mass which becomes infinite with the cut-off scale. The Kogut and Susskind fermions [10], also called staggered fermions, eliminate the doubling by reducing the Brillouin zone, *i.e.*, by doubling the effective lattice spacing. The situation is much more clouded for the full Standard Model. Here chiral symmetry plays a fundamental role, with neutrinos maximally violating parity. Nielsen and Ninomiya demonstrated a no-go theorem [27] whose most important consequence is that the weak interaction cannot be put on the lattice. For a general class of fermion theories on a lattice in the hamiltonian formalism an equal number of species of left- and right-handed Weyl particles, *i.e.* neutrinos, necessary appears in the continuum limit. They also proved that this disease is not peculiar to the lattice theory, but some trouble appears universally in all regularization schemes, for instance dimensional regularization. In any lattice theory of chirally invariant fermions with locality there is an equal number of production and annihilation of Weyl fermions. Thus there is no net production, so that the axial charges are conserved. An analogy or a simulation exists between the Weyl fermion theory and gapless semiconductors, where two energy bands have point-like degeneracies. In section (2.4) I shall discuss thoroughly this no-go theorem. At the moment no reliable lattice computation for the Standard Model does exist.

In section (2.1) I discuss the differences arising between boson and fermion fields on the lattice and I analyse the fermion doubling, an obstacle to put fermions on a lattice. Gauge fields on the lattice are discussed.

Section (2.2) is devoted to introduce staggered fermions, a particular type of lattice fermions which partially avoid the fermion doubling problem. Moreover, hamiltonian formulation of lattice gauge theories is introduced.

Section (2.3) explains the strong coupling approach to lattice gauge theories in the hamiltonian formalism.

In section (2.4) the Nielsen and Ninomiya no-go theorem is reviewed and the chiral symmetry and chiral anomaly on the lattice are analysed and the implications and analogs of these topics in condensed matter theory are discussed.

2.1 Bosons and fermions on the lattice

Any field (scalar, fermionic or gauge) can be defined on a lattice, but the result of putting a bosonic or a fermionic field on a lattice is distinctly different. While the procedure for a bosonic field is straightforward, placing the Dirac equation on a space-time lattice presents some surprisingly difficult problem.

In this section I shall first illustrate the way to put the scalar field on the lattice. Then I shall discuss the so called doubling problem [8] of lattice fermions. A prescription to cure it is discussed, the Wilson fermions [9], while section (2.2) is devoted to discuss the Kogut and Susskind fermions or staggered fermions [10], which have been used in my approach to the lattice Schwinger model. The link variable nature of gauge fields on the lattice is explained.

2.1.1 Bose fields on the lattice: scalar fields

Let us study how a scalar field $\phi(x)$ can be defined on a lattice. Consider the continuum field theory in Euclidean space

$$S(\phi) = \int d^d x \left[\frac{1}{2} (\partial_\mu \phi)^2 + V(\phi) \right] . \quad (2.1)$$

where

$$V(\phi) = \frac{1}{2} m^2 \phi^2 + \frac{\lambda}{4} \phi^4 . \quad (2.2)$$

A matter field is attributed to the lattice sites and it is natural to approximate a continuous field by its values at the lattice sites

$$\phi(x) \longrightarrow \phi_x \quad (2.3)$$

Clearly, in order for the lattice field ϕ_x to be a good approximation of a continuous field configuration $\phi(x)$, the lattice spacing should be much smaller than the characteristic size of this configuration. The derivative can be replaced by

$$\partial_\mu \phi \longrightarrow \frac{1}{a} (\phi_{x+\hat{\mu}} - \phi_x) \quad (2.4)$$

where $\hat{\mu}$ is a d -vector of length a in the direction of μ . The d dimensional integration is replaced by a sum

$$\int d^d x \longrightarrow a^d \sum_x \quad (2.5)$$

so that the scalar action on the lattice becomes

$$S(\phi) = \sum_x \left[\frac{a^{d-2}}{2} \sum_{\mu=1}^d (\phi_{x+\hat{\mu}} - \phi_x)^2 + a^d \left(\frac{m^2}{2} \phi_x^2 + \frac{\lambda}{4} \phi_x^4 \right) \right] . \quad (2.6)$$

It is instructive to go to momentum space to see the spectrum of the free field theory. For this I take the Fourier transform

$$\phi_x = \int \frac{d^d k}{(2\pi)^d} e^{ik \cdot x} \phi(k) . \quad (2.7)$$

Since it is meaningless to consider wavelengths less than twice the lattice spacing, the above integral is taken over only one ‘‘Brillouin zone’’ of the reciprocal lattice

$$-\frac{\pi}{a} \leq k_\mu \leq \frac{\pi}{a} \quad \text{for each } \mu \quad (2.8)$$

where $k_\mu = k \cdot \hat{\mu}$. Substituting Eq.(2.7) into Eq.(2.6) the free field action can be written as

$$S_0(\phi) = \frac{1}{2} \int \frac{d^d k}{(2\pi)^d} \left[\sum_\mu \frac{4}{a^{d-2}} \sin^2 \left(\frac{ak_\mu}{2} \right) + m^2 \right] \phi(-k) \phi(k) . \quad (2.9)$$

Each mode contributes to the action in the momentum space a quantity

$$S(k) = m^2 + \sum_x \frac{4}{a^{d-2}} \sin^2 \left(\frac{ak_\mu}{2} \right) \quad (2.10)$$

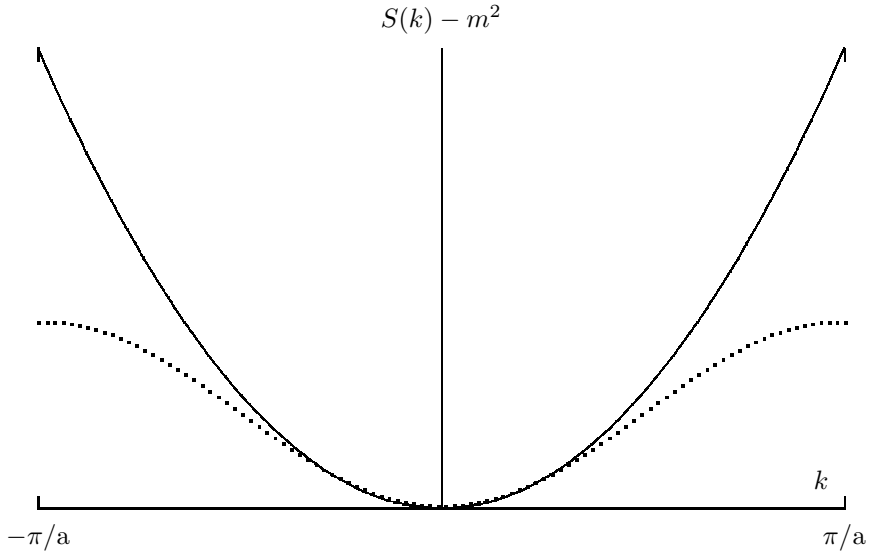


Figure 2.1: The dispersion relation $S(k)$ for a free scalar field. The solid line, k^2 , is for the continuum theory, the dotted line for the latticized system.

rather than the standard $m^2 + k^2$. Nevertheless these two expressions have the same continuum limit as they coincide at the minimum value of $k = 0$ (see fig. (2.1)).

The lattice action Eq.(2.6) is quantized by using the Feynman path-integral formalism, in which the expectation value of a product of fields is given by

$$\langle 0 | \phi_{x_1} \phi_{x_2} \dots \phi_{x_l} | 0 \rangle = \frac{1}{Z} \int \prod_x [d\phi_x] \phi_{x_1} \phi_{x_2} \dots \phi_{x_l} e^{-S(\phi)} \quad (2.11)$$

where

$$Z = \int \prod_x [d\phi_x] e^{-S(\phi)} \quad (2.12)$$

The meaning of the integrals should be clear as one recalls that the usual functional integrals are actually defined on a discretized space-time lattice and an appropriate continuum limit is taken at the end. If one rescales the field as

$$\phi'_x = \sqrt{\lambda} \phi_x \quad (2.13)$$

the lattice action scales as

$$S(\phi) = \frac{1}{\lambda} S'(\phi') \quad (2.14)$$

with

$$S'(\phi') = \sum_x \left[\frac{a^{d-2}}{2} \sum_{\mu=1}^d (\phi'_{x+\hat{\mu}} - \phi'_x)^2 + a^d \left(\frac{m^2}{2} \phi'^2_x + \frac{1}{4} \phi'^4_x \right) \right] \quad (2.15)$$

i.e. the coupling constant λ has become an overall factor in the action. In this way Eqs.(2.11) and (2.12) may be written as

$$\begin{aligned} \langle 0 | \phi'_{x_1} \phi'_{x_2} \dots \phi'_{x_l} | 0 \rangle &= \frac{1}{Z} \int \prod_x [d\phi'_x] \phi'_{x_1} \phi'_{x_2} \dots \phi'_{x_l} e^{-\frac{1}{\lambda} S'(\phi')} \\ Z &= \int \prod_x [d\phi'_x] e^{-\frac{1}{\lambda} S'(\phi')} \quad (2.16) \end{aligned}$$

Note that Eq.(2.16) has the same structure of the partition function in statistical mechanics, once the identification

$$\frac{1}{\lambda} \longrightarrow \beta \equiv \frac{1}{KT} \quad (2.17)$$

is made. The strong coupling expansion (in powers of λ^{-1}) corresponds to the high temperature expansion in statistical mechanics.

2.1.2 Fermi fields on the lattice

I shall now introduce the procedure to put Fermi fields on the lattice. A new phenomenon, the “fermion doubling” [8, 31] appears discretizing the Dirac equation, *i.e.* additional fermionic species are generated. Let us illustrate the fermion doubling problem starting from an example on a spatial lattice and continuum time in 1+1 dimensions. The massless Dirac equation in 1+1 dimensions in the continuum reads

$$i\dot{\psi} = -i\alpha\partial_x\psi = -i\gamma_5\partial_x\psi \quad (2.18)$$

with $\psi = \begin{pmatrix} \psi_1 \\ \psi_2 \end{pmatrix}$ and $\alpha = \gamma_5 = \sigma_1$. Choosing for the plane waves

$$\psi_{\pm}(x, t) = e^{-i(kx - Et)}\chi_{\pm} \quad (2.19)$$

with

$$\gamma_5\chi_{\pm} = \pm\chi_{\pm} \quad (2.20)$$

the dispersion relation is

$$E(k) = \pm k \quad , \quad -\infty < k < \infty \quad (2.21)$$

and the excitations are left- and right-handed particles and antiparticles – see fig.(2.2).

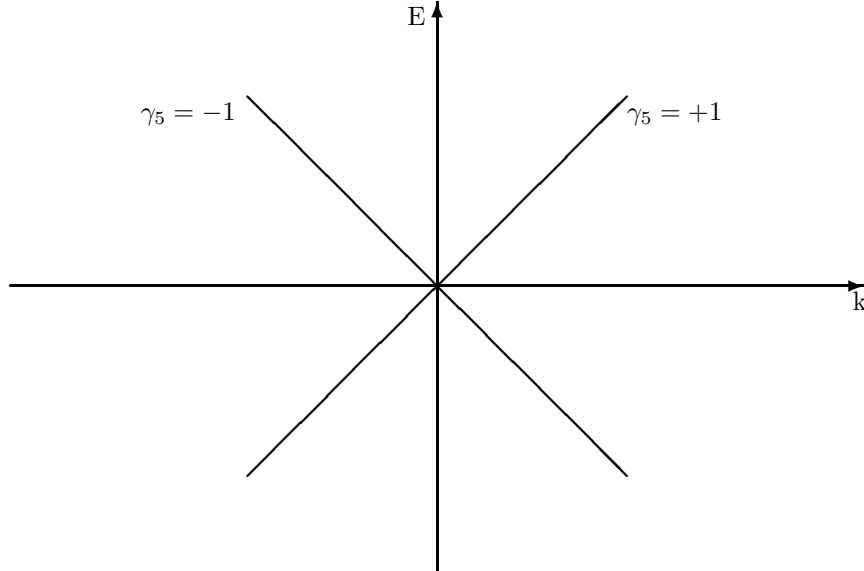


Figure 2.2: Spectrum of the free, continuum Dirac fermion in 1 + 1 dimensions.

Let us consider the naively latticized Dirac equation. I place the spinor $\psi = \begin{pmatrix} \psi_1 \\ \psi_2 \end{pmatrix}$ on each site of a spatial lattice and change the partial derivative ∂_x with a finite difference

$$i\dot{\psi}(x) = -\frac{i}{2a}\gamma_5[\psi(x+1) - \psi(x-1)] \quad . \quad (2.22)$$

The dispersion relation fig.(2.3) is now

$$E(k) = \pm \frac{\sin(ka)}{a} . \quad (2.23)$$

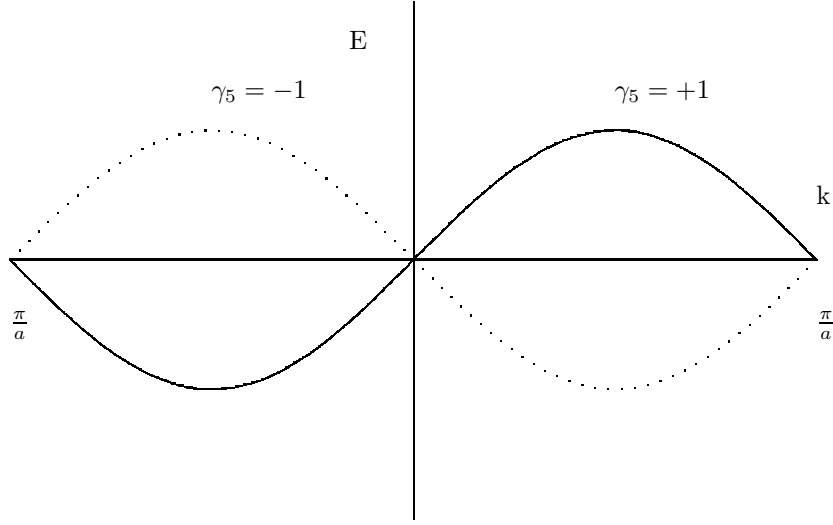


Figure 2.3: Spectrum of the naively latticized Dirac fermion in 1 + 1 dimensions.

This is a relativistic dispersion relation for $ka \ll 1$

$$E(k) \simeq \pm k + O(k^3 a^2) \quad (2.24)$$

and for $ka = \pi - k'a$, with $k'a \ll 1$,

$$E(k) \simeq \mp k' + O(k'^3 a^2) . \quad (2.25)$$

There are two two-component Dirac particles in the continuum limit, and the total chiral charge of the fermions is zero. Consider, for example, the excitations associated with the field ψ_+ on the lattice. There are right-movers ($k \simeq 0$) and left-movers ($k \simeq \pi$), and since chirality (helicity for particles) is just velocity in 1 + 1 dimensions this lattice field describes a pair of fermions with net chirality zero.

The same phenomenon happens in 3+1 dimensions, even if it is more difficult to visualize it. The Dirac Hamiltonian for massive fermions now reads

$$\mathcal{H} = -i\alpha_l \frac{\partial}{\partial x_l} + m\beta \quad (2.26)$$

with

$$\alpha_l = \gamma_5 \gamma_l \quad , \quad \beta = \gamma^0 . \quad (2.27)$$

The field operator describing the multifermion system will be denoted by $\psi_\alpha(\vec{x})$ where $\alpha = 0, 1, 2, 3$ is the Dirac index and the three-component vector \vec{x} denotes a space point. The Hamiltonian of the free fermion field is obtained from the single particle Hamiltonian Eq.(2.26) as

$$H = \int d^3x \psi_\alpha^\dagger(\vec{x}) \mathcal{H}_{\alpha\beta} \psi_\beta(\vec{x}) \quad (2.28)$$

or rewriting Eq.(2.28) with a symmetrized derivative, one gets

$$H = \int d^3x \psi_\gamma^\dagger(x) \left\{ m\beta + \frac{i}{2} \left(\overleftarrow{\frac{\partial}{\partial x_l}} - \overrightarrow{\frac{\partial}{\partial x_l}} \right) \alpha_l \right\}_{\gamma\delta} \psi_\delta(x) \quad . \quad (2.29)$$

Let us now introduce a regular cubic lattice in space with lattice spacing a and elementary cubes of volume a^3 . On a finite lattice with total volume $V = (aL)^3$ the lattice points have integer indices $\vec{x} = \{x_l \ ; \ l = 1, 2, 3\}$ satisfying $0 \leq x_l \leq L - 1$. The continuous field will be replaced by a discrete variable associated with elementary cubes, and the volume integral becomes a finite sum

$$\psi_\alpha(x) \rightarrow \psi_{\alpha\vec{x}} \quad , \quad \int d^3x \rightarrow \sum_x a^3 \quad . \quad (2.30)$$

The discrete field variables are assumed to satisfy the anticommutation relations

$$\{\psi_{\alpha\vec{x}}, \psi_{\beta\vec{y}}\} = \{\psi_{\alpha\vec{x}}^\dagger, \psi_{\beta\vec{y}}^\dagger\} = 0 \quad , \quad \{\psi_{\alpha\vec{x}}^\dagger, \psi_{\beta\vec{y}}\} = \frac{1}{a^3} \delta_{\alpha\beta} \delta_{\vec{x}\vec{y}} \quad (2.31)$$

and the continuous derivatives are discretized as

$$\frac{\partial}{\partial x_l} \psi_\alpha(\vec{x}) \rightarrow \frac{1}{a} (\psi_{\alpha\vec{x}+\vec{l}} - \psi_{\alpha\vec{x}}) \quad (2.32)$$

where \vec{l} denotes a unit vector on the lattice in direction \vec{l} . Applying these rules in the Hamiltonian Eq.(2.29) one obtains the naive discretized form

$$H = \sum_{\vec{x}} a^3 \left\{ \psi_{\gamma\vec{x}}^\dagger m\beta_{\gamma\delta} \psi_{\delta\vec{x}} + \frac{i}{2a} \sum_{l=1}^3 [\psi_{\gamma\vec{x}+\vec{l}}^\dagger (\alpha_l)_{\gamma\delta} \psi_{\delta\vec{x}} - \psi_{\gamma\vec{x}}^\dagger (\alpha_l)_{\gamma\delta} \psi_{\delta\vec{x}+\vec{l}}] \right\} \quad . \quad (2.33)$$

The free field Hamiltonian describes a collection of harmonic fermionic oscillators in momentum space. Assuming periodic boundary conditions in all three orthogonal directions of the L^3 cube, the allowed momentum components are discrete points in the Brillouin zone, namely

$$\vec{p} \equiv \left\{ p_l = \frac{2\pi}{L} n_l \quad ; \quad l = 1, 2, 3 \right\} \quad , \quad 0 \leq n_l \leq L - 1 \quad . \quad (2.34)$$

Due to periodicity, instead of $0 \leq p_l < 2\pi$, the Brillouin zone can also be equivalently defined in the interval $-\pi < p_l \leq \pi$. Fourier transformed field components read

$$\psi_{\alpha\vec{p}} = \sum_{\vec{x}} a^3 e^{-ip_l x_l} \psi_{\alpha\vec{x}} \quad (2.35)$$

$$\psi_{\alpha\vec{x}} = \frac{1}{(aL)^3} \sum_{\vec{p}} e^{ip_l x_l} \psi_{\alpha\vec{p}} \quad . \quad (2.36)$$

In momentum space the Hamiltonian (2.33) reads

$$H = \frac{1}{(aL)^3} \sum_{\vec{p}} \psi_{\gamma\vec{p}}^\dagger \left\{ m\beta + \frac{1}{a} \alpha_l \sin p_l \right\}_{\gamma\delta} \psi_{\delta\vec{p}} \quad . \quad (2.37)$$

The matrix in curly brackets in Eq.(2.37) has eigenvalues

$$E_{\vec{p}} = \pm \sqrt{m^2 + \frac{1}{a^2} \sum_{l=1}^3 \sin^2 p_l} \quad . \quad (2.38)$$

Eq.(2.38) gives the possible energies of the free naive lattice fermions. In the continuum limit $a \rightarrow 0$, Eq.(2.38) approaches the usual dispersion relation for free fermions, since the coordinate vector is $a\vec{x}$ and correspondingly, the momentum vector is $\vec{k} = \frac{1}{a}\vec{p}$. For fixed momentum \vec{k} and $a \rightarrow 0$ one has

$$E_{\vec{p}}^2 = m^2 + \vec{k}^2 + O(a^2) \quad . \quad (2.39)$$

This is as expected, but still the naive lattice Hamiltonian Eq.(2.33) is not entirely satisfactory. Due to the fact that $\sin(p + \pi) = -\sin p$ one has

$$E_{\vec{p}}^2 = E_{\vec{p}+\vec{\pi}}^2 \quad (2.40)$$

where $\vec{\pi}$ is one of the eight vectors

$$\vec{\pi} = \left\{ \begin{array}{l} (0, 0, 0), (\pi, 0, 0), (0, \pi, 0), (0, 0, \pi) \\ (\pi, \pi, 0), (\pi, 0, \pi), (0, \pi, \pi), (\pi, \pi, \pi) \end{array} \right\} . \quad (2.41)$$

These are the eight corners of the part of the Brillouin zone satisfying $0 \leq p_l \leq \pi$ ($l = 1, 2, 3$). The consequence of Eq.(2.40) is that in this naive lattice formulation there are eight fermion states per field component. This phenomena is called fermion doubling although a more appropriate name would be fermion octupling. The basic reason for fermion doubling is that the Dirac equation is of first order. In the case of free fermions one could, perhaps, tolerate this unwanted proliferation of degrees of freedom, but in an interacting theory the extra fermions influence the physical content in a non-trivial way, because the additional states can be pair-produced through the interactions of the fermion field. For example, even if the external particles in a process are the states at the zero $(0, 0, 0)$ corner of the Brillouin zone, the states of the other zones appear in virtual loops.

In order to cure the disease, Wilson introduced an additional second order term in the lattice Hamiltonian

$$\begin{aligned} H &= \sum_{\vec{x}} a^3 \left\{ \psi_{\gamma\vec{x}}^\dagger \left(m + \frac{3r}{a} \right) \beta_{\gamma\delta} \psi_{\delta\vec{x}} \right. \\ &+ \frac{i}{2a} \sum_{l=1}^3 \left[\psi_{\gamma\vec{x}+l}^\dagger (\alpha_l)_{\gamma\delta} \psi_{\delta\vec{x}} - \psi_{\gamma\vec{x}}^\dagger (\alpha_l)_{\gamma\delta} \psi_{\delta\vec{x}+l} \right] \\ &\left. - \frac{r}{2a} \sum_{l=1}^3 \left[\psi_{\gamma\vec{x}+l}^\dagger (\beta_l)_{\gamma\delta} \psi_{\delta\vec{x}} + \psi_{\gamma\vec{x}}^\dagger (\beta_l)_{\gamma\delta} \psi_{\delta\vec{x}+l} \right] \right\} . \quad (2.42) \end{aligned}$$

The Wilson parameter r is assumed to be in the interval $0 < r \leq 1$. In momentum space, instead of Eq.(2.37) one has now

$$\begin{aligned} H &= \frac{1}{(aL)^3} \sum_{\vec{p}} \psi_{\gamma\vec{p}}^\dagger \left\{ m\beta + \frac{r}{a} \beta \sum_{l=1}^3 (1 - \cos p_l) \right. \\ &\left. + \frac{1}{a} \alpha_l \sin p_l \right\}_{\gamma\delta} \psi_{\delta\vec{p}} \quad (2.43) \end{aligned}$$

and the correspondingly energy eigenvalues are

$$E_{\vec{p}} = \pm \sqrt{\left[m + \frac{r}{a} \sum_{l=1}^3 (1 - \cos p_l) \right]^2 + \sum_{l=1}^3 \frac{1}{a^2} \sin^2 p_l} . \quad (2.44)$$

In the continuum limit $a \rightarrow 0$ the mass m is replaced by $m + \frac{2r}{a} n_\pi$, where n_π is the number of momentum components equal to π . Therefore, the states with $n_\pi \neq 0$ become infinitely heavy. The only physical fermion state with finite energy is at the zero corner of the Brillouin zone. In section (2.2) I shall provide a detailed description of a different method to cure the doubling disease, *i.e.* the staggered fermions which are the closest possible analog to the lattice fermions in condensed matter physics.

2.1.3 Gauge fields on the lattice

Let us now discuss how to put gauge fields on the lattice and briefly review how one arrives at the gauge invariant action in the continuum with the simple example of QED. The starting

point is the action of the free Dirac field

$$S_F = \int d^4x \bar{\psi}(x)(i\gamma^\mu \partial_\mu - m)\psi(x) \quad . \quad (2.45)$$

The action is invariant under the transformation

$$\psi(x) \longrightarrow e^{i\Lambda}\psi(x) \quad (2.46)$$

$$\bar{\psi}(x) \longrightarrow \bar{\psi}(x)e^{-i\Lambda} \quad (2.47)$$

with Λ independent of x (*i.e.* a global transformation).

The next step is to require to the action to be also invariant under local $U(1)$ transformations with ψ ($\bar{\psi}$) transforming independently at different space-time points. This is accomplished by introducing a four-vector potential $A_\mu(x)$ and replacing the ordinary four derivative ∂_μ by the covariant derivative \mathcal{D}_μ defined by

$$\mathcal{D}_\mu = \partial_\mu + ieA_\mu \quad . \quad (2.48)$$

The resulting new action

$$S_F = \int d^4x \bar{\psi}(x)(i\gamma_\mu \mathcal{D}^\mu - m)\psi(x) \quad (2.49)$$

is then invariant under the local transformations

$$\psi(x) \longrightarrow e^{i\Lambda(x)}\psi(x) \quad (2.50)$$

$$\bar{\psi}(x) \longrightarrow \bar{\psi}(x)e^{-i\Lambda(x)} \quad (2.51)$$

$$A_\mu(x) \longrightarrow e^{i\Lambda(x)}(A_\mu(x) - \frac{i}{e}\partial_\mu)e^{-i\Lambda(x)} \quad . \quad (2.52)$$

The crucial property which ensures the gauge invariance of Eq.(2.49) is that, while A_μ transforms inhomogeneously, the transformation law for the covariant derivative Eq.(2.48) is homogeneous

$$\mathcal{D}_\mu \longrightarrow e^{i\Lambda(x)}\mathcal{D}_\mu e^{-i\Lambda(x)} \quad . \quad (2.53)$$

By introducing a four-vector field A_μ gauge invariance of the action (2.49) is ensured; one now must introduce a kinetic term which allows A_μ to propagate

$$S_G = -\frac{1}{4} \int d^4x F_{\mu\nu}F^{\mu\nu} \quad (2.54)$$

$F_{\mu\nu}$ is the gauge invariant field strength tensor

$$F_{\mu\nu} = \partial_\mu A_\nu - \partial_\nu A_\mu \quad . \quad (2.55)$$

The gauge invariant action describing the dynamics of the fermionic and gauge field is

$$S_{QED} = S_F + S_G \quad . \quad (2.56)$$

Let us start our approach to lattice QED by considering the lattice action of a free Dirac field. To parallel as closely as possible the steps in the continuum formulation, I shall consider Wilson fermions where every lattice site is occupied by all Dirac components ψ_α . The results presented in the following are valid also for staggered fermions. The Hamiltonian Eq.(2.42) is invariant under the global transformations

$$\psi_{\alpha x} \longrightarrow e^{i\Lambda}\psi_{\alpha x} \quad (2.57)$$

$$\bar{\psi}_{\alpha x} \longrightarrow \bar{\psi}_{\alpha x}e^{-i\Lambda} \quad (2.58)$$

where $e^{i\Lambda}$ is an element of the $U(1)$ group. The next step is in requiring the theory to be invariant under local $U(1)$ transformations, with the group element $e^{i\Lambda_x}$ depending on

the lattice site. Because of the non diagonal structure of the second and third term in the Hamiltonian Eq.(2.42) (whose origin is the derivative in the continuum formulation) one is forced to introduce new degrees of freedom. Since the group elements $e^{i\Lambda_x}$ do not act on the Dirac indices, it is sufficient for the following argument to focus our attention on a typical bilinear term

$$\bar{\psi}_{\vec{x}}\psi_{\vec{x}+\vec{l}} \quad . \quad (2.59)$$

In the continuum it is well known how such bilinear terms should be modified in order to arrive at a gauge invariant expression. Since the bilinear $\bar{\psi}(\vec{x})\psi(\vec{y})$ transforms under gauge transformations

$$\bar{\psi}(\vec{x})\psi(\vec{y}) \longrightarrow \bar{\psi}(\vec{x})e^{-i\Lambda(\vec{x})}e^{i\Lambda(\vec{y})}\psi(\vec{y}) \quad (2.60)$$

one must include a factor depending on the gauge potential which compensates the Eq.(2.60) gauge variation. This factor, called Schwinger line integral is given by

$$U(\vec{x}, \vec{y}) = e^{ie \int_{\vec{x}}^{\vec{y}} dz_{\mu} A^{\mu}(\vec{z})} \quad (2.61)$$

and the line integral is carried out along a path connecting the point \vec{x} with the point \vec{y} . $U(\vec{x}, \vec{y})$ is an element of the $U(1)$ group. Under a gauge transformation Eq.(2.52), Eq.(2.61) transforms as

$$U(\vec{x}, \vec{y}) \longrightarrow e^{i\Lambda(\vec{x})}U(\vec{x}, \vec{y})e^{-i\Lambda(\vec{y})} \quad . \quad (2.62)$$

From these considerations, one concludes that the following bilinear expression in the fermion fields ψ and $\bar{\psi}$ is gauge invariant

$$\bar{\psi}(\vec{x})U(\vec{x}, \vec{y})\psi(\vec{y}) = \bar{\psi}(\vec{x})e^{ie \int_{\vec{x}}^{\vec{y}} dz_{\mu} A^{\mu}(\vec{z})}\psi(\vec{y}) \quad . \quad (2.63)$$

Let us suppose now that $\vec{y} = \vec{x} + \vec{\epsilon}$. From Eq.(2.63) one concludes that the bilinears should be defined as

$$\bar{\psi}(\vec{x})\psi(\vec{x} + \vec{\epsilon}) \longrightarrow \bar{\psi}(\vec{x})U(\vec{x}, \vec{x} + \vec{\epsilon})\psi(\vec{x} + \vec{\epsilon}) \quad (2.64)$$

$$\bar{\psi}(\vec{x} + \vec{\epsilon})\psi(\vec{x}) \longrightarrow \bar{\psi}(\vec{x} + \vec{\epsilon})U^{\dagger}(\vec{x}, \vec{x} + \vec{\epsilon})\psi(\vec{x}) \quad (2.65)$$

with

$$U(\vec{x}, \vec{x} + \vec{\epsilon}) = e^{ie \vec{\epsilon} \cdot \vec{A}(\vec{x})} \quad (2.66)$$

and $\vec{\epsilon} \cdot \vec{A} = \sum_{\mu} \epsilon_{\mu} A^{\mu}$.

To arrive at a gauge-invariant expression for the fermionic action on the lattice, one should make the following substitution in Eq.(2.42)

$$\bar{\psi}_{\vec{x}+\vec{l}}(\gamma_0\gamma_l + ir)\psi_{\vec{x}} \longrightarrow \bar{\psi}_{\vec{x}+\vec{l}}(\gamma_0\gamma_l + ir)U_{\vec{x}+\vec{l},\vec{x}}\psi_{\vec{x}} \quad (2.67)$$

$$\bar{\psi}_{\vec{x}}(\gamma_0\gamma_l - ir)\psi_{\vec{x}+\vec{l}} \longrightarrow \bar{\psi}_{\vec{x}}(\gamma_0\gamma_l - ir)U_{\vec{x},\vec{x}+\vec{l}}\psi_{\vec{x}+\vec{l}} \quad (2.68)$$

where

$$U_{\vec{x}+\vec{l},\vec{x}} = U_{\vec{x},\vec{x}+\vec{l}}^{\dagger} \quad (2.69)$$

and $U_{\vec{x},\vec{x}+\vec{l}}$ is an element of the $U(1)$ gauge group and can therefore be written

$$U_{\vec{x},\vec{x}+\vec{l}} = e^{i\Phi_{\vec{x}}^l} \quad (2.70)$$

where $\Phi_{\vec{x}}^l$ is restricted to the compact domain $[0, 2\pi]$. The right hand side of Eqs.(2.67,2.68) are now invariant under the following set of local transformations

$$\psi_{\vec{x}} \longrightarrow e^{i\Lambda_{\vec{x}}}\psi_{\vec{x}} \quad (2.71)$$

$$\bar{\psi}_{\vec{x}} \longrightarrow \bar{\psi}_{\vec{x}}e^{-i\Lambda_{\vec{x}}} \quad (2.72)$$

$$U_{\vec{x},\vec{x}+\vec{l}} \longrightarrow e^{i\Lambda_{\vec{x}}}U_{\vec{x},\vec{x}+\vec{l}}e^{-i\Lambda_{\vec{x}+\vec{l}}} \quad (2.73)$$

$$U_{\vec{x}+\vec{l},\vec{x}} \longrightarrow e^{i\Lambda_{\vec{x}+\vec{l}}}U_{\vec{x}+\vec{l},\vec{x}}e^{-i\Lambda_{\vec{x}}} \quad . \quad (2.74)$$



Figure 2.4: Link variables.

At variance with the matter fields discussed before, the group element $U_{\vec{x}, \vec{x}+\vec{l}}$ lives on the links connecting two neighbouring lattice sites; hence I shall refer to them as link variables. The link variables have a direction and one can introduce a graphical representation - fig.(2.4).

The Hamiltonian Eq.(2.42) with the Wilson fermions can be written in the following gauge invariant form

$$\begin{aligned}
H &= \sum_{\vec{x}} a^3 \left\{ \left(m + \frac{3r}{a} \right) \bar{\psi}_{\alpha\vec{x}} \psi_{\alpha\vec{x}} \right. \\
&+ \frac{i}{2a} \sum_{l=1}^3 \left[\bar{\psi}_{\alpha\vec{x}+\vec{l}} (\gamma_0 \gamma_l + ir)_{\alpha\beta} U_{\vec{x}+\vec{l}, \vec{x}} \psi_{\beta\vec{x}} \right. \\
&\left. \left. - \bar{\psi}_{\alpha\vec{x}} (\gamma_0 \gamma_l - ir)_{\alpha\beta} U_{\vec{x}, \vec{x}+\vec{l}} \psi_{\beta\vec{x}+\vec{l}} \right] \right\} . \quad (2.75)
\end{aligned}$$

By requiring that $U_{\vec{x}, \vec{x}+\vec{l}}$ and $U_{\vec{x}+\vec{l}, \vec{x}}$ transform according to Eqs.(2.73,2.74), one naturally implements $U(1)$ -gauge invariance in the Hamiltonian and, a posteriori, one can state that the link variables are elements of the $U(1)$ gauge group due to the requirement that their gauge transforms must also be elements of $U(1)$.

Taking the continuum limit $a \rightarrow 0$ of Eq.(2.75) one should get the usual continuum Hamiltonian Eq.(2.29). This requirement is fulfilled by establishing a relation between the link variables and the vector potential $A_\mu(\vec{x})$. The vector potential $A_\mu(\vec{x})$ at the lattice site \vec{x} is real valued and carries a Lorentz index. The same happens for Φ_μ^μ which parametrizes the link variable $U_{\vec{x}, \vec{x}+\vec{\mu}}$. The difference is that Φ_μ^μ takes only values in the interval $[0, 2\pi]$, while the values taken by the vector potential $A_\mu(\vec{x})$ in the continuum theory extends over the entire real line.

Since A_μ carries the dimension of an inverse length, while Φ_μ is dimensionless one may try the ansatz

$$\Phi_\mu(\vec{x}) = ca A_\mu(\vec{x}) \quad (2.76)$$

where a is the lattice spacing and c is a constant to be determined. In the continuum limit $a \rightarrow 0$ the range of A_μ will be infinite.

By scaling m, ψ and $\bar{\psi}$ as $m \rightarrow am$, $\psi \rightarrow a^{\frac{3}{2}} \psi$ and $\bar{\psi} \rightarrow a^{\frac{3}{2}} \bar{\psi}$ and replacing $U_{\vec{x}, \vec{x}+\vec{\mu}}$ for small values of a with

$$U_{\vec{x}, \vec{x}+\vec{\mu}} \simeq 1 + ica A_\mu(\vec{x}) \quad (2.77)$$

Eq.(2.75) reduces to the continuum Eq.(2.49) if one sets $c = e$. From here on I use the notation

$$U_\mu(\vec{x}) = U_{\vec{x}, \vec{x}+\vec{\mu}} = e^{iea A_\mu(\vec{x})} \quad (2.78)$$

With this identification it is now an easy matter to verify that for $a \rightarrow 0$ $U_\mu(\vec{x})$ transforms as follows under gauge transformations

$$U_\mu(\vec{x}) \rightarrow e^{i\Lambda_{\vec{x}}} U_\mu(\vec{x}) e^{-i\Lambda_{\vec{x}+\vec{\mu}}} = e^{iea A_\mu^G(\vec{x})} \quad (2.79)$$

where $A_\mu^G(\vec{x})$ comes from the discretized version of Eq.(2.52).

To complete the construction of lattice QED one has to construct the lattice version of the kinetic term Eq.(2.54) for gauge fields which should be strictly gauge invariant and a functional of link variables only. Such gauge-invariant functionals are easily constructed by taking the product of link variables around closed loops on the euclidean space-time lattice. Moreover, because of the local structure of the integrand in Eq.(2.54) one should focus his attention on the smallest possible loops on the euclidean space time lattice. Hence one is led to consider the product of link variables around an elementary plaquette as shown in fig.(2.5). One then defines

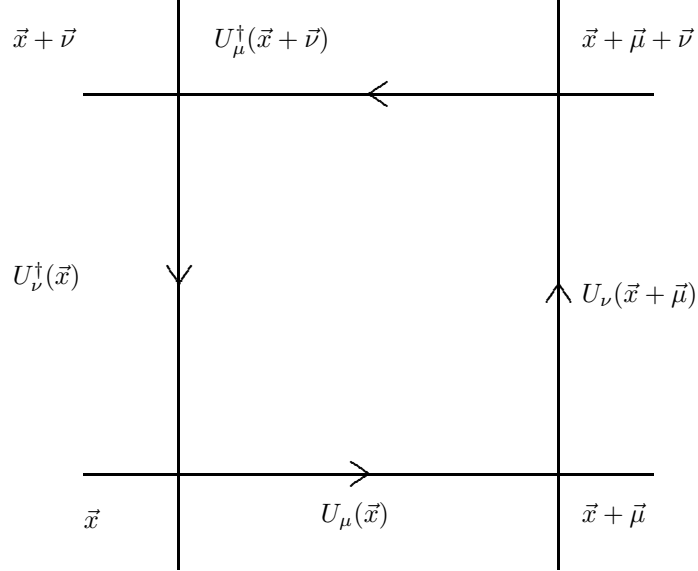


Figure 2.5: A plaquette.

$$U_{\mu\nu}(\vec{x}) = U_\mu(\vec{x})U_\nu(\vec{x} + \vec{\mu})U_\mu^\dagger(\vec{x} + \vec{\nu})U_\nu^\dagger(\vec{x}) \quad (2.80)$$

where I have path ordered the link variables. The path ordering is irrelevant in the Abelian case, but becomes important in *QCD*. Inserting Eq.(2.79) into Eq.(2.80) one gets

$$U_{\mu\nu}(\vec{x}) = e^{iea^2 F_{\mu\nu}(\vec{x})} \quad (2.81)$$

where $F_{\mu\nu}(\vec{x})$ is a discretized version of the continuum field strength tensor

$$F_{\mu\nu}(\vec{x}) = \frac{1}{a} [(A_\nu(\vec{x} + \vec{\mu}) - A_\nu(\vec{x})) - (A_\mu(\vec{x} + \vec{\nu}) - A_\mu(\vec{x}))] \quad (2.82)$$

From Eq.(2.81), in the limit of small lattice spacing a , one has

$$\frac{1}{e^2} \sum_{\vec{x}} \sum_{\mu < \nu} \left[1 - \frac{1}{2}(U_{\mu\nu}(\vec{x}) + U_{\mu\nu}^\dagger(\vec{x})) \right] \simeq \frac{1}{4} \sum_{\vec{x}, \mu, \nu} a^4 F_{\mu\nu}(\vec{x}) F^{\mu\nu}(\vec{x}) \quad (2.83)$$

where the sum appearing on the left hand side extends over the contributions coming from all distinct plaquettes on the lattice. The lattice action [3] for the gauge potential in a compact form reads

$$S_G(U) = \frac{1}{e^2} \sum_P \left\{ 1 - \frac{1}{2}(U_P + U_P^\dagger) \right\} \quad (2.84)$$

where U_P , the plaquette variable, stands for the product of link variables around the boundary of the plaquette P , taken in a counterclockwise direction.

2.2 Staggered fermions

In what follows I shall introduce the staggered fermion formalism [10] that I used to study the lattice Schwinger models. In this formalism one eliminates the unwanted fermion modes by reducing the Brillouin zone, *i.e.* by doubling the effective lattice spacing. In the case of a d -dimensional lattice, one subdivides it into elementary d -dimensional hypercubes of unit length. At each site within a given hypercube one places a different degree of freedom and repeats this structure periodically throughout the lattice. Since there are 2^d sites within a hypercube, but only $2^{\frac{d}{2}}$ components of a Dirac field, one needs $2^{\frac{d}{2}}$ different Dirac fields to reduce the Brillouin zone by a factor of $\frac{1}{2}$.

In the continuum, the massless Dirac spinors are invariant under the chiral rotations

$$\psi(x) \longrightarrow e^{i\gamma_5\theta} \psi(x) \quad , \quad \bar{\psi}(x) \longrightarrow \bar{\psi}(x) e^{-i\gamma_5\theta} \quad (2.85)$$

The continuum axial symmetry (2.85) is broken explicitly by the staggered fermions, but a discrete axial symmetry remains. It is a chiral rotation of $\theta = \pi/2$ and corresponds to the continuum transformation

$$\psi(x) \longrightarrow \gamma_5 \psi(x) \quad , \quad \bar{\psi}(x) \longrightarrow -\bar{\psi}(x) \gamma_5 \quad (2.86)$$

and appears on the lattice as a translation by one site.

Let us start to see how staggered fermions work in $(1+1)$ -dimensions. The main idea is to reduce the number of degrees of freedom by using a single component Fermi field ψ_x on each site of the lattice

$$\{\psi_x, \psi_y\} = 0 \quad , \quad \{\psi_x^\dagger, \psi_y\} = \delta_{xy} \quad (2.87)$$

so that the lattice Dirac Hamiltonian reads

$$H_D = -\frac{it}{2a} \sum_x (\psi_{x+1}^\dagger \psi_x - \psi_x^\dagger \psi_{x+1}) \quad (2.88)$$

and the equations of motion are

$$\dot{\psi}_x = -i[H_D, \psi_x] = \frac{t}{2a} [\psi_{x+1} - \psi_{x-1}] \quad . \quad (2.89)$$

If one decomposes the lattice into even and odd sublattices (characterized by x even and odd), one can identify a single two component Dirac spinor by associating the upper component with even sites and the lower component with odd sites (or vice versa). In this way the equations of motion become

$$\dot{\psi}_1(x) = \frac{1}{2a} [\psi_2(x+1) - \psi_2(x-1)] \quad (2.90)$$

$$\dot{\psi}_2(x) = \frac{1}{2a} [\psi_1(x+1) - \psi_1(x-1)] \quad . \quad (2.91)$$

Comparing Eq.(2.90) and Eq.(2.91) with the the continuum Dirac equation, one immediately sees that the staggered fermion formalism avoids the species doubling problem by doubling the lattice spacing and so halving the size of the Brillouin zone.

Let us now discuss the symmetries of the lattice Dirac Hamiltonian Eq.(2.88). It is invariant under translations of the spatial lattice by an even number of sites. Translation by two lattice spacings is the ordinary continuum translation, whose generator is

$$p = -i \int dx \psi^\dagger \partial_x \psi = -i \int dx (\psi_1^\dagger \partial_x \psi_1 + \psi_2^\dagger \partial_x \psi_2) \quad (2.92)$$

and it does not mix upper and lower spinor components. Consequently, one expects the lattice generator not to mix the two sublattices

$$p = -i \sum_x (\psi_{x+2}^\dagger \psi_x + \psi_x^\dagger \psi_{x+2}) \quad . \quad (2.93)$$

The Hamiltonian Eq.(2.88) is also invariant under translations by an odd number of sites. The lattice generator of this symmetry is

$$Q_5 = \sum_x (\psi_x^\dagger \psi_{x+1} + \psi_{x+1}^\dagger \psi_x) \quad (2.94)$$

which in the continuum would be $Q_5 = \int dx \psi^\dagger \gamma_5 \psi$. The matrix γ_5 applied to the bispinor interchanges upper and lower component, this on the lattice corresponds to translation by one lattice site.

I illustrate now staggered fermions on a $(d-1)$ -dimensional hypercubic lattice and continuum time (hamiltonian formalism) which are obtained by spin-diagonalization [33] of the naively latticized Dirac Hamiltonian

$$H_f = -\frac{i}{2} \sum_{\vec{x}, \vec{j}} \left(\psi_\sigma^\dagger(\vec{x} + \vec{j}) \alpha_{\sigma\sigma'}^j \psi_{\sigma'}(\vec{x}) - \psi_\sigma^\dagger(\vec{x}) \alpha_{\sigma\sigma'}^j \psi_{\sigma'}(\vec{x} + \vec{j}) \right) \quad (2.95)$$

where $\psi_\sigma(x)$ are the fermion field operators, $\sigma = 1, 2, \dots, 2^{[d/2]}$ is the spin index, $\vec{x} \equiv (x_1, x_2 \dots x_{(d-1)}) = \sum_{j=1}^{d-1} x_j \hat{j}$ (the x_j are integers) refers to lattice sites, \hat{j} are unit vectors and α^j are the $2^{[d/2]} \times 2^{[d/2]}$ Hermitean Dirac matrices - here $[d/2]$ is the largest integer less than or equal to $d/2$. Hamiltonian (2.95) describes a fermion hopping problem in a $U(2^{[d/2]})$ background gauge field given by the unitary² matrices α^j . The crucial observation which allows spin diagonalization is that this background field has only $U(1)$ curvature, i.e. if one considers the product around any plaquette

$$\alpha^j \alpha^k (\alpha^j)^\dagger (\alpha^k)^\dagger = -1 \quad . \quad (2.96)$$

Hence the only information carried by the α -matrices which is invariant under a space dependent change of phase of the fermion fields is that a product of α 's around any plaquette is -1 . This allows diagonalization of the α 's using a gauge transformation such as

$$\psi(\vec{x}) \rightarrow (\alpha^1)^{x_1} (\alpha^2)^{x_2} \dots (\alpha^{(d-1)})^{x_{(d-1)}} \psi(\vec{x}) \quad (2.97)$$

resulting in the Hamiltonian

$$H_f = -\frac{i}{2} \sum_{\vec{x}, \vec{j}} (-1)^{\sum_{p=1}^{j-1} x_p} \left(\psi^\dagger(\vec{x} + \vec{j}) \psi(\vec{x}) - \psi^\dagger(\vec{x}) \psi(\vec{x} + \vec{j}) \right) \quad (2.98)$$

which describes $2^{[d/2]}$ species of lattice fermions with background $U(1)$ magnetic flux π through every plaquette of the lattice. This flux is contained in the background $U(1)$ field $U^0[\vec{x}, \vec{j}] = (-1)^{\sum_{p=1}^{j-1} x_p}$. Each species of fermion must have the same spectrum as the original one given by the Dirac Hamiltonian (2.95). This allows reduction of the fermion multiplicity by a factor of $2^{[d/2]}$ (by dropping the fermion spin index σ). The result resembles a condensed matter hopping problem with a single species of fermion where there is a background magnetic field π per plaquette.

²Dirac's α -matrices are Hermitean,

$$\alpha^{i\dagger} = \alpha^i \quad ,$$

and, due to their anticommutator algebra,

$$\{ \alpha^i, \alpha^j \} = 2\delta^{ij} \quad ,$$

they are also unitary.

Discrete Chiral symmetry interchanges the even ($\sum_{p=1}^{d-1} x_p = \text{even}$) and odd ($\sum_{p=1}^{d-1} x_p = \text{odd}$) sublattices. The substitutions

$$\psi(\vec{x}) \rightarrow (-1)^{\sum_{p=j+1}^{d-1} x_p} \psi(\vec{x} + \vec{j}) \quad (2.99)$$

for $j = 1, \dots, (d-1)$ leave the Hamiltonian in Eq.(2.98) invariant. A candidate for Dirac mass operator, which changes sign under the transformations in Eq.(2.99), is the staggered charge density operator

$$\mu = m \sum_{\vec{x}} (-1)^{\sum_{p=1}^{d-1} x_p} \psi^\dagger(\vec{x}) \psi(\vec{x}) \quad (2.100)$$

To obtain the continuum limit and the number of fermion species, one first divides the lattice into 2^{d-1} sublattices according to whether the components of their coordinates are even or odd. For example, when $(d-1) = 3$, I label 8 fermion species as

$$\begin{aligned} \psi(\text{even, even, even}) &\equiv \psi_1 \quad , \quad \psi(\text{even, odd, odd}) \equiv \psi_2 \\ \psi(\text{odd, even, odd}) &\equiv \psi_3 \quad , \quad \psi(\text{odd, odd, even}) \equiv \psi_4 \\ \psi(\text{even, even, odd}) &\equiv \psi_5 \quad , \quad \psi(\text{even, odd, even}) \equiv \psi_6 \\ \psi(\text{odd, even, even}) &\equiv \psi_7 \quad , \quad \psi(\text{odd, odd, odd}) \equiv \psi_8 \quad . \end{aligned} \quad (2.101)$$

Then, if one adds the mass operator (2.100), in momentum space the Hamiltonian (2.98) has the form

$$H_f = \int_{\Omega_B} d^3 k \psi^\dagger(\vec{k}) (A^i \sin k_i + Bm) \psi(\vec{k}) \quad (2.102)$$

with

$$\psi^\dagger(\vec{k}) \equiv (\psi_1^\dagger(\vec{k}), \dots, \psi_8^\dagger(\vec{k})) \quad (2.103)$$

and 8×8 matrices

$$\begin{aligned} A^i &= \begin{pmatrix} 0 & \alpha^i \\ \alpha^i & 0 \end{pmatrix} \quad , \quad B = \begin{pmatrix} 1 & 0 \\ 0 & -1 \end{pmatrix} \\ \alpha^1 &= \begin{pmatrix} 0 & 1 \\ 1 & 0 \end{pmatrix} \quad , \quad \alpha^2 = \begin{pmatrix} \sigma^1 & 0 \\ 0 & -\sigma^1 \end{pmatrix} \quad , \quad \alpha^3 = \begin{pmatrix} \sigma^3 & 0 \\ 0 & -\sigma^3 \end{pmatrix} \end{aligned} \quad (2.104)$$

with σ^i the Pauli matrices; I used the Fourier transform

$$\psi(\vec{x}) = \int_{\Omega_B} \frac{d^3 k}{(2\pi)^{3/2}} e^{-i\vec{k} \cdot \vec{x}} \psi(\vec{k}) \quad (2.105)$$

where $\Omega_B = \{\vec{k} = (k_1, k_2, k_3), -\pi/2 < k_i \leq \pi/2\}$ is the Brillouin zone of the (even,even,even) sublattice. The fermion spectrum is

$$\omega(\vec{k}) = \sqrt{\sum_{i=1}^3 \sin^2 k_i + m^2}, \quad (2.106)$$

and only the region $k_i \sim 0$ is relevant to the continuum limit. I have normalized $\psi(k)$ so that

$$\{\psi(x), \psi^\dagger(y)\} = \delta(x-y) \quad , \quad \{\psi(k), \psi^\dagger(l)\} = \delta^3(k-l) \quad (2.107)$$

If one defines $\beta = \begin{pmatrix} \sigma^2 & 0 \\ 0 & -\sigma^2 \end{pmatrix}$ and the unitary matrix

$$M = \frac{1}{2} \begin{pmatrix} 1-\beta & 1+\beta \\ 1+\beta & 1-\beta \end{pmatrix} \quad (2.108)$$

and

$$\psi = M\psi' \quad (2.109)$$

with

$$\psi' = \begin{pmatrix} \psi_a \\ \psi_b \end{pmatrix}, \quad (2.110)$$

the Hamiltonian is

$$H_f = \int_{\Omega_B} d^3k \begin{pmatrix} \psi_a^\dagger & \psi_b^\dagger \end{pmatrix} \begin{pmatrix} \alpha^i \sin k_i - \beta m & 0 \\ 0 & \alpha^i \sin k_i + \beta m \end{pmatrix} \begin{pmatrix} \psi_a \\ \psi_b \end{pmatrix}. \quad (2.111)$$

the low momentum limit, $\sin k_i \sim k_i$, with fermion density 1/2 per site so that the Fermi level is at the intersection point of the positive and negative energy bands, one obtains 2 continuum Dirac fermions. Furthermore, the staggered charge operator gives a Dirac mass of differing sign for the two species.

If one considers $\mathcal{N}\mathcal{N}_C$ lattice species in d dimensions, i.e. fermions ψ_A^α with $\alpha = 1, \dots, \mathcal{N}$ and $A = 1, \dots, \mathcal{N}_C$ a lattice flavor and color index, respectively, this yields $\mathcal{N}\mathcal{N}_C 2^{(d-1)}/2^{[d/2]}$ continuum species of Dirac fermions where the lattice fermion density is $\mathcal{N}\mathcal{N}_C/2$ per site. For the Dirac mass operator one may choose

$$\mu = \sum_{\vec{x}} (-1)^{\sum_{p=1}^{d-1} x_p} \psi_A^{\alpha\dagger}(\vec{x}) m_{\alpha\beta} \psi_B^\beta(\vec{x}), \quad (2.112)$$

with $m_{\alpha\beta} = \text{diag}(m_1, \dots, m_{\mathcal{N}})$, and this gives the fermion spectrum

$$\omega(k) = \sqrt{\sum_{i=1}^{d-1} \sin^2 k_i + m_\alpha} \quad (2.113)$$

where $-\pi/2 \leq k_i < \pi/2$ and $\alpha = 1, \dots, \mathcal{N}$.

Here, I count the number of flavors of fermions obtained in the continuum limit by noting that Eq.(2.98) describes a 2^{d-1} -component fermion. In d dimensions the Dirac matrices are $[d/2]$ dimensional, therefore the continuum limit of Eq.(2.98) describes $2^{d-1}/2^{[d/2]}$ species of Dirac fermions.

d	no. of flavors	no. of spinor components	
2	1	2	(2.114)
3	2	2	
4	2	4	

2.3 Strong coupling lattice gauge theory

This section is devoted to a detailed analysis of the strong coupling limit of hamiltonian lattice gauge theories. I shall give a general introduction to the subject by considering a gauge theory with colour group $U(\mathcal{N}_C)$ or $SU(\mathcal{N}_C)$ and $SU(\mathcal{N})$ -flavor groups. The Hamiltonian formalism is particularly suitable for illustrating the relationship between several gauge and spin systems and was already exploited in some of the earliest studies of chiral symmetry breaking in the strong coupling limit [15]. The strong coupling limit, though far from the scaling regime is often used to study qualitative properties related to confinement and chiral symmetry breaking. In chapter 4, 5 and 6 I shall study the one-flavor and multiflavor lattice Schwinger models. The one-flavor model will be mapped in the strong coupling limit onto an antiferromagnetic Ising model with long range Coulomb interaction. The multiflavor Schwinger models are effectively described by spin-1/2 antiferromagnetic $SU(\mathcal{N})$ Heisenberg models.

2.3.1 Hamiltonian formulation of lattice gauge theory

Let us consider an hamiltonian lattice gauge theory [13] where space is a $(d-1)$ -dimensional hypercubic lattice with oriented plaquettes $[x, i, j]$ with corners $x, x + \hat{i}, x + \hat{i} + \hat{j}, x + \hat{j}$ and orientation $\hat{i} \times \hat{j}$. The gauge field $U[x, i]$ associated with the link $[x, i]$ is a group element in the fundamental representation $[\mathcal{N}_C]$ of $SU(\mathcal{N}_C)$ and, if the color group is $U(\mathcal{N}_C)$, also carries a representation of $U(1)$. It has the property $U[x, -i] = U^\dagger[x - \hat{i}, i]$. The electric field operator $E^a[x, i]$ associated with link $[x, i]$ has the Lie algebra

$$[E^a[x, i], E^b[y, j]] = if^{abc}E^c[x, i]\delta([x, i] - [y, j]) \quad (2.115)$$

and

$$E[x, -i] = -U^\dagger[x - \hat{i}, i]E[x - \hat{i}, i]U[x - \hat{i}, i] \quad (2.116)$$

where

$$E[x, i] \equiv E^a[x, i]T^a \quad (2.117)$$

with $T^a = (T^a)^\dagger$, $a = 0 \dots, \mathcal{N}_C^2 - 1$ the generators of the Lie algebra of $U(\mathcal{N}_C)$ obeying

$$[T^a, T^b] = if^{abc}T^c, \quad (2.118)$$

$T^0 = \mathbf{1}$ the $\mathcal{N}_C \times \mathcal{N}_C$ unit matrix representing $U(1)$ and T^a , $a \neq 0$, in the representation $[\mathcal{N}_C]$ of $SU(\mathcal{N}_C)$. It generates the left-action of the Lie algebra on $U[x, i]$, i.e.,

$$[E^a[x, i], U[y, j]] = -T^a U[x, i]\delta([x, i] - [y, j]) \quad (2.119)$$

The Hamiltonian for lattice gauge theory with staggered fermions and discrete chiral symmetry is

$$H = \sum_{[x, i], a} \frac{g^2}{2} E^a[x, i]^2 + \left(\sum_{[x, i, j]} \frac{1}{2g^2} \text{Tr}(U[x, i]U[x + \hat{i}, j]U^\dagger[x + \hat{j}, i]U^\dagger[x, j]) + \text{h.c.} \right) + \left(\sum_{[x, i]} t_{[x, i]} \psi_A^{\alpha\dagger}(x + \hat{i}) U_{AB}[x, i] \psi_B^\alpha(x) + \text{h.c.} \right) \quad (2.120)$$

where $\text{Tr}(\cdot)$ is the $\mathcal{N}_C \times \mathcal{N}_C$ matrix trace and where

$$t_{[x, i]} = t \frac{i}{2} (-)^{\sum_{p=1}^i x_p}, \quad t_{[x, -i]} = t_{[x - \hat{i}, i]}^* \quad (2.121)$$

and the generators of static gauge transformations are

$$\mathcal{G}^a(x) = \sum_{i=-(d-1)}^{(d-1)} E^a[x, i] + \psi_A^{\alpha\dagger}(x) T_{AB}^a \psi_B^\alpha(x) \quad (2.122)$$

with $a = 1, \dots, \mathcal{N}_C^2 - 1$. If the gauge group is $U(\mathcal{N}_C)$ rather than $SU(\mathcal{N}_C)$ there is also the $U(1)$ generator

$$\mathcal{G}^0(x) = \sum_{i=1}^{(d-1)} (E^0[x, i] - E^0[x - \hat{i}, i]) + \frac{1}{2} [\psi_A^{\alpha\dagger}(x), \psi_A^\alpha(x)] \quad (2.123)$$

with the fermionic $U(1)$ charge operator ordered so that, like E , it changes sign under charge conjugation. (Note that there is no ordering ambiguity for the \mathcal{G}^a , $a \neq 0$.) These generators obey the Lie algebra

$$[\mathcal{G}^a(x), \mathcal{G}^b(y)] = if^{abc}\mathcal{G}^c(x)\delta(x - y) \quad (2.124)$$

The Hamiltonian is gauge invariant,

$$[\mathcal{G}^a(x), H] = 0 \quad . \quad (2.125)$$

The dynamical problem of lattice gauge theory is to find the eigenstates of the Hamiltonian operator Eq.(2.120) which are also gauge invariant, i.e. which obey the physical state condition

$$\mathcal{G}^a(x)|\psi_{\text{phys}}\rangle = 0 \quad . \quad (2.126)$$

2.3.2 Strong coupling

In order to perform a strong-coupling expansion [31], let us rewrite Eq.(2.120)

$$H = H_0 + H_1 + H_2$$

where $H_0 = \sum \frac{g^2}{2} E^2$, $H_1 = \sum (t\psi^\dagger U\psi + \text{h.c.})$ and $H_2 = \sum \frac{1}{2g^2} (\text{Tr}UUUU + \text{h.c.})$. Each term is gauge invariant,

$$[\mathcal{G}^a(x), H_i] = 0.$$

Therefore, if one finds a gauge invariant eigenstate of H_0 , perturbations in H_1 and H_2 remain gauge invariant. H_0 is the sum of group manifold Laplacians for each link. If $|0\rangle$ is a singlet of the algebra (2.115), i.e.

$$E^a[x, i]|0\rangle = 0,$$

then

$$H_0|0\rangle = 0$$

and

$$H_0 U[x, i]|0\rangle = \frac{g^2}{2} C_2(\mathcal{N}_C) U[x, i]|0\rangle \quad (2.127)$$

In Eq.(2.127) the Casimir operator is

$$C_2(\mathcal{N}_C)\mathbf{1} = \sum_a T^a T^a$$

and a runs either from 0 (for $U(\mathcal{N}_C)$) or 1 (for $SU(\mathcal{N}_C)$) to $\mathcal{N}_C^2 - 1$.

Consider the empty vacuum which is a singlet of (2.115) and which has no fermions,

$$\psi_A^\alpha(x)|0\rangle = 0 \quad , \quad \forall x, A, \alpha.$$

It is necessary to find the lowest energy ($E_0 =$ eigenvalue of H_0) eigenstates $|\Psi\rangle$ of H_0 which are gauge invariant,

$$\mathcal{G}^a(x)|\Psi\rangle = 0 \quad \forall a, x,$$

with the constraint that the fermion states are half-filled, i.e. half of the fermion states are filled.

I shall first review the simplest case of $SU(\mathcal{N}_C \geq 3)$ gauge theory with 1 lattice flavor ($\mathcal{N} = 1$) and $2^d/2^{[d/2]}$ continuum flavors [11]. The density is $\mathcal{N}_C/2$ fermions per site. The lowest energy eigenstates of H_0 with $E_0 = 0$ are the states which are singlets of the electric field algebra (2.115) and, since they are gauge invariant they must also be color singlets, i.e. singlets of the algebra (2.124). Then, they must also be singlets of the algebra of the fermion currents $\psi^\dagger(x)T^a\psi(x)$. One can form a ‘‘baryon’’ (=color singlet) at a site by either

leaving it unoccupied or putting \mathcal{N}_C fermions with antisymmetrized singlet wave-function by applying the creation operator

$$S^\dagger(x) = \epsilon_{A_1 \dots A_{\mathcal{N}_C}} \psi_{A_1}^\dagger(x) \dots \psi_{A_{\mathcal{N}_C}}^\dagger(x) \quad (2.128)$$

($\epsilon_{A_1, \dots, A_{\mathcal{N}_C}}$ is the usual antisymmetric tensor).

Fermi statistics allows at most one singlet per site. Otherwise one can distribute the $N/2$ singlets arbitrarily (N is the total number of lattice sites). Thus, there are $N!/((N/2)!)^2$ degenerate ground states with a typical state being

$$|\{\rho_x\}_x\rangle = \prod_{\text{occupied } x} S^\dagger(x)|0\rangle$$

I label them by the eigenvalues ρ_x of the local Fermion number operators

$$\rho(x) = \frac{1}{2}[\psi^\dagger(x), \psi(x)] = \psi^\dagger(x)\psi(x) - \mathcal{N}_C/2.$$

All matrix elements in the vector space of degenerate vacua of the first order Hamiltonian vanish,

$$\langle \{\rho_x\}_x | H_1 | \{\rho'_x\}_x \rangle = 0$$

so second order perturbation theory must be considered and the matrix with elements

$$\langle \{\rho_x\}_x | H_2 | \{\rho'_x\}_x \rangle - \langle \{\rho_x\}_x | H_1 \frac{1}{H_0 - E_0} H_1 | \{\rho'_x\}_x \rangle .$$

must be diagonalized. The first term is zero and diagonalizing the second term is equivalent to diagonalizing the four-fermion Hamiltonian

$$H_{\text{eff}} = -K \sum_{[x,i]} \psi_A^\dagger(x + \hat{i}) \psi_B(x) \psi_B^\dagger(x) \psi_A(x + \hat{i}) = K \sum_{[x,i]} \rho(x + \hat{i}) \rho(x) \quad (2.129)$$

(up to an additive constant), with

$$K = \frac{t^2}{2g^2 \mathcal{N}_C C_2(\mathcal{N}_C)} > 0 \quad , \quad (2.130)$$

in the space of pure fermion states where $\rho(x)$ has eigenvalues

$$\rho_x = \pm \mathcal{N}_C/2$$

and

$$\sum_x \rho_x = 0.$$

This is the antiferromagnetic Ising model.

Now I consider arbitrary \mathcal{N} . Then the density is $\mathcal{N}_C \mathcal{N}/2$ fermions per site and the ‘‘baryon’’ (= color singlet) creation operator is

$$S_{\alpha_1 \dots \alpha_{\mathcal{N}_C}}^\dagger(x) = \epsilon_{A_1 \dots A_{\mathcal{N}_C}} \psi_{A_1}^{\alpha_1 \dagger}(x) \dots \psi_{A_{\mathcal{N}_C}}^{\alpha_{\mathcal{N}_C} \dagger}(x) \quad . \quad (2.131)$$

Since this operator is symmetric in the lattice flavor indices $\alpha_1, \dots, \alpha_{\mathcal{N}_C}$, it carries an irreducible representation of $SU(\mathcal{N})$ with Young Tableau with \mathcal{N}_C columns and 1 row. Fermi statistics allows at most \mathcal{N} singlets on a given site. Thus, the allowed representations of the flavor $SU(\mathcal{N})$ algebra at one site are the empty singlet and those with the Young tableaux given in fig. (2.6) and which are distinguished by the fermion numbers

$$\rho_x = \mathcal{N}_C(2\nu - \mathcal{N})/2, \quad \nu = 0, 1, 2, \dots, \mathcal{N} \quad (2.132)$$

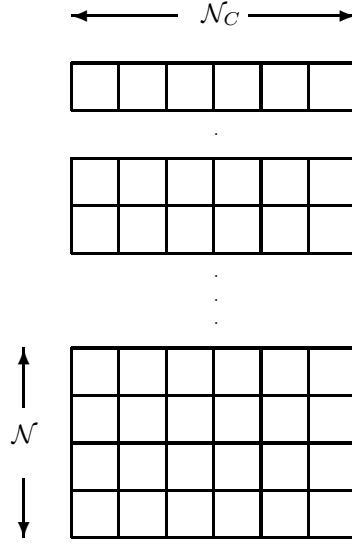


Figure 2.6: Young tableaux representations allowed at a given site.

respectively. A ground state of H_0 is obtained by creating $N\mathcal{N}/2$ color singlets. The states are labeled by the local fermion densities ρ_x and the vector in the corresponding $SU(\mathcal{N})$ representation at each site and are degenerate.

Again this degeneracy must be resolved by diagonalizing perturbations. The first-order perturbation to the vacuum energy vanishes and diagonalizing the second order perturbations is equivalent to diagonalizing the effective Hamiltonian

$$H_{\text{eff}} = -K \sum_{[x,i]} \psi_A^{\alpha\dagger}(x + \hat{i}) \psi_B^\alpha(x) \psi_B^{\beta\dagger}(x) \psi_A^\beta(x + \hat{i}) = K \sum_{[x,i]} J^{\alpha\beta}(x + \hat{i}) J^{\beta\alpha}(x) \quad (2.133)$$

(up to an additive constant) where the operators

$$J^{\alpha\beta}(x) = \frac{1}{2} \left[\psi_A^{\alpha\dagger}(x), \psi_A^\beta(x) \right] = \psi_A^{\alpha\dagger}(x) \psi_A^\beta(x) - \delta^{\alpha\beta} \frac{\mathcal{N}_C}{2} = (J^{\beta\alpha}(x))^\dagger \quad (2.134)$$

are generators of the Lie algebra of $U(\mathcal{N})$,

$$\left[J^{\alpha\beta}(x), J^{\alpha'\beta'}(y) \right] = \delta(x-y) \left(\delta^{\beta\alpha'} J^{\alpha\beta'}(x) - \delta^{\beta'\alpha} J^{\alpha'\beta}(x) \right) . \quad (2.135)$$

Thus, the effective Hamiltonian is that of a $U(\mathcal{N})$ quantum antiferromagnet with representations given in fig. (2.7) and with the constraint $\sum_x \rho_x = 0$, and I have shown that it is equivalent to the strong coupling limit of $SU(\mathcal{N}_C)$ lattice gauge theory with \mathcal{N} lattice flavors of staggered fermions.

The $SU(2)$ color group is peculiar and this can be traced back to the fact that for 2 colors the singlet creation and annihilation operators involve only 2 fermion field operators, and in second order perturbation theory terms are generated describing the hopping of these singlets [24]. Due to this Eq.(2.133) is not the right effective Hamiltonian but

$$\begin{aligned} H_{\text{eff}} &= -K \sum_{[x,i]} \left(\psi_A^{\alpha\dagger}(x) \psi_B^\alpha(x + \hat{i}) \psi_B^{\beta\dagger}(x + \hat{i}) \psi_A^\beta(x) - \epsilon_{AC} \epsilon_{BD} \psi_A^{\alpha\dagger}(x + \hat{i}) \psi_B^\alpha(x) \psi_C^{\beta\dagger}(x + \hat{i}) \psi_D^\beta(x) \right) \\ &= K \sum_{[x,i]} \left(J^{\alpha\beta}(x) J^{\beta\alpha}(x + \hat{i}) + S_+^{\alpha\beta}(x) S_-^{\beta\alpha}(x + \hat{i}) \right) \end{aligned} \quad (2)$$

(up to a constant), with

$$S_+^{\alpha\beta}(x) = \epsilon_{AB} \psi_A^{\alpha\dagger}(x) \psi_B^{\beta\dagger}(x) , \quad (2.137)$$

$$S_-^{\alpha\beta}(x) = \epsilon_{AB}\psi_A^\alpha(x)\psi_B^\beta(x) = (S_+^{\beta\alpha}(x))^\dagger , \quad (2.138)$$

and the $J^{\alpha\beta}(x)$ as above. One can check that the operators $J^{\alpha\beta}(x)$ and $S_\pm^{\alpha\beta}(x)$ obey the relations of the Lie algebra of the symplectic group $\text{Sp}(2N_L)$, i.e. Eqs. (2.135) and

$$\left[S_+^{\alpha\beta}(x), S_-^{\alpha'\beta'}(y) \right] = \delta(x-y) \left(\delta^{\beta\alpha'} J^{\alpha\beta'}(x) + \delta^{\alpha\beta'} J^{\beta\alpha'}(x) + \delta^{\alpha\alpha'} J^{\beta\beta'}(x) + \delta^{\beta\beta'} J^{\alpha\alpha'}(x) \right) , \quad (2.139)$$

$$\left[J^{\alpha\beta}(x), S_+^{\alpha'\beta'}(y) \right] = \delta(x-y) \left(\delta^{\beta\alpha'} S_+^{\alpha\beta'}(x) + \delta^{\beta\beta'} S_+^{\alpha\alpha'}(x) \right) , \quad (2.140)$$

$$\left[J^{\alpha\beta}(x), S_-^{\alpha'\beta'}(y) \right] = -\delta(x-y) \left(\delta^{\alpha\alpha'} S_-^{\beta\beta'}(x) + \delta^{\alpha\beta'} S_-^{\beta\alpha'}(x) \right) , \quad (2.141)$$

hence (2.136) is a $\text{Sp}(2N_L)$ antiferromagnet. Especially for $\mathcal{N} = 1$ it is the spin 1/2 Heisenberg antiferromagnet as originally found in [24].

If, instead of $SU(\mathcal{N}_C)$ one had the gauge group $U(\mathcal{N}_C)$, gauge invariance would require that one imposes the extra constraint

$$\mathcal{G}^0(x)|\Psi\rangle = 0 , \quad \forall x.$$

This can be fulfilled without electric fields, i.e. with $\rho_x = 0 \forall x$, only when \mathcal{N} is even. Then the allowed $SU(\mathcal{N}_C)$ representation at each site is the one with the Young Tableau given in fig. (2.7), and, with the constraint

$$\sum_\alpha J^{\alpha\alpha}(x) = 0 ,$$

$J^{\alpha\beta}(x)$ generate the $SU(\mathcal{N})$ algebra in this representation. Thus, $U(\mathcal{N}_C)$ gauge theory is equivalent to an $SU(\mathcal{N})$ quantum antiferromagnet in the representation fig. (2.7). This actually is true for all $\mathcal{N}_C \geq 1$ ($\mathcal{N}_C = 2$ is *not* special here as no hopping of color singlets is allowed for $U(\mathcal{N}_C)$ color groups [24]).

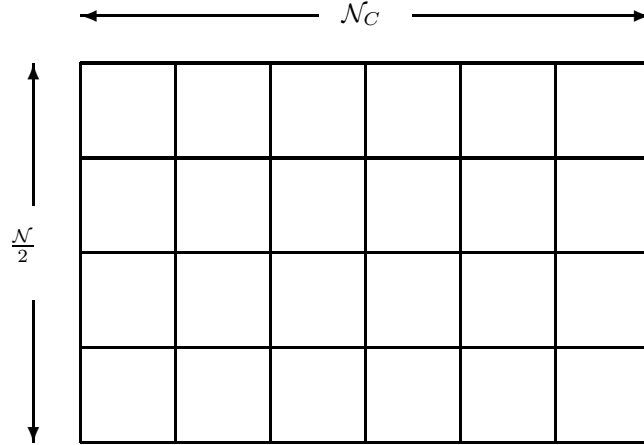


Figure 2.7: Young tableau with \mathcal{N}_C columns and $\mathcal{N}/2$ rows.

As a concrete example, let us consider the case $\mathcal{N} = 2$ which gives 4 continuum flavors in $d = 4$. The $SU(\mathcal{N}_C \leq 3)$ gauge theory is equivalent to a $U(2)$ antiferromagnet. Using the identity

$$2\delta_{\beta\gamma}\delta_{\alpha\epsilon} = \vec{\sigma}_{\alpha\beta} \cdot \vec{\sigma}_{\gamma\epsilon} + \delta_{\alpha\beta}\delta_{\gamma\epsilon} \quad (2.142)$$

(with $\vec{\sigma}$ the Pauli matrices) one can change basis in the $U(2)$ Lie algebra to find the effective strong coupling Hamiltonian

$$H_{\text{eff}} = \frac{K}{2} \sum_{[x,i]} \left(\psi^\dagger(x) \vec{\sigma} \psi(x) \cdot \psi^\dagger(x+i) \vec{\sigma} \psi(x+i) + \rho(x) \rho(x+i) \right) \quad (2.143)$$

where

$$(\psi^\dagger \vec{\sigma} \psi \equiv \psi_A^{\alpha\dagger} \vec{\sigma}_{\alpha\beta} \psi_A^\beta) \quad (2.144)$$

and the representation at a given site has either $\rho_x = 0$ and the spin $S = \mathcal{N}_C/2$ representation of $SU(2)$ or $\rho_x = \pm \mathcal{N}_C$ and the spin $S = 0$.

If the gauge group is $U(\mathcal{N}_C)$ then the density is constrained, $\rho_x = 0$ and each site is occupied by the $S = \mathcal{N}_C/2$ representation of $SU(2)$ and (2.143) is the Hamiltonian of the quantum Heisenberg antiferromagnet.

The most subtle case is that of a $U(\mathcal{N}_C)$ lattice gauge theory with odd \mathcal{N} . There I first solve the problem of minimizing the contribution of $U(1)$ electric fields to the energy. This is done by solving the auxilliary problem of minimizing the energy function

$$\frac{1}{2g^2} \sum_{[x,i]} (E^0[x, i])^2$$

with the constraint

$$\sum_i (E^0[x, i] - E^0[x - \hat{i}, i]) + \rho(x) \sim 0 \quad (2.145)$$

where

$$\rho(x) = \psi_A^{\alpha\dagger}(x) \psi_A^\alpha(x) - \mathcal{N}_C \mathcal{N} / 2 \quad .$$

If $\mathcal{N}_C \mathcal{N}$ is odd, the charge density $\rho(x)$ has only half-odd-integer eigenvalues ρ_x . Since they have no zero eigenvalue, the constraint Eq.(2.145) cannot be satisfied unless the $U(1)$ electric field is non-zero. This is also true of $SU(\mathcal{N}_C)$ color singlet states, since they always contain an integral multiple of \mathcal{N}_C particles. Then the operator $\psi^\dagger \psi$ has eigenvalue which is an integer multiple of \mathcal{N}_C and when \mathcal{N} is odd, the charge density $\rho(x)$ again has no nonzero eigenvalues. The configuration which minimizes the $U(1)$ energy is the most symmetric one,

$$E^0[x, \pm i] = \pm \frac{\mathcal{N}_C}{4(d-1)} (-1)^{\sum_{p=1}^{d-1} x_p}$$

with the accompanying eigenvalues of the charge density

$$\rho_x = \pm \frac{\mathcal{N}_C}{2} (-1)^{\sum_{p=1}^{d-1} x_p} \quad .$$

If, instead of $U(1)$ electric fields, one had color non-singlets, the energy would be higher. In chapter 4 the one-flavor lattice Schwinger model is studied as a concrete example with $\mathcal{N}_c = 1$ and $\mathcal{N} = 1$.

2.4 Chiral anomaly on the lattice

We shall see in section (2.4.1) that under some mild assumption about the lattice action, there are always an equal number of left- and right-handed Weyl particles in the continuum limit of a lattice fermionic theory. In the continuum the axial or chiral charge Q_5 is defined as the integral of the chiral density of the current $j_5^\mu(x) = \bar{\psi}(x) \gamma^\mu \gamma_5 \psi(x)$

$$Q_5 = \int d^3x j_5^0(x) = \int d^3x \psi^\dagger(\vec{x}, t) \gamma_5 \psi(\vec{x}, t) \quad (2.146)$$

According to Eq.(2.146) Q_5 is the number of right-handed fermions minus the number of left-handed fermions minus the number of right-handed antifermions plus the number of left-handed antifermions. In the case of massless fermions Q_5 is conserved at the classical level, not only in the case of free theories, but also in the case of interacting theories like

QED or σ -models [6]. At the quantum level the chiral symmetry is broken by the anomaly. For example in massless QED the divergence of the axial current is given by [26]

$$\partial_\mu j_5^\mu(x) = \frac{e^2}{16\pi^2} \epsilon_{\mu\nu\rho\sigma} F^{\mu\nu}(x) F^{\rho\sigma}(x) \quad (2.147)$$

There is no way to avoid the physical consequences of the anomaly; one might also define a conserved axial vector current, but it is not gauge invariant and the physical consequences are unchanged. The axial anomaly appears in perturbation theory as a consequence of the linear divergences in the triangle graph with an internal fermion loop, and either three axial vector current insertions or one axial vector and two vector current insertions. The one-loop quantum corrections to a chirally symmetric classical action are not chirally symmetric. It is impossible to regularize a quantum field theory preserving both axial and gauge invariance. Since lattice gauge theories are manifestly gauge invariant, it is an interesting question how axial anomaly appears there. In general the fermion doublers do contribute to the anomaly. Since the doublers appear with opposite chiralities, one might conclude that the anomaly on the lattice is zero. However the question is more involved [31].

I am interested in analyzing how the anomaly manifests itself in the lattice Schwinger models with different flavor groups. I already illustrated that staggered fermions explicitly break the $U_A(1)$ symmetry but possess a discrete chiral symmetry corresponding to translations by one lattice spacing. As we shall see in chapters 4, 5 and 6 in the continuum the $U_A(1)$ symmetry is broken by the anomaly either in the one-flavor or in the multiflavor Schwinger models. In chapter 4 we shall see that on the lattice in the one-flavor case the discrete chiral symmetry is broken spontaneously. At variance, in the two-flavor model we shall see in chapter 5 that the ground state is translationally invariant, *i.e.* does not break the discrete chiral symmetry. The only relic of the continuum axial anomaly is the non-zero VEV of the umklapp operator.

2.4.1 The Nielsen-Ninomiya no-go theorem

Nielsen and Ninomiya [27] demonstrated that fermion theories on a lattice have an equal number of species of left- and right-handed Weyl particles, *i.e.* neutrinos, in the continuum limit. The consequence of this behavior is a no-go theorem for putting theories of weak interactions on a lattice. Moreover it is not possible in strong interaction models to solve the species doubling problem on a lattice in a chirally invariant way. The appearance of equally many right- and left-handed species of Weyl particles is an unavoidable consequence of a lattice theory under some mild assumptions.

The hypothesis of this theorem are locality of the theory and exact conservation of discrete valued quantum numbers and charges assumed to have a density defined from a finite region.

If one is interested in the strong interactions and wants to study a Dirac particle rather than a Weyl particle, there is no unsurmountable problem because a Dirac particle can be thought of as a composite of two Weyl particles, a right-handed one and a left-handed one. However there is no way to construct chiral invariant lattice models for QCD .

Let us consider the general class of lattice fermion theories for which the bilinear part of the action for the N -component complex fermion field $\psi(\vec{x})$ is of the form

$$S_F = -i \int dt \sum_{\vec{x}} \dot{\bar{\psi}}(\vec{x}) \psi(\vec{x}) - \int dt \sum_{\vec{x}, \vec{y}} \bar{\psi}(\vec{x}) H(\vec{x} - \vec{y}) \psi(\vec{y}) \quad (2.148)$$

$$\psi = \begin{pmatrix} \psi_1 \\ \vdots \\ \psi_N \end{pmatrix}$$

with H an Hamiltonian where interactions of quartic or higher degree in ψ are neglected. In fact, one can define the number of species of Weyl fermions depending only on the bilinear part of the action, while the interactions do not change the dispersion relation but just cause scattering processes. The action S_F should fulfill the following three conditions

- Locality of the interaction, *i.e.* $H(\vec{x}) \rightarrow 0$ fast enough as $|\vec{x}| \rightarrow \infty$ that its Fourier transform $\tilde{H}(\vec{p})$ is a smooth function. Thus the eigenvalues $\omega_i(\vec{p})$ ($i = 1, \dots, N$) are smooth except in the case that two eigenvalues $\omega_i(\vec{p})$ and $\omega_{i+1}(\vec{p})$ coincide
- Translational invariance on the lattice
- Hermiticity of the $N \times N$ matrix Hamiltonian H .

The assumptions made for the charges Q (lepton number, for instance) are

- Exact conservation of Q , even at the scales where the lattice cut-off is relevant
- Q is locally defined $Q = \sum_{\vec{x}} \rho(\vec{x})$. The charge density $\rho(\vec{x})$ is a function of the field variables $\psi(\vec{y})$ related to \vec{y} within a bounded distance from \vec{x} .
- Q is quantized
- Q is bilinear in the fermion field $\psi(\vec{x})$.

The weak interactions and the Standard Model exhibit right- and left-handed particles that do not have the same hypercharge, so that parity and charge conjugation are broken in weak interaction processes. This implies that if nature were indeed built on a lattice, it should be possible to realize Weyl fermions with different quantum numbers for left- and right-handed ones.

One has thus to understand where is the problem: one must give up the idea that nature is based on a fundamental lattice cut-off or some assumption of the no-go theorem, or weak interactions phenomenology, *i.e.* the usual understanding of parity violation.

Nielsen and Ninomiya gave two proofs of their no-go theorem, a very technical one based on algebraic topology and homotopy and a more intuitive topological proof. The proof is mainly supported by the fact that the momentum space of lattice theory is periodic, *i.e.* there is the Brillouin zone

$$-\frac{\pi}{a} \leq p_i \leq \frac{\pi}{a} \tag{2.149}$$

where the end points π/a and $-\pi/a$ are identified. From a topological point of view p_i runs on a circle S^1 , thus the momentum space makes up a hypertorus $S^1 \otimes S^1 \otimes S^1$.

Let review the intuitive proof of the no-go theorem for a general class of 1+1 dimensional lattice fermion theories, whose action is the 1+1 dimensional version of the 3+1 dimensional case Eq.(2.148). One thus takes ψ to be a complex N -component field in order to keep generality. A generic 1+1 dimensional Hamiltonian has non degenerate energy levels, in fact, in order to have just two-level degeneracy $\omega_i(p) = \omega_{i+1}(p)$ three parameters must be restricted in the Hamiltonian $H(p)$, but there is only one p . However the wave packet velocity

$$v_i = \left. \frac{d\omega_i}{dp} \right|_{p=p_f} \tag{2.150}$$

is non zero at the Fermi energy

$$\omega_i(p_f) = 0 \quad (2.151)$$

Low energy excitations are such that fermion states with p close to p_f are excited and for particles relevant at low energies one has

$$\omega_i(p) = (p - p_f) \left. \frac{d\omega_i}{dp} \right|_{p=p_f} + O((p - p_f)^2) \quad (2.152)$$

The particle at the crossing point with $\omega_i = 0$ line is called a right(left) mover when

$$\left. \frac{d\omega_i}{dp} \right|_{p=p_f} > 0 \quad (< 0) \quad (2.153)$$

Antiparticles and particles have the same velocity. Assuming locality $\omega_i(p)$ is analytic in p except for degeneracy points and a smooth curve $\omega_i(p)$ is defined in $\omega_i - p$ space. The curve is closed since on a lattice p is defined modulo $2\pi/a$ and thus runs on a circle S_1 . Such curves must cross equally many times from $\omega_i(p) < 0$ to $\omega_i(p) > 0$ as they cross from $\omega_i(p) > 0$ to $\omega_i(p) < 0$. One can orient the curve such that it is along the increasing p direction. The curve going up through $\omega_i = 0$ represents a right-mover and that going down a left-mover. From a topological point of view there must be the same number of upgoings and downgoings for the closed curve – see fig. (2.8). Therefore, there appear equally many

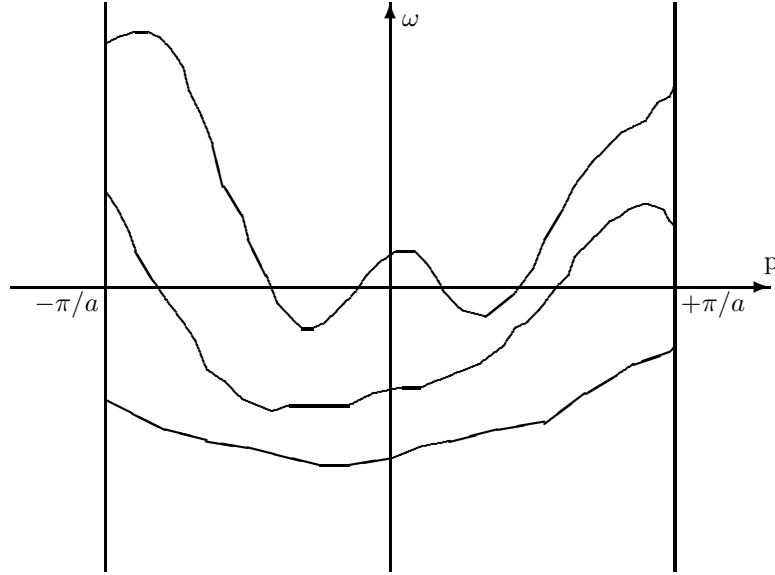


Figure 2.8: Dispersion relations for 1 + 1 dimensional lattice Weyl fermions. Each curve is closed since end points are identified. Each crossing point at $\omega = 0$ is a Fermi “surface” describing one species of Weyl fermions.

right and left movers in the low energy regime. Let us introduce the shifted momentum

$$\tilde{p} = p - p_f \quad (2.154)$$

The dispersion relation reads

$$\omega_i = \left. \frac{d\omega_i}{dp} \right|_{\tilde{p}=0} \tilde{p} \quad (2.155)$$

This is a relativistically invariant dispersion relation for a massless mover along the right or left direction. This is true only when $\left. \frac{d\omega_i}{dp} \right|_{p=p_f}$ is considered equal to the velocity of light.

Let us now turn our attention to the 3 + 1 dimensional case. The eigenvalue equation for the Hamiltonian Eq.(2.148) reads

$$H(\vec{p})\psi(\vec{p}) = \omega_i(\vec{p})\psi(\vec{p}) \quad i = 1, \dots, N \quad (2.156)$$

with N ordered eigenvalues $\omega_1 > \omega_2 > \dots > \omega_N$. When two energy levels, the i-th and (i+1)-th coincide, *i.e.* are degenerate, at the momentum \vec{p}_{deg} ,

$$\omega_i(\vec{p}_{deg}) = \omega_{i+1}(\vec{p}_{deg}) = 0 \quad (2.157)$$

one can expand the $N \times N$ matrix $H(p)$ near the degeneracy point \vec{p}_{deg} . The most general Hamiltonian $H^{(2)}(\vec{p})$ for the two component spinor $U(p)$ describing the i-th and (i+1)-th levels, is of the form

$$H^{(2)}(\vec{p}) = \omega_{deg}(\vec{p}_{deg}) + (\vec{p} - \vec{p}_{deg})\vec{b} + (\vec{p} - \vec{p}_{deg})_k V_\alpha^k \sigma^\alpha + O((\vec{p} - \vec{p}_{deg})^2) \quad (2.158)$$

with \vec{b} and \vec{V} constants. By introducing the shifted variables

$$\tilde{\vec{p}} = \vec{p} - \vec{p}_{deg} \quad \tilde{\omega} = \omega - \omega_{deg} \quad (2.159)$$

$H^{(2)}(\vec{p})$ reads

$$H^{(2)}(\vec{p}) = \tilde{\vec{p}}_k V_\alpha^k \sigma^\alpha + \tilde{\vec{p}} \cdot \vec{b} \quad (2.160)$$

let us define further a new momentum

$$P_0 = \tilde{\omega} - (\vec{p} - \vec{p}_{deg})\vec{b} \quad (2.161)$$

$$P_\alpha = \pm \tilde{\vec{p}}_k V_\alpha^k \quad (2.162)$$

The sign \pm depends on the sign of $\det V$ which determines the relative handedness of the $\tilde{\vec{p}}$ and \vec{p} coordinates. Take conventionally $\tilde{\vec{p}}$ to be the right handed one. $H^{(2)}(\vec{p})$ becomes

$$H^{(2)}(\vec{p}) = \vec{\sigma} \cdot \vec{P} \quad (2.163)$$

and one obtains the right and left handed Weyl equation

$$\vec{P}\vec{\sigma}U(\vec{p}) = \pm P_0U(\vec{p}) \quad (2.164)$$

corresponding to the sign of $\det V$. Whether one has right- or left- handed Weyl fermions depends on the degeneracy point since the constant tensor \vec{V} depends on \vec{p}_{deg} .

One may call the degeneracy point a right or left handed one according to Eq.(2.164). Each degeneracy point represents one species of Weyl fermions. If the Fermi energy surface lies at the degeneracy points of the i-th and (i+1)-th, each degeneracy point represents one species of Weyl particles.

Let us consider curves in 4-dimensional $\omega - \vec{p}$ space or on the 3-dimensional dispersion relation surface defined by

$$\{(\vec{p}, \omega_i(\vec{p})) \mid \langle a | \omega_i(\vec{p}) \rangle = 0\} \quad (2.165)$$

where

$$\langle a | \omega_i(\vec{p}) \rangle = a_1 \psi_1^{(i)} + a_2 \psi_2^{(i)} + \dots + a_N \psi_N^{(i)} \quad (2.166)$$

The vector $|a \rangle = (a_1, a_2, \dots, a_N)$ is an arbitrarily chosen constant in the complex N-dimensional vector space, which may be chosen to be the basic vector corresponding to the field number one. Eq.(2.166) specifies a 1-dimensional curve in the generic case, in fact Eq.(2.166) fixes two variables since $\langle a | \omega_i(\vec{p}) \rangle$ is a complex number and it is a continuous and analytic complex-valued function of \vec{p} . The set of curves always passes through all the degeneracy points, as can be shown explicitly using the continuum 2-component Weyl equation near the degeneracy point \vec{p}_{deg} . Then one can construct a new state

$$|\bar{\omega}_i(\vec{p}) \rangle = \alpha |\omega_i(\vec{p}) \rangle + \beta |\omega_{i+1}(\vec{p}) \rangle \quad (2.167)$$

near $\vec{p} = \vec{p}_{deg}$. One can always choose α and β such that

$$\langle a|\bar{\omega}_i(\vec{p}) \rangle = 0 \quad (2.168)$$

which is the condition of Eq.(2.166) for the curve. Due to the existence of the Brillouin zone and the fact that the curves continuously pass through all the degeneracy points between the energy levels ω_i and ω_{i+1} , such a curve must be closed or consists of a number of closed curves. If the curves are oriented they must pass equally many times upward and downward between the energy levels ω_i and ω_{i+1} , through all the degeneracy points. Let us now orient the curves and show that, when the curve crosses the level $\omega = 0$ between the levels ω_i and ω_{i+1} upward (or downward), the crossing point, *i.e.* the degeneracy point is a right- (or left-) handed degeneracy point. The eigenstate determined by Eq.(2.156) is unique modulo a phase factor if one imposes the normalization condition $\langle \omega_i(\vec{p})|\omega_i(\vec{p}) \rangle = 1$. One can choose the phase of $|\omega_i(\vec{p}) \rangle$ to be analytic in a simply connected region which should not include the degeneracy points. An orientation of the curves is assigned by means of the phase rotation of $\langle a|\omega_i(\vec{p}) \rangle$ on a small circle S_1 around the curve (2.166). The convention is that an increase of phase on S_1 should form a right-handed screw together with the oriented curve when one takes a right-handed coordinate convention for \vec{p} . Let us consider for example the case the curve is along $p_z > 0$ on the upper cone $p_0 > 0$ near the right handed degeneracy points. The two component field U satisfies the equation

$$\vec{P}\vec{\sigma}U(\vec{p}) = P_0U(\vec{p}) \quad (2.169)$$

One draws a circle S_1 with radius R around a point on the curve at a distance d from the degeneracy point and let us take $R \ll d$. The point Q on S_1 is parametrized in the following way

$$p_x = R \cos \theta \quad (2.170)$$

$$p_y = R \sin \theta \quad (2.171)$$

$$p_z = d \quad (2.172)$$

The normalized eigenvector U of Eq.(2.169) is solved in the limit $\frac{R}{d} \ll 1$

$$U = \begin{pmatrix} 1 \\ \frac{R}{2d} e^{i\theta} \end{pmatrix} . \quad (2.173)$$

Since one obtains

$$U = \begin{pmatrix} 1 \\ 0 \end{pmatrix} . \quad (2.174)$$

on the curve $R = 0$, the vector $\langle a|$ must be $\langle a| = (0, 1)$ so that on S_1

$$\langle a|\omega_i \rangle = \frac{R}{2p_z} e^{i\theta} \quad (2.175)$$

and according to the orientation convention the curve is oriented in the positive p_z direction because it forms a right handed screw. Computing the case of $p_0 > 0$ and $p_z < 0$, $p_0 < 0$ and $p_z < 0$, $p_0 < 0$ and $p_z > 0$ one obtains fig. (2.9a) for the right handed degeneracy point. The case of left handed degeneracy point is depicted in fig. (2.9b). As one can see in fig. (2.9), the curve continues through the degeneracy points conserving the orientation. The orientation determined in this way becomes the same all along the curve. The important fact is that the curve must be oriented away from the degeneracy point on the level sheet with right-handed particles (*i.e.* with positive helicity), while the curve must be inward oriented on the level with left-handed particles. Finally the oriented curve is closed and thus must go equally many times upward and downward through all the degeneracy points $\omega_i(\vec{p}_{deg}) = \omega_{i+1}(\vec{p}_{deg}) = 0$ between the energy levels $\omega_i(\vec{p})$ and $\omega_{i+1}(\vec{p})$. When the Dirac sea (ω_{i+1} level) is filled and the Fermi surface lies at the degeneracy point $\omega = 0$, there appear equally many species of right- and left-handed Weyl fermions. This concludes the proof of this no-go theorem of Nielsen and Ninomiya.

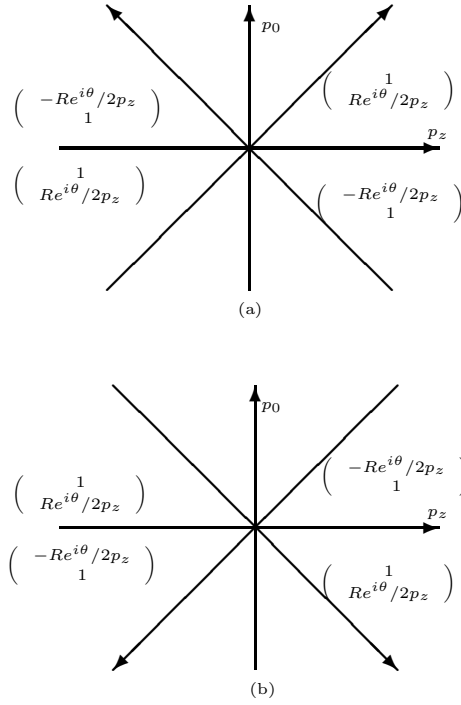


Figure 2.9: Around a degeneracy point all the curves of the type $\langle a|\omega_i(\vec{p})\rangle$ are oriented away on one level and inward on the other one.

The strong interaction lattice models for QCD invented by Wilson, Susskind and Banks and Casher break chiral invariance in order to avoid the fermion doubling. Drell, Weinstein and Yankielowicz were able to construct a chiral invariant model for lattice QCD but it breaks locality of the interaction. There is some proposal in the literature to avoid the no-go theorem, giving up some of its hypothesis, and to put the Standard Model on the lattice; but up to now no generally accepted scheme does exist.

Nielsen and Ninomiya pointed also out a similarity between the fermion system of lattice gauge theories and the electron system of crystals. More precisely they pointed out that there exists an effect analogous to the mechanism of the Adler-Bell-Jackiw (ABJ) axial anomaly in solid state physics. The main similarity between lattice fermions and “real” electrons in crystals is that in both systems there is only the lattice translational invariance which implies the Brillouin zone existence. The crystal electrons are described by a one component non-relativistic Schrödinger equation, but the energy eigenvalues form bands. It is possible to write the electron theory as a multicomponent lattice fermion theory with a matrix Hamiltonian. At points where two energy bands of the electrons make a contact in the energy-momentum dispersion law space, the two band wave functions of the electrons can be approximated by the Weyl equation, and so, according to the no-go theorem, such degeneracy points occur in pairs of the right-handed and left-handed type. There is no net production of electrons like the absence of the net production of Weyl fermions in lattice fermions theories when parallel electric, E , and magnetic, H , fields are put on. This leads to the conservation of axial charge. The ABJ anomaly manifests itself by transferring electrons from the neighborhood of the left-handed degeneracy point to the right-handed one in energy-momentum space. In a parity non-invariant zero-gap semiconductor the effect analogous to the ABJ anomaly gives rise to a peculiar behavior of the conductivity of the electric current in the presence of the magnetic field.

In chapter 5 I shall compute the VEV of the operator $F = \overline{\psi}_L^{(2)} \overline{\psi}_L^{(1)} \psi_R^{(1)} \psi_R^{(2)}$, describing an umklapp process in which two right-movers are annihilated and two left-movers are created.

I shall show that VEV of the umklapp operator is non-zero due to the coupling of left- and right-movers by the gauge field. Right-handed fermions are annihilated and left-handed are created at a degeneracy point so that there is no net production of electrons.

Chapter 3

Antiferromagnetic spin chains

The title of this chapter deserves an entire book to be properly developed, and in fact some books, reviews and long articles about spin chains do already exist [34]. Spin chains interested mathematical physicists for their exact solvability, field theorists for the possibility to test their methods by comparison with exact results and condensed matter physicists for the possibility to understand the spectra of real physical systems. It is my purpose to report a self-contained analysis of antiferromagnetic spin chains, useful to understand chapter 5 and 6 where I shall show that the multiflavor lattice Schwinger models in the strong coupling limit are effectively described by the spin-1/2 $SU(\mathcal{N})$ antiferromagnetic Heisenberg chains.

A common tool to study spin systems is spin-wave theory. Spin-wave theory was developed by Anderson, Kubo and others [35] in the 1950s and it is a very powerful approach to quantum magnetic systems in dimensions greater than one, predicting long-range order and gapless Goldstone bosons. The situation remained clouded for magnetic chains because it was known that long-range order could not occur in one dimension, but the Bethe ansatz predicts massless excitations. There is “quasi-long-range-order” corresponding to a power law decay of spin-spin correlators and there are gapless excitations which are not true Goldstone bosons.

Quantum spin chains have been extensively studied in the literature, starting from the seminal paper by Hans Bethe [36] in 1931 for the spin-1/2 case, where he introduced an ansatz to write down the eigenfunctions of the Heisenberg Hamiltonian, describing a chain with periodic boundary conditions. Seven years later Hulthen [37] was able to compute the ground state energy of the antiferromagnetic Heisenberg chain. We had to wait until 1984 to know exactly the spectrum of this model, when Faddeev and Takhtadzhyan [30] analyzed the model using the algebraic Bethe ansatz and showed that the only one-particle excitation is a doublet of spin-1/2 quantum excitations with gapless dispersion relation. This excitation is a kink rather than an ordinary particle and is called spinon. All the eigenstates of the antiferromagnetic Heisenberg Hamiltonian contain an even number of kinks, nevertheless the kinks are localizable objects and one can consider their scattering. There are no bound states of kinks in this model.

The one dimensional spin systems are not only unusual because they are exactly solvable but also for their incompatibility with long range order. Actually solvability and absence of long range order are deeply related concepts; systems with spontaneously broken symmetries are more difficult to describe and resist analytical solutions. All isotropic antiferromagnetic quantum spin chains with short range interactions exhibit quantum spin-liquid ground states – *i.e.* states with short range antiferromagnetic correlations and no order. Moreover these chains have strange quantum elementary excitations above these ground states, that are not

ordinary spin waves but are usually called spinons – neutral spin-1/2 kinks.

As R. B. Laughlin [38] points out: “spinons are not “like” anything familiar to most of us, but are instead an important and beautiful instance of fractional quantization, the physical phenomenon in which particles carrying pieces of a fundamental quantum number, such as charge or spin, are created as a collective motion of many conventional particles obeying quantum mechanical laws. The fractional quantum number of the spinon is its spin. It is fractional because the particles out of which the magnetic states are constructed are spin flips, which carry spin 1.”

One significant result of my research [39, 40] has been to show explicitly how spinons appear in lattice gauge theories. More precisely I showed that the massless excitations of the two-flavor Schwinger model coincide with the spinons of the spin-1/2 antiferromagnetic Heisenberg model.

Section (3.1) shows the failure of spin wave theory in one dimension, due to the infrared divergencies. Spin-spin correlation functions are computed in the spin wave theory and are compared with exact expressions.

In section (3.2) I review the Haldane-Shastry model [41], a spin model discovered independently by Haldane and Shastry and in the context of one dimensional Bose gas by Sutherland. The Haldane-Shastry model is a realization of the spin-1/2 Heisenberg chain in which the quantum disordered ground state and spinon excitations are particularly easy to understand.

Section (3.3) is devoted to review the Bethe ansatz solution of the antiferromagnetic Heisenberg chain. Moreover I shall compare the exact solution given in [30] with a study of finite size chains of 4,6, and 8 sites. An original result presented is the thermodynamic limit coefficient of the states with $N - 2$ domain walls composing the ground state. The spin-spin correlation function $\sum_x \langle g.s. | \vec{S}_x \cdot \vec{S}_{x+2} | g.s. \rangle$ originally computed by M. Takahashi [42], is derived in a slightly different way. The vacuum expectation value of the square of the vector $\vec{V} = \sum_x \vec{S}_x \wedge \vec{S}_{x+1}$ is computed in an approximate way.

In section (3.4) I introduce the spin-1/2 $SU(\mathcal{N})$ antiferromagnetic Heisenberg chains. To provide an intuitive picture I study the $SU(3)$ two sites chain and I find the ground state. A short review of the literature on $SU(\mathcal{N})$ antiferromagnetic Heisenberg chains is provided.

3.1 Failure of spin wave theory in D=1

In the limit of large spin $S \rightarrow \infty$ the quantum nature of a magnetic system can be forgotten, and one can consider the spin \vec{S} as a classical vector in the three dimensional space. In fact in this limit the spin commutator is much smaller than the square of the spin variables

$$[S^a, S^b] = i\epsilon^{abc} S^c = O(S) \ll O(S^2) \tag{3.1}$$

The classical ground states of the Heisenberg model are states with spins parallel for the ferromagnetic case

↑↑↑↑↑↑↑↑ ...

or neighbouring spins antiparallel for the antiferromagnetic case

$$\uparrow\downarrow\uparrow\downarrow\uparrow\downarrow\uparrow\downarrow\dots$$

The classical ground state of the antiferromagnet is called Néel state. By introducing the raising and lowering spin operators

$$S_x^\pm = S_x^1 \pm iS_x^2 \quad (3.2)$$

the antiferromagnetic ($J > 0$) Heisenberg Hamiltonian reads

$$H_J = J \sum_{x=1}^N \left\{ S_x^3 S_{x+1}^3 + \frac{1}{2} (S_x^+ S_{x+1}^- + S_x^- S_{x+1}^+) \right\} \quad (3.3)$$

The classical ferromagnetic ground state coincides with the quantum one, but the Néel state is not an eigenstate of H_J due to the raising and lowering spin operators action.

It is an interesting question to investigate whether or not long-range antiferromagnetic order occurs

$$\langle S_x^3 S_0^3 \rangle = \pm m \quad (3.4)$$

where the sign depends whether x belongs to the even or odd sublattice. The spin wave approach to this problem is to perturb away from the limit in which the Néel state is exact. This happens of course for a spin- S Heisenberg antiferromagnet in the limit $S \rightarrow \infty$. In this limit one expects that the fluctuations of S^3 around $+S$ on one sublattice and $-S$ on the other sublattice are very small. It is customary to study the effects of these fluctuations using the Holstein-Primakov transformation, which consists in parametrizing the spin operators in terms of boson operators a and a^\dagger on the sublattice of even sites A and b and b^\dagger on the sublattice of odd sites B. On the sublattice A one writes

$$S^3 = S - a^\dagger a \quad (3.5)$$

$$S^- = (2S)^{\frac{1}{2}} a^\dagger \left(1 - \frac{a^\dagger a}{2S} \right)^{\frac{1}{2}} \quad (3.6)$$

Eqs.(3.5,3.6) for spin operators correctly reproduce the spin algebra. The state with maximal $S^3 = S$ is a state with zero bosons. Applying S^- on this state one creates a boson and so lowers S^3 by one. The state with $S^3 = -S$ has $2S$ bosons and is annihilated by S^- . On sublattice B one writes

$$S^3 = -S + b^\dagger b \quad (3.7)$$

$$S^- = (2S)^{\frac{1}{2}} \left(1 - \frac{b^\dagger b}{2S} \right)^{\frac{1}{2}} b \quad (3.8)$$

Using the Holstein-Primakov representation given by Eqs.(3.5,3.6) and Eqs.(3.7,3.8) and studying the small fluctuations around the Néel state so that $a^\dagger a$ and $b^\dagger b$ are $O(1) \ll S$ in the large S limit, one may develop an expansion in $\frac{1}{S}$ by expanding the square roots in the definition of S^- in Eqs.(3.6,3.8). To quadratic order the Hamiltonian (3.3) reads

$$H = J \sum_{x=1}^N \left\{ -S^2 + S(a_x^\dagger a_x + b_{x+1}^\dagger b_{x+1} + a_x b_{x+1} + a_x^\dagger b_{x+1}^\dagger) \right\} \quad (3.9)$$

where higher orders in $\frac{1}{S}$ have been dropped. In momentum space the Hamiltonian (3.9) reads

$$H_J = 2JS \sum_k \left\{ \gamma_k (a_k b_{-k} + a_k^\dagger b_{-k}^\dagger) + (a_k^\dagger a_k + b_k^\dagger b_k) \right\} \quad (3.10)$$

where

$$\gamma_k = \frac{e^{ik} + e^{-ik}}{2} = \cos k = \gamma_{-k} \quad . \quad (3.11)$$

The Hamiltonian (3.10) describes free bosons. Let us take the Bogoliubov transformation

$$C_k = U_k a_k - V_k b_{-k}^\dagger \quad D_k = U_k b_k - V_k a_{-k}^\dagger \quad (3.12)$$

where, since a and b are bosonic operators, one has

$$|U|^2 - |V|^2 = 1 \quad . \quad (3.13)$$

To put to zero the off diagonal terms inverting Eqs.(3.12) one has

$$\gamma(U^2 + V^2) + 2UV = 0 \quad (3.14)$$

Solving Eq.(3.13) and Eq.(3.14) one gets

$$U_k = \frac{1}{2} \frac{1}{(1 - \gamma_k^2)^{\frac{1}{4}}} \left[\sqrt{1 - \gamma_k} + \sqrt{1 + \gamma_k} \right] \quad (3.15)$$

$$V_k = \frac{1}{2} \frac{1}{(1 - \gamma_k^2)^{\frac{1}{4}}} \left[\sqrt{1 - \gamma_k} - \sqrt{1 + \gamma_k} \right] \quad . \quad (3.16)$$

Using Eqs.(3.12) the Hamiltonian Eq.(3.10) reads

$$H_J = 2JS \sum_k (1 - \gamma_k^2)^{\frac{1}{2}} (C_k^\dagger C_k + D_k^\dagger D_k) \quad (3.17)$$

The free excitations created by C and D are known as spin waves and correspond to the infinitesimal deviations of the spins away from the Néel state. The dispersion relation for spin waves is

$$E(k) = 2JS(1 - \gamma_k^2)^{\frac{1}{2}} \quad (3.18)$$

that vanishes linearly at $k = 0$

$$E(k) \approx v|k| \quad (3.19)$$

where the effective “light velocity” is

$$v = 2JS \quad (3.20)$$

In a field theoretical language spin waves are gapless due to the Goldstone theorem. In fact there are two Goldstone modes C and D corresponding to the breaking of $SO(3)$ down to the $SO(2)$ rotations about the z axis. Low energy long-wavelength spin waves correspond to configurations where all regions are locally in some Néel ground state but the direction of the sublattice magnetization vector makes long-wavelength rotations. The two different modes C and D have spin $S^3 = \pm 1$ and correspond to raising S^3 on one sublattice or lowering it on the other.

Now one can compute the reduction in the sublattice magnetization due to quantum fluctuations

$$\langle S^3(x) \rangle = S - \int \frac{dk}{2\pi} \frac{1}{2} \left[\frac{1}{\sqrt{1 - \gamma_k^2}} - 1 \right] \quad (3.21)$$

Quantum spins like quantum harmonic oscillators have zero point motion. In one dimension one finds that Eq.(3.21) is divergent for small wavelengths

$$\Delta \langle S^3(x) \rangle = \langle S^3(x) \rangle - S = - \int \frac{dk}{2\pi} \frac{1}{2k} = -\infty \quad (3.22)$$

Eq.(3.22) indicates that the Néel state is destabilized by quantum fluctuations in one dimension even in the large S limit. The divergence of Eq.(3.22) is in agreement with the Coleman and Mermin-Wagner theorems [43] preventing the spontaneous breaking of continuous symmetries in (1+1)-dimensions due to infrared divergences connected with the Goldstone bosons.

3.1.1 Spin-spin correlators in spin wave theory

We have seen that the Néel state is destabilized by quantum fluctuations in D=1 even in the classical limit $S \rightarrow \infty$. The spin-spin correlation function to next order in $\frac{1}{S}$ is

$$\langle \vec{S}_0 \cdot \vec{S}_r \rangle \approx \pm S^2 \left[1 - \frac{1}{\pi S} \log \frac{r}{a} + O\left(\frac{1}{S^2}\right) \right] \quad (3.23)$$

Eq.(3.23) indicates that at large S the system is ordered at small distances while the disorder occurs at exponentially large scales

$$\xi \simeq e^{\pi S} \quad (3.24)$$

More precisely, one should distinguish the r odd and even cases. To see this, it is instructive to compute the finite distance correlators from spin wave theory. If r belongs to the odd sublattice, the spin-spin correlator reads

$$\begin{aligned} \langle \vec{S}_0 \cdot \vec{S}_r \rangle &= -S^2 \left[1 + \frac{1}{S} \left(1 - \frac{1}{N} \sum_k \frac{1 - \cos rk \cos k}{|\sin k|} \right) + O(S^{-2}) \right] \\ &= -S^2 \left[1 + \frac{1}{S} (1 - I_o(r)) + O(S^{-2}) \right] \end{aligned} \quad (3.25)$$

while if r belongs to the even sublattice one has

$$\begin{aligned} \langle \vec{S}_0 \cdot \vec{S}_r \rangle &= -S^2 \left[1 + \frac{1}{S} \left(1 - \frac{1}{N} \sum_k \frac{1 - \cos rk}{|\sin k|} \right) + O(S^{-2}) \right] \\ &= -S^2 \left[1 + \frac{1}{S} (1 - I_e(r)) + O(S^{-2}) \right] \end{aligned} \quad (3.26)$$

In Eqs.(3.25,3.26)

$$I_o(r) = \frac{1}{2\pi} \int_0^{2\pi} \frac{1 - \cos rk \cos k}{|\sin k|} dk \quad (3.27)$$

$$I_e(r) = \frac{1}{2\pi} \int_0^{2\pi} \frac{1 - \cos rk}{|\sin k|} dk \quad (3.28)$$

and up to the distance $r = 10$ one gets the values given in table (3.1) The spin-spin correlator

Table 3.1: $I_o(r)$ and $I_e(r)$

$I_o(r)$	$I_e(r)$
$I_o(1) = \frac{2}{\pi}$	$I_e(2) = \frac{4}{\pi}$
$I_o(3) = \frac{14}{3\pi}$	$I_e(4) = \frac{16}{3\pi}$
$I_o(5) = \frac{86}{15\pi}$	$I_e(6) = \frac{92}{15\pi}$
$I_o(7) = \frac{674}{105\pi}$	$I_e(8) = \frac{704}{105\pi}$
$I_o(9) = \frac{2182}{315\pi}$	$I_e(10) = \frac{2252}{315\pi}$

$G(r) = \langle \vec{S}_0 \cdot \vec{S}_r \rangle$ are given in table (3.2). It is interesting to compare table (3.2) with the numerical correlators given in table (3.7). While it is quite impressive the agreement of $G(r)$ for $r = 1, 2$ with the exact results, increasing the distance r the agreement becomes very

Table 3.2: Spin-wave theory spin-spin correlation functions

r	$G(r)$
1	-0.4317
2	0.1817
3	-0.0073
4	0.0756
5	0.1625
6	0.0119
7	0.2716
8	-0.0335
9	0.3525
10	-0.0689

poor already for $r = 3$, and starts to have no meaning at $r = 5$, where one gets even a wrong sign, opposite to the right answer. I think that this is an interesting lesson that one can learn from the failure of spin-wave theory. While, in studying short distance correlations ($r = 1, 2$) one gets very good results in the spin-wave theory, quantum disorder prevails for larger distances and so a Néel state approximation cannot pick up the main features of the system. The expected scale for the appearance of quantum disorder for $S = \frac{1}{2}$ is, from Eq.(3.24), $\xi = e^{\frac{\pi}{2}} \approx 5$.

3.2 The Haldane-Shastry spin model

The Haldane-Shastry spin model [41] is a generalized spin-1/2 Heisenberg Hamiltonian with long range inverse-square exchange interaction between spins. The inverse-square interaction makes the model more easy to solve than the original Heisenberg model and the description of the excitation spectrum in terms of spin-1/2 spinons is particularly easy to understand. The model can be considered as a discretized version of the Calogero-Sutherland model [44] describing a one-dimensional Bose gas with inverse square repulsions.

This paragraph shortly reviews the approach to the Haldane-Shastry model given by Laughlin et al. in [34]. My purpose is to stress some feature of one-dimensional antiferromagnetic chains that are more intuitive to understand in this model than in the Heisenberg model. The Haldane-Shastry Hamiltonian describes N spin-1/2 particles distributed equidistantly on a circle, coupled with an exchange interaction that decays proportional to the inverse square of the chord between the spins

$$H_{HS} = J \left(\frac{2\pi}{N} \right)^2 \sum_{\alpha < \beta = 1}^N \frac{\vec{S}_\alpha \cdot \vec{S}_\beta}{|z_\alpha - z_\beta|^2} \tag{3.29}$$

where each site is parametrized by the roots of the unity

$$z_\alpha^N - 1 = 0 \tag{3.30}$$

and \vec{S}_α is the spin operator on site α . The Hamiltonian Eq.(3.29) is invariant, due to periodic boundary conditions, under translations generated by \hat{T}

$$\hat{T} : \vec{S}_\alpha \longrightarrow \vec{S}_{\alpha+1} \tag{3.31}$$

and under global rotations in the spin space generated by

$$\vec{S} = \sum_{x=1}^N \vec{S}_x \quad . \quad (3.32)$$

Of course,

$$[\vec{S}, \hat{T}] = 0 \quad . \quad (3.33)$$

Moreover the Hamiltonian Eq.(3.29) is invariant under the special internal Yangian symmetry [45]

$$[H_{HS}, \vec{\Lambda}] = 0 \quad (3.34)$$

where

$$\vec{\Lambda} = \frac{i}{2} \sum_{\alpha \neq \beta} \left(\frac{z_\alpha + z_\beta}{z_\alpha - z_\beta} \right) (\vec{S}_\alpha \wedge \vec{S}_\beta) \quad (3.35)$$

The ground state of this model has the same functional form as the fractional quantum Hall ground state [46, 47]; it is a spin singlet in the case of N even and exhibits quantum disorder: *i.e.* it has the same relation to the antiferromagnetically ordered Néel state that a quantum liquid has to a conventional crystal.

In the hard-core bosons picture, the spin \uparrow on a site corresponds to the presence of a boson, the spin \downarrow to the absence of a boson. The ground state wavefunction is the complex coefficient assigned to each configuration with $N/2$ bosons. The ground state of the Hamiltonian (3.29) reads

$$\psi_{g.s.}(z_1, \dots, z_{\frac{N}{2}}) = \prod_{\alpha < \beta}^{\frac{N}{2}} (z_\alpha - z_\beta)^2 \prod_{\alpha=1}^{\frac{N}{2}} z_\alpha \quad (3.36)$$

and its energy is

$$E_{g.s.} = -J \left(\frac{\pi^2}{24} \right) \left(N + \frac{5}{N} \right) \quad (3.37)$$

where $z_1, \dots, z_{\frac{N}{2}}$ denote the localization of the $N/2$ bosons. It is easy to verify that the ground state wave function Eq.(3.36) is real, and it is translationally invariant with momentum 0 or π for $N/2$ even or odd. In fact the translated expression of one site of $\psi_{g.s.}$ is obtained by multiplying each of its arguments by $z = e^{i\frac{2\pi}{N}}$ and due to the fact $\psi_{g.s.}$ is an homogeneous polynomial of degree $(N/2)^2$ one gets

$$\psi_{g.s.}(z_1 z, \dots, z_{\frac{N}{2}} z) = e^{i\frac{N\pi}{2}} \psi_{g.s.}(z_1, \dots, z_{\frac{N}{2}}) \quad (3.38)$$

One can immediately verify that $\psi_{g.s.}$ is a spin singlet. Due to the fact that z_j is constrained to take $N/2$ possible values, *i.e.* that there are $N/2$ spins up (and $N/2$ down), $S^z \psi_{g.s.} = 0$. Moreover it is the lowest weight state

$$S^- \psi_{g.s.} = 0 \quad (3.39)$$

It is worth stressing that it is very peculiar of this model the possibility to write down in a closed form, so simple to read, the exact quantum ground state (3.36). In general, it is very difficult to write down in an easy compact form the ground state of a quantum antiferromagnetic chain. In the case of the Heisenberg antiferromagnet this is not possible for a general N .

$\psi_{g.s.}$ exhibits quantum disorder, *i.e.* the spin-spin correlation function

$$\langle \vec{S}_\alpha \cdot \vec{S}_\beta \rangle = \frac{\langle \psi_{g.s.} | \vec{S}_\alpha \cdot \vec{S}_\beta | \psi_{g.s.} \rangle}{\langle \psi_{g.s.} | \psi_{g.s.} \rangle} \quad (3.40)$$

goes to zero as $|z_\alpha - z_\beta| \rightarrow \infty$ so that it is a spin-liquid state. However the fall-off of Eq.(3.40) is slow and this is typical of half-integer spin systems that exhibit gapless excitations [48]. Different is the case of integer spin systems that are strongly-disordered spin liquids with exponential decay of correlations on a length scale ξ and have an energy gap for excitations $\Delta = \frac{\hbar v}{\xi}$, where v is the spin-wave velocity of a nearby ordered state.

The ground state Eq.(3.36) is not degenerate, but the state

$$\psi'_{g.s.}(z_1, \dots, z_{\frac{N}{2}}) = \prod_{\alpha < \beta = 1}^{\frac{N}{2}} (z_\alpha - z_\beta)^2 \left[1 - \prod_{\alpha}^{\frac{N}{2}} z_\alpha^2 \right] \quad (3.41)$$

is almost degenerate with $\psi_{g.s.}$.

$$H_{HS}|\psi'_{g.s.}\rangle = -J\left(\frac{\pi^2}{24}\right)\left(N - \frac{7}{N}\right)|\psi'_{g.s.}\rangle \quad (3.42)$$

and it has momentum π greater than $\psi_{g.s.}$. The state $\psi'_{g.s.}$ can be thought as $\psi_{g.s.}$ plus a pair of spinons excited out in a singlet state of momentum π . When the number of sites N is odd, the ground state cannot be a spin singlet, but it is a spin-1/2 state, *i.e.* it describes a spinon of momentum $\pm\pi/2$. The wave function

$$\psi_\alpha(z_1, \dots, z_{\frac{N-1}{2}}) = \prod_{\gamma=1}^{\frac{N-1}{2}} (z_\alpha - z_\gamma) \prod_{\gamma < \delta = 1}^{\frac{N-1}{2}} (z_\gamma - z_\delta)^2 \prod_{\gamma=1}^{\frac{N-1}{2}} z_\gamma \quad (3.43)$$

describes a \downarrow spinon at site α and it can be interpreted as a \downarrow spin on site α surrounded by an otherwise featureless singlet sea. The linear combination of the states given by

$$\psi_m(z_1, \dots, z_M) = \sum_{\alpha=1}^N (z_\alpha^*)^m \psi_\alpha(z_1, \dots, z_M) \quad (3.44)$$

with $0 \leq m \leq \frac{N-1}{2}$, is an exact eigenstate of H_{HS} with eigenvalue

$$H_{HS}|\psi_m\rangle = \left\{ -J\left(\frac{\pi^2}{24}\right)\left(n - \frac{1}{N}\right) + \frac{J}{2}\left(\frac{2\pi}{N}\right)^2 m\left(\frac{N-1}{2} - m\right) \right\} |\psi_m\rangle \quad (3.45)$$

The state $|\psi_m\rangle$ represents a \downarrow spinon travelling with crystal momentum

$$q = \frac{\pi}{2}N - \frac{2\pi}{N}\left(m + \frac{1}{4}\right) \pmod{2\pi} \quad (3.46)$$

due to the definition

$$\psi_m(z_1 z, \dots, z_M z) = e^{iq} \psi(z_1, \dots, z_M) \quad (3.47)$$

Rewriting Eq.(3.45) as

$$H_{HS}|\psi_m\rangle = \left\{ -J\left(\frac{\pi^2}{24}\right)\left(N + \frac{5}{N} - \frac{3}{N^2}\right) + E_q \right\} |\psi_m\rangle \quad (3.48)$$

one obtains the dispersion relation

$$E_q = \frac{J}{2} \left[\left(\frac{\pi}{2}\right)^2 - q^2 \right] \pmod{\pi} \quad (3.49)$$

The allowed momenta for the spinon are only half of the Brillouin zone (the inner $-\frac{\pi}{2} \leq q \leq \frac{\pi}{2}$ or the outer part $-\pi \leq q \leq -\frac{\pi}{2}$ and $\frac{\pi}{2} \leq q \leq \pi$, depending on whether $N-1$ is divisible by 4). The spinon dispersion relation is linear in q close to $\pm\frac{\pi}{2}$ with velocity

$$v_{spinon} = \frac{\pi}{2} \frac{J}{\hbar} \frac{2\pi}{N} \quad (3.50)$$

Spinons are “relativistic” excitations travelling with velocity v_{spinon} and they exist because quantum disorder exists whenever the total spin in the unit cell is half integral. A spin liquid singlet ground state can exist only if the total number of spins is even. If N is odd the total spin cannot be less than $1/2$. Since in the thermodynamic $N \rightarrow \infty$ there can be no difference between N even and odd, the spin system must have already had a neutral spin- $\frac{1}{2}$ spinon excitation at the beginning, *i.e.* Eq.(3.47) describes a spinon. In the case of N odd, the ground state is 4-times degenerate and is given by Eq.(3.47) for $m = 0$ and $\frac{N-1}{2}$ and their \uparrow counterparts. Even if more than one spinon is present in the chain, they keep their identity. In the thermodynamic limit spinons are non-interacting excitations, some kind of quantum kink-excitations. Spinons are neither bosons nor fermions but they are semions, *i.e.* particles obeying $1/2$ statistics. The two-spinon wave function is given by

$$\psi_{AB} = \prod_j (z_j - z_A)(z_j - z_B) \prod_{j < k} (z_j - z_k)^2 \quad (3.51)$$

where z_A and z_B are not necessarily lattice sites, and it has the property

$$\psi_{AB}^*(z_1, \dots, z_{\frac{N}{2}-1}) = (z_A z_B)^{1-\frac{N}{2}} \psi_{AB}(z_1, \dots, z_{\frac{N}{2}-1}) \quad (3.52)$$

The phase for adiabatic motion of spinon A in the presence of spinon B, called Berry phase, is

$$\frac{1}{2 \langle \psi_{AB} | \psi_{AB} \rangle} \left[\langle \psi_{AB} | z_A \frac{\partial}{\partial z_A} \psi_{AB} \rangle + \langle z_A \frac{\partial}{\partial z_A} \psi_{AB} | \psi_{AB} \rangle \right] = \frac{1}{2} \left(1 - \frac{N}{2} \right) \quad (3.53)$$

By moving spinon A around the loop to exchange it with B, one gets the phase

$$\Delta \Phi_S = \oint \frac{1}{2} \left(1 - \frac{N}{2} \right) \frac{dz_\alpha}{z_\alpha} = \pm \frac{\pi}{2} \pmod{2\pi} \quad (3.54)$$

One would get in the case of bosons or fermions

$$\begin{aligned} \Delta \Phi_B &= 0 \\ \Delta \Phi_F &= \pi \end{aligned} \quad (3.55)$$

Fractional statistics has nothing to do with the symmetry properties of ψ_{AB} under the exchange of A with B, but it has to do with state-counting.

Last I want to say that the the Yangian symmetry operator Eq.(3.35) represents a scaled spin current. Acting on the propagating spinon Eq.(3.44) one gets

$$\Lambda^z |\psi_m \rangle = \left\{ \frac{N-1}{4} - m \right\} |\psi_m \rangle \quad (3.56)$$

So the eigenvalue of Λ^z is proportional to the spinon velocity

$$\frac{dE_q}{dq} = \frac{2\pi J}{N} \left\{ \frac{N-1}{4} - m \right\} \quad (3.57)$$

The action of Λ^z on a multispinon state is the sum of all the spinon velocities.

I analysed the model at half filling, *i.e.* when every site is occupied by one particle. In the presence of doping the possible configurations on each site are spin up, spin down and empty site. When the filling is less than half, new quantum excitations called holons are created. Holons are charged quantum excitations of spin 0. New phenomena appear in presence of holons and it is necessary to add to H_{HS} a term describing the holon dynamics. Since my thesis is concerned with the relationships between spin chains and field theories, the half filling constraint is required. The reader interested in knowing more about holons can look up Ref. [49].

3.3 The Bethe Ansatz solution of the antiferromagnetic Heisenberg chain

In this paragraph the Bethe ansatz solution of the antiferromagnetic Heisenberg chain [30] is discussed in detail. Moreover I shall compare the exact solution given by L.D. Faddeev and L.A. Takhtadzhyan in [30] with a study of finite size chains of 4, 6 and 8 sites. I show that already these very small finite systems exhibit spectra that match very well with the thermodynamic limit solution. I suggest to the reader interested in the subject the references [34].

The Bethe ansatz is a method of solution of a number of quantum field theory and statistical mechanics models in two space-time dimensions. This method was first suggested by Bethe [36] in 1931 from which takes its name. Historically one can call this formulation the Coordinate Bethe ansatz to distinguish it from the modern formulation known as Algebraic Bethe ansatz. The eigenfunctions of some (1+1)-dimensional Hamiltonians can be constructed imposing periodic boundary conditions which lead to a system of equations for the permitted values of momenta. These are known as the Bethe equations which are also useful in the thermodynamic limit. The energy of the ground state may be calculated in this limit and its excitations can be investigated.

I review here the method applied to the study of the antiferromagnetic Heisenberg chain [30]. In particular it is shown that there is only one excitation with spin-1/2 which is a kink: physical states have only an even number of kinks, therefore they always have an integer spin. The one dimensional isotropic Heisenberg model describes a system of N interacting spin- $\frac{1}{2}$ particles. The Hamiltonian of the model is

$$H_J = J \sum_{x=1}^N (\vec{S}_x \cdot \vec{S}_{x+1} - \frac{1}{4}) \quad . \quad (3.58)$$

where $J > 0$ ($J < 0$ would describe a ferromagnet) and the spin operators have the following form

$$\vec{S}_x = 1_1 \otimes 1_2 \otimes \dots \otimes \frac{\vec{\sigma}_x}{2} \otimes \dots \otimes 1_N \quad . \quad (3.59)$$

They act nontrivially only on the Hilbert space of the x^{th} site. Periodic boundary conditions are assumed.

The Hamiltonian (3.58) is invariant under global rotations in the spin space, generated by

$$\vec{S} = \sum_{x=1}^N \vec{S}_x \quad . \quad (3.60)$$

Due to the periodic boundary conditions, under translations generated by the operator \hat{T} ,

$$\hat{T} : \vec{S}_x \longrightarrow \vec{S}_{x-1} \quad (3.61)$$

the Hamiltonian is invariant and $[\vec{S}, \hat{T}] = 0$.

In order to diagonalize H_J it is convenient to use an eigenfunction basis of operators commuting with H_J , so obviously \vec{S}^2 , S^z and also \hat{T} . Let us sketch the Coordinate Bethe ansatz technique. One has to introduce the “false vacuum”

$$|\Omega \rangle = \prod_{x=1}^N |\uparrow\rangle_x \quad (3.62)$$

with

$$S_x^+ |\uparrow\rangle_x = 0 \quad (3.63)$$

$$S_x^3 |\uparrow\rangle_x = \frac{1}{2} |\uparrow\rangle_x \quad (3.64)$$

where

$$S_x^\pm = S_x^1 \pm S_x^2 \quad (3.65)$$

$$S^3 |\Omega\rangle = \frac{N}{2} |\Omega\rangle \quad (3.66)$$

$$\tilde{S}^2 |\Omega\rangle = \frac{N}{2} \left(\frac{N}{2} + 1 \right) |\Omega\rangle \quad (3.67)$$

$$\hat{T} |\Omega\rangle = |\Omega\rangle \quad (3.68)$$

All the other basis vectors have $S^3 < \frac{N}{2}$ and one can get them by properly acting on $|\Omega\rangle$ with the lowering operators S_x^- . Let us start from the generic state with $S^3 = \frac{N}{2} - 1$, with $N - 1$ spins up and $M = 1$ spin down

$$|M = 1\rangle = \sum_{x=1}^N \phi_x |x\rangle \quad \text{with} \quad |x\rangle = S_x^- |\Omega\rangle \quad (3.69)$$

where the coefficients ϕ_x must be such that $|M = 1\rangle$ is a translationally and rotationally invariant state

$$\hat{T} |M = 1\rangle = \sum_{x=1}^N \phi_x |x-1\rangle = \sum_{x=1}^N \phi_{x+1} |x\rangle = \mu \sum_{x=1}^N \phi_x |x\rangle \quad (3.70)$$

and from Eq.(3.70) one gets

$$\phi_{x+1} = \mu \phi_x \quad (3.71)$$

$$\phi_{x+1} = \mu^x \phi_1 \quad x \neq N \quad (3.72)$$

$$\phi_1 = \mu \phi_N = \mu^N \phi_1 \longrightarrow \mu^N = 1 \quad (3.73)$$

Setting $\phi_1 = 1$ one has $\phi_x = \mu^{x-1}$. There are N possible values for ϕ_x , corresponding to the N roots of the unity. One of these roots corresponds to a state with $S = \frac{N}{2}$

$$\sum_{x=1}^N |x\rangle = S^- |\Omega\rangle \longrightarrow \mu = 1 \quad (3.74)$$

while the other $N - 1$ roots have $S = \frac{N}{2} - 1$.

The generic case with M spins down is more complicated. Let us consider the case $M = 2$ to understand what happens

$$|M = 2\rangle = \sum_{x_1 < x_2 = 1}^N \phi(x_1, x_2) |x_1, x_2\rangle \quad \text{with} \quad |x_1, x_2\rangle = S_{x_1}^- S_{x_2}^- |\Omega\rangle \quad (3.75)$$

By requiring the translational invariance of the state $|M = 2\rangle$ one has

$$\hat{T} |M = 2\rangle = T |M = 2\rangle \quad (3.76)$$

and for $x_2 < N$ one has

$$\phi(x_1 + 1, x_2 + 1) = T \phi(x_1, x_2) \quad (3.77)$$

that would easily give

$$\phi(x_1, x_2) = \mu_1^{x_1-1} \mu_2^{x_2-1} \quad , \quad T = \mu_1 \mu_2 \quad (3.78)$$

but due to the periodic boundary conditions one has to find coefficients $\phi(x_1, x_2)$ that satisfy not only Eq.(3.77) but also

$$\phi(1, x+1) = T\phi(x, N) \quad . \quad (3.79)$$

Eq.(3.79) is no more satisfied by (3.78). Bethe proposed the following ansatz for the coefficients $\phi(x_1, x_2)$

$$\phi(x_1, x_2) = A_{1,2}\mu_1^{x_1-1}\mu_2^{x_2-1} + A_{2,1}\mu_2^{x_1-1}\mu_1^{x_2-1} \quad . \quad (3.80)$$

Eq.(3.77,3.79) are satisfied if the following equations hold

$$A_{12} = A_{21}\mu_1^N \quad (3.81)$$

$$A_{21} = A_{12}\mu_2^N \quad . \quad (3.82)$$

By imposing to $|M=2\rangle$ to be an highest weight state

$$S^+|M=2\rangle = 0 \quad (3.83)$$

taking into account Eq.(3.81,3.82) and introducing the following change of variables

$$\mu_\alpha = \frac{\lambda_\alpha - \frac{i}{2}}{\lambda_\alpha + \frac{i}{2}} \quad (3.84)$$

one gets the so called Bethe ansatz equations

$$\left(\frac{\lambda_\alpha - \frac{i}{2}}{\lambda_\alpha + \frac{i}{2}}\right)^N = - \prod_{\beta=1}^2 \frac{\lambda_\alpha - \lambda_\beta - i}{\lambda_\alpha - \lambda_\beta + i} \quad . \quad (3.85)$$

In the general case of M spins flipped one gets

$$\left(\frac{\lambda_\alpha - \frac{i}{2}}{\lambda_\alpha + \frac{i}{2}}\right)^N = - \prod_{\beta=1}^M \frac{\lambda_\alpha - \lambda_\beta - i}{\lambda_\alpha - \lambda_\beta + i} \quad . \quad (3.86)$$

The energy and the momentum of a given state with M spins down can be expressed in terms of the parameters λ_α

$$E_M = \sum_{\alpha=1}^M \epsilon_\alpha = -\frac{J}{2} \sum_{\alpha=1}^M \frac{1}{\lambda_\alpha^2 + \frac{1}{4}} \quad (3.87)$$

$$P_M = i \ln T = \sum_{\alpha=1}^M p_\alpha = i \sum_{\alpha=1}^M \ln \frac{\lambda_\alpha - \frac{i}{2}}{\lambda_\alpha + \frac{i}{2}} \quad . \quad (3.88)$$

Energy and momentum are thus additive as if there were M independent particles and the λ_α must satisfy the Bethe ansatz equations (3.86) in order for E_M and P_M to be eigenvalues of the Hamiltonian and momentum operators.

The solution of the antiferromagnetic Heisenberg chain is reduced to the solution of the system of the M algebraic equations (3.86). This, in general, is not an easy task. It can be shown [30], however, that, in the thermodynamic limit $N \rightarrow \infty$, the complex parameters λ have the form

$$\lambda_l = \lambda_{j,L} + il \quad , \quad l = -L, -L+1, \dots, L-1, L; \quad (3.89)$$

where L is a non-negative integer or half-integer, $\lambda_{j,L}$ is the real part of the solution of (3.86) and I shall define shortly the set of allowed values for the integer index j . The λ 's that, for a given $\lambda_{j,L}$, are obtained varying l between $[-L, L]$ by integer steps, form a string of length $2L+1$, see fig.(3.1). This arrangement of λ 's in the complex plane is called the "string hypothesis" [30]. In the following I shall verify that, even on finite size systems, the "string hypothesis" is very well fulfilled.

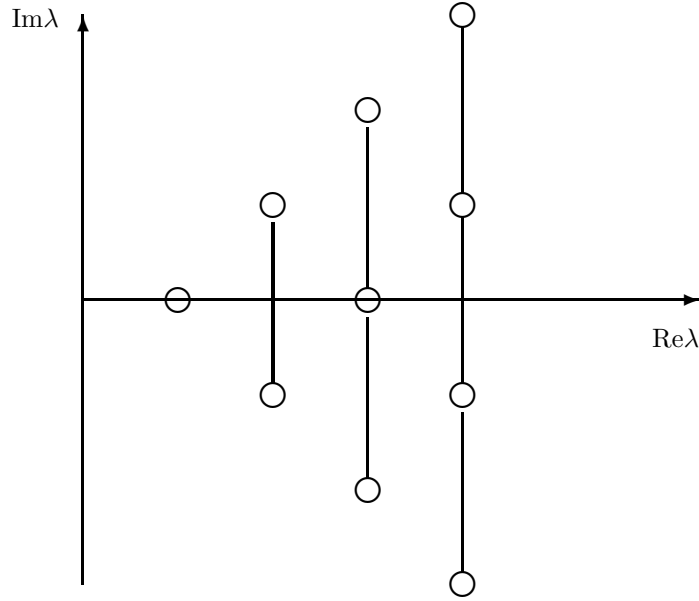


Figure 3.1: Strings for $L = 0, \frac{1}{2}, 1, \frac{3}{2}$

In a generic Bethe state with M spins down, there are M solutions to (3.86), which can be grouped according to the length of their strings. Let us denote by ν_L the number of strings of length $2L + 1$, $L = 0, \frac{1}{2}, \dots$; strings of the same length are obtained by changing the real parts, $\lambda_{j,L}$, of the λ 's in (3.89); as a consequence $j = 1, \dots, \nu_L$. If one denotes the total number of strings by q one has

$$q = \sum_L \nu_L \quad , \quad M = \sum_L (2L + 1)\nu_L \quad . \quad (3.90)$$

The set of integers $(M, q, \{\nu_L\})$ constrained by (3.90), characterizes Bethe states up to the fixing of the q numbers $\lambda_{j,L}$; this set is called the ‘‘configuration’’. Varying M , q and ν_L , one is able to construct all the 2^N eigenstates of an Heisenberg antiferromagnetic chain of N sites [30]. The energy and momentum of the Bethe's state, corresponding to a given configuration – within exponential accuracy as $N \rightarrow \infty$ – consist of q summands representing the energy and momentum of separate strings. For the parameters $\lambda_{j,L}$ of the given configuration, taking the logarithm of (3.86) the following system of equations is obtained in the thermodynamic limit

$$2N \arctan \frac{\lambda_{j,L_1}}{L_1 + \frac{1}{2}} = 2\pi Q_{j,L_1} + \sum_{L_2} \sum_{k=1}^{\nu_{L_2}} \Phi_{L_1 L_2}(\lambda_{j,L_1} - \lambda_{k,L_2}) \quad , \quad (3.91)$$

where

$$\Phi_{L_1 L_2}(\lambda) = 2 \sum_{L=|L_1-L_2| \neq 0}^{L_1+L_2} \left(\arctan \frac{\lambda}{L} + \arctan \frac{\lambda}{L+1} \right) \quad . \quad (3.92)$$

Integer and half integer numbers $Q_{j,L}$ parametrize the branches of the arctangents and, consequently, the possible solutions of the system of Eqs.(3.91). In ref.[30] it was shown that the $Q_{j,L}$ are limited as

$$- Q_L^{max} \leq Q_{1,L} < Q_{2,L} < \dots < Q_{\nu_L,L} \leq Q_L^{max} \quad (3.93)$$

with Q_L^{max} given by

$$Q_L^{max} = \frac{N}{2} - \sum_{L'} J(L, L') \nu_{L'} - \frac{1}{2} \quad (3.94)$$

and

$$J(L_1, L_2) = \begin{cases} 2\min(L_1, L_2) + 1 & \text{if } L_1 \neq L_2 \\ 2L_1 + \frac{1}{2} & \text{if } L_1 = L_2 \end{cases} . \quad (3.95)$$

The admissible values for the numbers $Q_{j,L}$ are called the ‘‘vacancies’’ and their number for every L is denoted by P_L

$$P_L = 2Q_L^{max} + 1 \quad . \quad (3.96)$$

The main hypothesis formulated in [30] is that to every admissible collection of $Q_{j,L}$ there corresponds a unique solution of the system of equations (3.91). The solution always provides, in a multiplet, the state with the highest value of the third spin component S^3 .

Let us now consider some simple example. The simplest configuration has only strings of length 1, *i.e.* all the λ 's are real. The singlet associated to this configuration

$$M = q = \nu_0 = \frac{N}{2} \quad , \quad \nu_L = 0 \quad , \quad L > 0 \quad , \quad (3.97)$$

is the ground state. The vacancies of the strings of length 1, *i.e.* the admissible values of $Q_{j,0}$, due to eqs.(3.93,3.94,3.95), belong to the segment

$$-\frac{N}{4} + \frac{1}{2} \leq Q_{j,0} \leq \frac{N}{4} - \frac{1}{2} \quad . \quad (3.98)$$

Therefore they are $N/2$. All these vacancies must then be used to find the $N/2$ strings of length 1. As a consequence this state is uniquely specified and no degeneracy is possible.

Next I consider the configuration that provides a singlet with 1 string of length 2 and all the others of length 1:

$$M = \frac{N}{2} \quad , \quad q = \frac{N}{2} - 1 \quad , \quad \nu_0 = \frac{N}{2} - 2 \quad , \quad \nu_{\frac{1}{2}} = 1 \quad , \quad \nu_L = 0 \quad , \quad L > \frac{1}{2} \quad . \quad (3.99)$$

For the strings of length 1 the number of vacancies is again $N/2$; for the string of length 2 there is one vacancy and the only admissible $Q_{j,1}$ equals 0. Thus, since the number of strings of length 1 is $\nu_0 = \frac{N}{2} - 2$, there are two vacancies for which Eqs.(3.91) have no solution; they are called ‘‘holes’’ and are denoted $Q_1^{(h)}$ and $Q_2^{(h)}$. This configuration is determined by two parameters: the positions of two ‘‘holes’’ which vary independently in the interval (3.98).

There is another state with only 2 holes: the triplet corresponding to the configuration

$$M = q = \nu_0 = \frac{N}{2} - 1 \quad , \quad \nu_L = 0 \quad , \quad L > 0 \quad (3.100)$$

The number of vacancies for the strings of length 1 equals $\frac{N}{2} + 1$, while $\nu_0 = \frac{N}{2} - 1$.

The excitations determined by the configurations (3.99,3.100) belong to the configuration class called in [30] $\mathcal{M}_{\mathcal{AF}}$. The class $\mathcal{M}_{\mathcal{AF}}$ is characterized as follows: the number of strings of length 1 in each configuration belonging to this class differs by a finite quantity from $N/2$, $\nu_0 = \frac{N}{2} - k_0$ where k_0 is a positive finite constant, so that the number of strings of length greater than 1 is finite. From (3.96) one then has

$$P_0 = \frac{N}{2} + k_0 - 2 \sum_{L>0} \nu_L \quad (3.101)$$

$$P_L = 2k_0 - 2 \sum_{L'>0} J(L, L') \nu_{L'} \quad , \quad L > 0 \quad (3.102)$$

so that

$$P_0 \geq \frac{N}{2} \quad , \quad P_L < 2k_0 \quad , \quad L > 0 \quad . \quad (3.103)$$

From (3.101) follows that the number of holes for the strings of length 1 is always even and equals 2 only for the singlet and the triplet excitations discussed above. One can imagine the class $\mathcal{M}_{\mathcal{AF}}$ as a “sea” of strings of length 1 with a finite number of strings of length greater than 1 immersed into it. It was proven in [30] that, in the thermodynamic limit, the states belonging to $\mathcal{M}_{\mathcal{AF}}$ have finite energy and momentum with respect to the antiferromagnetic vacuum, whereas each of the states which corresponds to a configuration not included in the class $\mathcal{M}_{\mathcal{AF}}$ has an infinite energy relative to the antiferromagnetic vacuum.

Let us now sketch the computation of the thermodynamic limit ground state energy. Eqs.(3.91) for the ground state have the form

$$\arctan 2\lambda_j = \frac{\pi Q_j}{N} + \frac{1}{N} \sum_{k=1}^{N/2} \arctan(\lambda_j - \lambda_k) \quad . \quad (3.104)$$

Taking the thermodynamic limit $N \rightarrow \infty$, one has

$$\frac{Q_j}{N} \rightarrow x \quad , \quad -\frac{1}{4} \leq x \leq \frac{1}{4} \quad , \quad \lambda_j \rightarrow \lambda(x) \quad , \quad (3.105)$$

and Eqs.(3.104) can be rewritten in the form

$$\arctan 2\lambda(x) = \pi x + \int_{-\frac{1}{4}}^{\frac{1}{4}} \arctan(\lambda(x) - \lambda(y)) dy \quad . \quad (3.106)$$

Upon introducing the density of the numbers $\lambda(x)$ in the interval $d\lambda$

$$\rho(\lambda) = \frac{1}{\frac{d\lambda(x)}{dx} \Big|_{x=\lambda(x)}} \quad (3.107)$$

and differentiating Eqs.(3.106), one gets

$$\rho(\lambda) = \frac{1}{2\pi} \int_{-\infty}^{\infty} \frac{e^{-\frac{1}{2}|\xi|}}{1 + e^{-|\xi|}} e^{-i\lambda|\xi|} d\xi = \frac{1}{2 \cosh \pi \lambda} \quad . \quad (3.108)$$

The density $\rho(\lambda)$ introduced in this way is normalized to 1/2. It is now easy to compute the energy and the momentum of the ground state

$$E_{g.s.} = \sum_{\alpha=1}^{\frac{N}{2}} \epsilon_{\alpha} = N \int_{-\infty}^{\infty} \epsilon(\lambda) \rho(\lambda) d\lambda = -\frac{JN}{4} \int_{-\infty}^{\infty} d\lambda \frac{1}{(\lambda^2 + \frac{1}{4}) \cosh \pi \lambda} = -JN \ln 2 \quad (3.109)$$

$$P_{g.s.} = \sum_{\alpha=1}^{\frac{N}{2}} p_{\alpha} = N \int_{-\infty}^{\infty} p(\lambda) \rho(\lambda) d\lambda = -\frac{N}{2} \int_{-\infty}^{\infty} d\lambda \frac{\pi}{\cosh \pi \lambda} = \frac{N}{2} \pi \pmod{2\pi} \quad . \quad (3.110)$$

According to Eq.(3.110), $P_{g.s.} = 0 \pmod{2\pi}$ for $\frac{N}{2}$ even, and $P_{g.s.} = \pi \pmod{2\pi}$ for $\frac{N}{2}$ odd. The ground state, as expected, is a singlet, in fact the spin S is given by

$$S = \frac{N}{2} - \sum_{\alpha=1}^{N/2} 1 = \frac{N}{2} - N \int_{-\infty}^{\infty} \rho(\lambda) d\lambda = 0 \quad . \quad (3.111)$$

Let us analyze the triplet described by Eq.(3.100); Eqs.(3.91) take the form

$$\arctan 2\lambda_j = \frac{\pi Q_j}{N} + \frac{1}{N} \sum_{k=1}^{\frac{N}{2}-1} \arctan(\lambda_j - \lambda_k) \quad (3.112)$$

where now the numbers Q_j lie in the segment $[-\frac{N}{4}, \frac{N}{4}]$ and have two holes, $Q_1^{(h)}$ and $Q_2^{(h)}$ with $Q_1^{(h)} < Q_2^{(h)}$. Taking the thermodynamic limit one gets

$$\frac{Q_1^{(h)}}{N} \rightarrow x_1 \quad , \quad \frac{Q_2^{(h)}}{N} \rightarrow x_2 \quad , \quad \frac{Q_j}{N} \rightarrow x + \frac{1}{N}(\theta(x - x_1) + \theta(x - x_2)) \quad (3.113)$$

where $\theta(x)$ is the Heaviside function. Eqs.(3.112) become

$$\arctan 2\lambda(x) = \pi x + \frac{\pi}{N}(\theta(x - x_1) + \theta(x - x_2)) + \int_{-\frac{1}{4}}^{\frac{1}{4}} \arctan(\lambda(x) - \lambda(y)) dy \quad . \quad (3.114)$$

Eq.(3.114) gives, for this triplet, the density of λ , $\rho(\lambda) = \frac{d\lambda}{dx}$

$$\rho_t(\lambda) = \rho(\lambda) + \frac{1}{N}(\sigma(\lambda - \lambda_1) - \sigma(\lambda - \lambda_2)) \quad (3.115)$$

where $\rho(\lambda)$ is given in Eq.(3.108) and

$$\sigma(\lambda) = -\frac{1}{2\pi} \int_{-\infty}^{\infty} \frac{1}{1 + e^{-|\xi|}} e^{-i\lambda\xi} d\xi \quad . \quad (3.116)$$

λ_1 and λ_2 are the parameters of the holes, $\lambda_i = \lambda(x_i)$, $i = 1, 2$. The energy and the momentum of this state measured from the ground state are now easily computed

$$\epsilon_T(\lambda_1, \lambda_2) = N \int_{-\infty}^{\infty} \epsilon(\lambda)(\rho_t(\lambda) - \rho(\lambda)) d\lambda = \epsilon(\lambda_1) + \epsilon(\lambda_2) \quad (3.117)$$

$$p_T(\lambda_1, \lambda_2) = N \int_{-\infty}^{\infty} p(\lambda)(\rho_t(\lambda) - \rho(\lambda)) d\lambda = p(\lambda_1) + p(\lambda_2) \quad (mod \quad 2\pi) \quad (3.118)$$

where

$$\epsilon(\lambda) = \int_{-\infty}^{\infty} \epsilon(\mu)\sigma(\lambda - \mu) d\mu = J \frac{\pi}{2 \cosh \pi\lambda} \quad (3.119)$$

$$p(\lambda) = \int_{-\infty}^{\infty} p(\mu)\sigma(\lambda - \mu) d\mu = \arctan \sinh \pi\lambda - \frac{\pi}{2}, \quad -\pi \leq p(\lambda) \leq 0 \quad . \quad (3.120)$$

From Eqs.(3.119,3.120) one gets

$$\epsilon = -\frac{J\pi}{2} \sin p \quad . \quad (3.121)$$

The momentum $p_T(\lambda_1, \lambda_2)$ varies over the interval $[0, 2\pi)$, when λ_1 and λ_2 run independently over the whole real axis. The spin of this state can be computed by the formula

$$S = - \int_{-\infty}^{\infty} (\sigma(\lambda - \lambda_1) + \sigma(\lambda - \lambda_2)) d\lambda = 1 \quad . \quad (3.122)$$

Let us finally analyze the singlet excitation characterized by the configuration (3.99). Denoting by λ_S the only number among the $\lambda_{j,1/2}$ which characterizes the string of length 2 and by λ_j the numbers $\lambda_{j,0}$ for the strings of length 1, Eqs.(3.91) read

$$\arctan 2\lambda_j = \frac{\pi Q_j}{N} + \frac{1}{N} \Phi(\lambda_j - \lambda_S) + \frac{1}{N} \sum_{k=1}^{\frac{N}{2}-2} \arctan(\lambda_j - \lambda_k) \quad (3.123)$$

$$\arctan \lambda_S = \frac{1}{N} \sum_{j=1}^{\frac{N}{2}-2} \Phi(\lambda_S - \lambda_j) \quad (3.124)$$

with

$$\Phi(\lambda) = \arctan 2\lambda + \arctan \frac{2}{3}\lambda \quad . \quad (3.125)$$

The $\frac{N}{2} - 2$ numbers Q_j vary in the segment $[-\frac{N}{4} + \frac{1}{2}, \frac{N}{4} - \frac{1}{2}]$; among them there are the two holes $Q_1^{(h)}$ and $Q_2^{(h)}$. Taking the thermodynamic limit one finds the density of λ 's for the singlet

$$\rho(\lambda_S) = \rho(\lambda) + \frac{1}{N}(\sigma(\lambda - \lambda_1) + \sigma(\lambda - \lambda_2) + \omega(\lambda - \lambda_S)) \quad (3.126)$$

where ρ and σ were given in Eqs.(3.108, 3.116) and where

$$\omega(\lambda) = -\frac{1}{2\pi} \int_{-\infty}^{\infty} e^{-\frac{1}{2}|\xi| - i\lambda\xi} d\xi = -\frac{2}{\pi(1 + 4\lambda^2)} \quad (3.127)$$

In [30] it was demonstrated that the string parameter λ_S is uniquely determined by the λ 's parametrizing the two holes

$$\lambda_S = \frac{\lambda_1^{(h)} + \lambda_2^{(h)}}{2} \quad (3.128)$$

In [30] it was also proved the remarkable fact that the string of length 2 does not contribute to the energy and momentum of the excitation, so that the singlet and the triplet have the same dispersion relations

$$\epsilon_S(\lambda_1, \lambda_2) = \epsilon_T(\lambda_1, \lambda_2) = \epsilon(\lambda_1) + \epsilon(\lambda_2) \quad (3.129)$$

$$p_S(\lambda_1, \lambda_2) = p_T(\lambda_1, \lambda_2) = p(\lambda_1) + p(\lambda_2) \pmod{2\pi} \quad (3.130)$$

The spin of this excitation is, of course, zero

$$S = -2 - \int_{-\infty}^{\infty} (2\sigma(\lambda) + \omega(\lambda)) d\lambda = 0 \quad (3.131)$$

The only difference between the state whose configuration is given in Eq.(3.100) and the state of Eq.(3.99) is the spin.

To summarize, the finite energy excitations of the antiferromagnetic Heisenberg chain are only those belonging to the class $\mathcal{M}_{\mathcal{AF}}$ and are described by scattering states of an even number of quasiparticles or kinks. The momentum p of these kinks runs over half the Brillouin zone $-\pi \leq p \leq 0$, the dispersion relation is $\epsilon(p) = \frac{J\pi}{2} \sin p$, Eq.(3.121), and the spin of a kink is $1/2$. The singlet and the triplet excitations described above are the only states composed of two kinks, the spins of the kinks being parallel for the triplet and antiparallel for the singlet. For vanishing total momentum all the states belonging to $\mathcal{M}_{\mathcal{AF}}$ have the same energy of the ground state so that they are gapless excitations. Since the eigenstates of H_J always contain an even number of kinks, the dispersion relation is determined by a set of two-parameters: the momenta of the even number of kinks whose scattering provides the excitation. There are no bound states of kinks.

3.3.1 Finite size antiferromagnetic Heisenberg chains

Let us now turn to the computation of the spectrum of finite size quantum antiferromagnetic chains by exact diagonalization. We shall see that already for very small chains, the spectrum is well described by the Bethe ansatz solution in the thermodynamic limit. Furthermore, an intuitive picture of the ground state and of the lowest lying excitations of the strongly coupled two-flavor lattice Schwinger model emerges, due to the mapping of the gauge model onto the spin chain – see chapter 5.

The states of an antiferromagnetic chain are classified according to the quantum numbers of spin, third spin component, energy and momentum $|S, S^3, E, p\rangle$. For a 4 site chain the momenta allowed for the states are: $0, \frac{\pi}{2}, \frac{3\pi}{2} \pmod{2\pi}$. The ground state is

$$|g.s.\rangle = |0, 0, -3J, 0\rangle = \frac{1}{\sqrt{12}} (2|\uparrow\uparrow\downarrow\downarrow\rangle + 2|\downarrow\downarrow\uparrow\uparrow\rangle - |\uparrow\uparrow\downarrow\downarrow\rangle - |\downarrow\downarrow\uparrow\uparrow\rangle - |\downarrow\uparrow\uparrow\downarrow\rangle - |\uparrow\downarrow\downarrow\uparrow\rangle) \quad (3.132)$$

This state is P -parity even. In fact, by the definition of P -parity given in Eq.(5.29), the P -parity inverted state (3.132) is obtained by reverting the order of the spins in each vector $|\dots\rangle$ appearing in (3.132), e.g. $|\downarrow\downarrow\uparrow\uparrow\rangle \xrightarrow{P} |\uparrow\uparrow\downarrow\downarrow\rangle$.

The λ 's associated to the ground state (solution of the Bethe ansatz equations (3.86)) are $\lambda_1 = -\frac{1}{2\sqrt{3}}$ and $\lambda_2 = \frac{1}{2\sqrt{3}}$. There is also an excited singlet

$$|0, 0, -J, \pi\rangle = \frac{1}{\sqrt{4}}(|\downarrow\downarrow\uparrow\uparrow\rangle - |\downarrow\uparrow\uparrow\downarrow\rangle - |\uparrow\downarrow\downarrow\uparrow\rangle + |\uparrow\uparrow\downarrow\downarrow\rangle) \quad (3.133)$$

It is P -even, so that it is a $S^P = 0^+$ excitation, with the same quantum numbers (the isospin is replaced by the spin) of the lowest lying singlet excitation of the strongly coupled Schwinger model discussed by Coleman [50]. The state (3.133) also coincides with the excited singlet described by the configuration (3.99). It has only two complex λ 's which arrange themselves in a string approximately of length 2, $\lambda_1 = -\lambda_2 = i\sqrt{\frac{\sqrt{481}-17}{8}}$ and there are two holes with $Q_1^{(h)} = -\frac{1}{2}$ and $Q_2^{(h)} = \frac{1}{2}$.

There are also three excited triplets, whose highest weight states are

$$|1, 1, -J, \frac{\pi}{2}\rangle = \frac{1}{\sqrt{4}}(|\downarrow\uparrow\uparrow\uparrow\rangle + i|\uparrow\downarrow\uparrow\uparrow\rangle - |\uparrow\uparrow\downarrow\uparrow\rangle - i|\uparrow\uparrow\downarrow\downarrow\rangle) \quad (3.134)$$

$$|1, 1, -2J, \pi\rangle = \frac{1}{\sqrt{4}}(|\downarrow\uparrow\uparrow\uparrow\rangle - |\uparrow\downarrow\uparrow\uparrow\rangle + |\uparrow\uparrow\downarrow\uparrow\rangle - |\uparrow\uparrow\downarrow\downarrow\rangle) \quad (3.135)$$

$$|1, 1, -J, \frac{3\pi}{2}\rangle = \frac{1}{\sqrt{4}}(|\downarrow\uparrow\uparrow\uparrow\rangle - i|\uparrow\downarrow\uparrow\uparrow\rangle - |\uparrow\uparrow\downarrow\uparrow\rangle + i|\uparrow\uparrow\downarrow\downarrow\rangle) \quad (3.136)$$

Among these, only the non-degenerate state with the lowest energy has a well defined P -parity (3.135). It is a $S^P = 1^-$ like the lowest lying triplet of the two-flavor strongly coupled Schwinger model. The degenerate states can be always combined to form a P -odd state.

We thus see that within the states in a given configuration there is always a representative state with well defined parity, the others are degenerate and can be used to construct state of well defined energy and parity. Moreover the parity of the representative states (with respect to the parity of the ground state) is the same of the one of the lowest-lying Schwinger model excitations in strong coupling.

All the triplets in (3.136) have one real λ and two holes; they can be associated with the family of triplets (3.100). In table (3.3) I summarize the triplet λ 's and $Q^{(h)}$'s. The

Table 3.3: Triplet internal quantum numbers

TRIPLET	λ	$Q_1^{(h)}$	$Q_2^{(h)}$
$ 1, 1, -J, \frac{\pi}{2}\rangle$	$\frac{1}{2}$	-1	0
$ 1, 1, -2J, \pi\rangle$	0	-1	1
$ 1, 1, -J, \frac{3\pi}{2}\rangle$	$-\frac{1}{2}$	0	1

spectrum exhibits also a quintet, whose highest weight state is

$$|2, 2, 0, 0\rangle = |\uparrow\uparrow\uparrow\uparrow\rangle \quad (3.137)$$

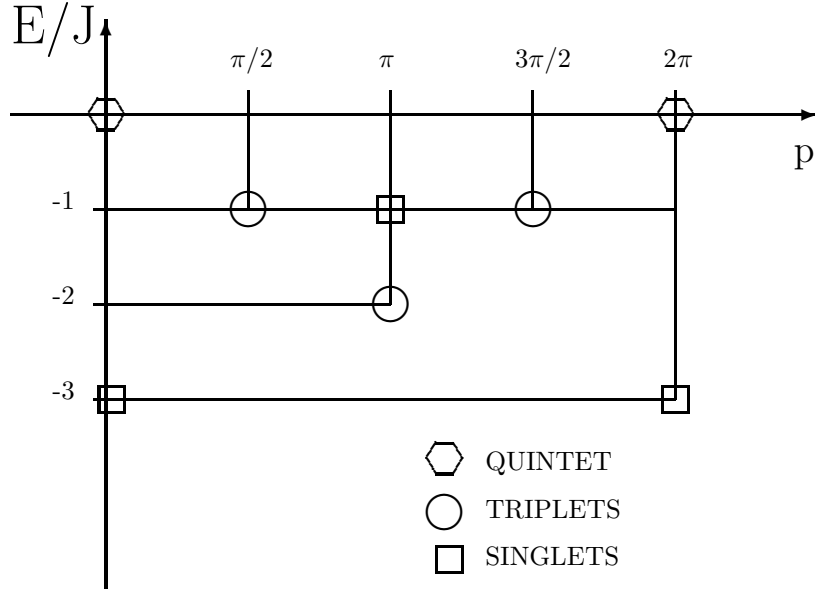


Figure 3.2: Four sites chain spectrum

I report in fig.(3.2) the spectrum of the 4 sites chain.

Let us analyze the spectrum of the 6 site antiferromagnetic chain. The momenta allowed for the states are now $0, \frac{\pi}{3}, \frac{2\pi}{3}, \pi, \frac{4\pi}{3}, \frac{5\pi}{3} \bmod 2\pi$. The ground state is

$$\begin{aligned}
|g.s. \rangle &= |0, 0, -\frac{J}{2}(5 + \sqrt{13}), \pi \rangle = \frac{1}{\sqrt{26 - 6\sqrt{13}}} \{ | \downarrow \downarrow \downarrow \uparrow \uparrow \uparrow \rangle - | \uparrow \uparrow \uparrow \downarrow \downarrow \downarrow \rangle \\
&+ \frac{1 - \sqrt{13}}{6} (| \uparrow \uparrow \downarrow \uparrow \downarrow \rangle - | \uparrow \downarrow \uparrow \downarrow \uparrow \rangle + | \downarrow \uparrow \downarrow \uparrow \uparrow \rangle - | \uparrow \downarrow \uparrow \uparrow \downarrow \rangle + | \downarrow \uparrow \uparrow \downarrow \uparrow \rangle - | \uparrow \uparrow \downarrow \uparrow \downarrow \rangle \\
&- | \downarrow \downarrow \uparrow \uparrow \uparrow \rangle + | \downarrow \uparrow \uparrow \uparrow \downarrow \rangle - | \uparrow \downarrow \uparrow \uparrow \downarrow \rangle + | \downarrow \uparrow \uparrow \uparrow \downarrow \rangle - | \uparrow \uparrow \downarrow \uparrow \downarrow \rangle + | \uparrow \downarrow \uparrow \uparrow \downarrow \rangle) \\
&+ \frac{4 - \sqrt{13}}{3} (| \uparrow \uparrow \downarrow \uparrow \downarrow \rangle - | \uparrow \uparrow \downarrow \downarrow \uparrow \rangle + | \uparrow \downarrow \downarrow \uparrow \uparrow \rangle - | \downarrow \downarrow \uparrow \uparrow \uparrow \rangle + | \downarrow \uparrow \uparrow \uparrow \downarrow \rangle - | \downarrow \uparrow \uparrow \downarrow \uparrow \rangle) \} \quad (3.138)
\end{aligned}$$

This state is odd under P -parity. The spectrum of the six sites chain is reported in fig.(3.3). There are 9 triplets in the spectrum. In [51] it was already pointed out that the number of lowest lying triplets for a finite system with N sites is $N(N+2)/8$, so for $N=6$ there are 6 lowest lying triplet states. In order to identify these 6 states among the 9 that are exhibited by the spectrum of fig.(3.3), it is necessary to compute their λ 's and their Q 's. In this way in fact, I can find out which are the triplets characterized by two holes and thus belonging to the triplet of type (3.100). In table (3.4) I report the internal quantum numbers of the lowest lying triplets. The $Q^{(h)}$'s vary in the segment $[-\frac{3}{2}, \frac{3}{2}]$. The highest weight state of the triplet of zero momentum and energy $-(J/2)(5 + \sqrt{5})$ reads

$$\begin{aligned}
|0, 0, -\frac{J}{2}(5 + \sqrt{5}), 0 \rangle &= \frac{1}{\sqrt{45 - 15\sqrt{5}}} \{ \frac{-3 + \sqrt{5}}{2} (| \downarrow \downarrow \uparrow \uparrow \uparrow \uparrow \rangle + | \downarrow \uparrow \uparrow \uparrow \uparrow \downarrow \rangle + | \uparrow \uparrow \uparrow \uparrow \downarrow \downarrow \rangle + | \uparrow \uparrow \uparrow \downarrow \downarrow \uparrow \rangle \\
&+ | \uparrow \uparrow \downarrow \downarrow \uparrow \uparrow \rangle + | \uparrow \downarrow \downarrow \uparrow \uparrow \uparrow \rangle) \\
&+ (| \downarrow \downarrow \uparrow \uparrow \uparrow \uparrow \rangle + | \uparrow \downarrow \uparrow \uparrow \uparrow \downarrow \rangle + | \downarrow \uparrow \uparrow \uparrow \downarrow \uparrow \rangle + | \uparrow \uparrow \downarrow \uparrow \downarrow \uparrow \rangle + | \uparrow \uparrow \downarrow \uparrow \downarrow \uparrow \rangle + | \uparrow \downarrow \downarrow \uparrow \uparrow \uparrow \rangle) \\
&+ (1 - \sqrt{5})(| \downarrow \uparrow \uparrow \uparrow \uparrow \uparrow \rangle + | \uparrow \uparrow \downarrow \uparrow \uparrow \uparrow \rangle + | \uparrow \downarrow \uparrow \uparrow \uparrow \uparrow \rangle) \} \quad (3.139)
\end{aligned}$$

One can get the triplet of energy $-(J/2)(5 - \sqrt{5})$ from (3.139) by changing $\sqrt{5} \rightarrow -\sqrt{5}$. As can be explicitly checked from (3.139), the two non-degenerate triplets of zero momentum are then P -parity even, namely they have opposite parity with respect to that of the ground state, as it happens for the lowest lying triplet excitations of the two-flavor Schwinger model.

For what concerns the degenerate triplets of momenta $\pi/3$ and $5\pi/3$ (or $2\pi/3$ and $4\pi/3$) they do not have definite P -parity, but it is always possible to take a linear combination of them with parity opposite to the ground state.

Table 3.4: Triplet internal quantum numbers

TRIPLET	λ_1	λ_2	$Q_1^{(h)}$	$Q_2^{(h)}$
$ 1, 1, -\frac{5+\sqrt{5}}{2}J, 0 \rangle$	$-\sqrt{\frac{5-2\sqrt{5}}{20}}$	$\sqrt{\frac{5-2\sqrt{5}}{20}}$	$-\frac{1}{2}$	$\frac{1}{2}$
$ 1, 1, -\frac{5-\sqrt{5}}{2}J, 0 \rangle$	$-\sqrt{\frac{5+2\sqrt{5}}{20}}$	$\sqrt{\frac{5+2\sqrt{5}}{20}}$	$-\frac{3}{2}$	$\frac{3}{2}$
$ 1, 1, -\frac{5}{2}J, \frac{\pi}{3} \rangle$	$-\frac{\sqrt{3}+\sqrt{\pi}}{8}$	$-\frac{\sqrt{3}-\sqrt{\pi}}{8}$	$-\frac{3}{2}$	$\frac{1}{2}$
$ 1, 1, -\frac{7+\sqrt{17}}{4}J, \frac{2\pi}{3} \rangle$	$\frac{-2\sqrt{3}-\sqrt{-2+2\sqrt{17}}}{2+2\sqrt{17}}$	$\frac{-2\sqrt{3}+\sqrt{-2+2\sqrt{17}}}{2+2\sqrt{17}}$	$-\frac{3}{2}$	$-\frac{1}{2}$
$ 1, 1, -\frac{7+\sqrt{17}}{4}J, \frac{4\pi}{3} \rangle$	$\frac{2\sqrt{3}-\sqrt{-2+2\sqrt{17}}}{2+2\sqrt{17}}$	$\frac{2\sqrt{3}+\sqrt{-2+2\sqrt{17}}}{2+2\sqrt{17}}$	$\frac{1}{2}$	$\frac{3}{2}$
$ 1, 1, -\frac{5}{2}J, \frac{5\pi}{3} \rangle$	$\frac{\sqrt{3}-\sqrt{\pi}}{8}$	$\frac{\sqrt{3}+\sqrt{\pi}}{8}$	$-\frac{1}{2}$	$\frac{3}{2}$

The remaining three triplets in fig.(3.3) have no real λ 's and are characterized by a string of length 2 and four holes for $Q = -\frac{3}{2}, -\frac{1}{2}, \frac{1}{2}, \frac{3}{2}$, *i.e.* do not belong to the type (3.100). More precisely, two triplets have a string approximately of length 2, due to the finite size of the system, while the triplet of momentum π has a string exactly of length 2. In table (3.5) I summarize the quantum numbers of these triplets.

Table 3.5: Four holes triplet internal quantum numbers

TRIPLET	λ_1	λ_2
$ 1, 1, -\frac{7-\sqrt{17}}{4}J, \frac{2\pi}{3} \rangle$	$\frac{2\sqrt{3}-i\sqrt{2+2\sqrt{17}}}{-2+2\sqrt{17}}$	$\frac{2\sqrt{3}+i\sqrt{2+2\sqrt{17}}}{-2+2\sqrt{17}}$
$ 1, 1, -J, \pi \rangle$	$-\frac{i}{2}$	$\frac{i}{2}$
$ 1, 1, -\frac{7-\sqrt{17}}{4}J, \frac{4\pi}{3} \rangle$	$\frac{2\sqrt{3}+i\sqrt{2+2\sqrt{17}}}{2-2\sqrt{17}}$	$\frac{2\sqrt{3}-i\sqrt{2+2\sqrt{17}}}{2-2\sqrt{17}}$

In fig.(3.3) it is shown that the spectrum exhibits five singlet states. The lowest lying state at momentum π is the ground state. Then there are three excited singlets characterized by the configuration with two holes (3.99), *i.e.* they have one real λ and a string of length almost 2. In table (3.6) I summarize their quantum numbers. Among these singlets, those which are not degenerate, have P -parity equal to that of the ground state (odd) as it happens in the two-flavor Schwinger model. The non- singlet in fact reads

$$\begin{aligned}
|0, 0, -3J, 0 \rangle &= \frac{1}{\sqrt{12}} \{ |\uparrow\uparrow\downarrow\downarrow\rangle + |\uparrow\downarrow\uparrow\downarrow\rangle + |\downarrow\downarrow\uparrow\uparrow\rangle + |\uparrow\downarrow\uparrow\downarrow\rangle + |\downarrow\uparrow\downarrow\uparrow\rangle + |\downarrow\uparrow\downarrow\uparrow\rangle \\
&- |\downarrow\downarrow\uparrow\uparrow\rangle - |\downarrow\uparrow\downarrow\uparrow\rangle - |\uparrow\downarrow\uparrow\downarrow\rangle - |\uparrow\downarrow\uparrow\downarrow\rangle - |\uparrow\uparrow\downarrow\downarrow\rangle - |\uparrow\uparrow\downarrow\downarrow\rangle \} \quad .(3.140)
\end{aligned}$$

The degenerate singlets are again not eigenstates of the P -parity, but it is always possible to take a linear combination of them with the a P -parity that coincides with that of the representative state (3.140) of the configuration.

Table 3.6: Singlet internal quantum numbers

SINGLET	λ	λ_S	$Q_1^{(h)}$	$Q_2^{(h)}$
$ 0, 0, -3J, 0 \rangle$	0	0	-1	1
$ 0, 0, -2J, \frac{\pi}{3} \rangle$	$-\frac{\sqrt{3+2\sqrt{6}}}{14}$	$\frac{-2+3\sqrt{2}}{\sqrt{3(4+\sqrt{2})}}$	0	1
$ 0, 0, -2J, \frac{5\pi}{3} \rangle$	$\frac{\sqrt{3+2\sqrt{6}}}{14}$	$\frac{2-3\sqrt{2}}{\sqrt{3(4+\sqrt{2})}}$	-1	0

The remaining singlet $|0, 0, -\frac{5-\sqrt{13}}{2}J, \pi \rangle$ it is not of the type (3.99). It is characterized by a string approximately of length 3 with $\lambda_{1,1} = i\sqrt{\frac{5+2\sqrt{13}}{12}}$, $\lambda_{2,1} = 0$ and $\lambda_{3,1} = -i\sqrt{\frac{5+2\sqrt{13}}{12}}$.

Even in finite systems very small like the 4 and 6 sites chains, the “string hypothesis” is a very good approximation and it allows us to classify and distinguish among states with the same spin.

The ground state of the antiferromagnetic Heisenberg chain with N sites is a linear combination of all the $\binom{N}{\frac{N}{2}}$ states with $\frac{N}{2}$ spins up and $\frac{N}{2}$ spins down. These states group themselves into sets with the same coefficient in the linear combination according to the fact that the ground state is translationally invariant (with momentum 0 (π) for $\frac{N}{2}$ even (odd)), it is an eigenstate of P -parity and it is invariant under the exchange of up with down spins. The states belonging to the same set have the same number of domain walls, which ranges from N , for the two Néel states, to 2 for the states with $\frac{N}{2}$ adjacent spins up and $\frac{N}{2}$ adjacent spins down.

The ground state of the 8 sites chain is

$$|g.s.\rangle = \frac{1}{\sqrt{\mathcal{N}}}(|\psi_8\rangle + \alpha|\psi_6^{(1)}\rangle + \beta|\psi_6^{(2)}\rangle + \gamma|\psi_4^{(1)}\rangle + \delta|\psi_4^{(2)}\rangle + \epsilon|\psi_4^{(3)}\rangle + \zeta|\psi_2\rangle) \quad (3.141)$$

where

$$|\psi_8\rangle = |\uparrow\downarrow\uparrow\downarrow\uparrow\downarrow\uparrow\downarrow\rangle + |\downarrow\uparrow\downarrow\uparrow\downarrow\uparrow\downarrow\rangle \quad (3.142)$$

$$|\psi_6^{(1)}\rangle = |\uparrow\uparrow\downarrow\downarrow\uparrow\uparrow\rangle + |\downarrow\downarrow\uparrow\uparrow\downarrow\downarrow\rangle + \text{translated states} \quad (3.143)$$

$$|\psi_6^{(2)}\rangle = |\uparrow\uparrow\downarrow\downarrow\uparrow\uparrow\rangle + |\downarrow\downarrow\uparrow\uparrow\downarrow\downarrow\rangle + \text{translated states} \quad (3.144)$$

$$|\psi_4^{(1)}\rangle = |\uparrow\uparrow\downarrow\downarrow\rangle + \text{translated states} \quad (3.145)$$

$$|\psi_4^{(2)}\rangle = |\uparrow\uparrow\downarrow\downarrow\rangle + |\downarrow\downarrow\uparrow\uparrow\rangle + \text{translated states} \quad (3.146)$$

$$|\psi_4^{(3)}\rangle = |\uparrow\uparrow\downarrow\downarrow\rangle + |\downarrow\downarrow\uparrow\uparrow\rangle + \text{translated states} \quad (3.147)$$

$$|\psi_2\rangle = |\uparrow\uparrow\rangle + |\downarrow\downarrow\rangle + \text{translated states} . \quad (3.148)$$

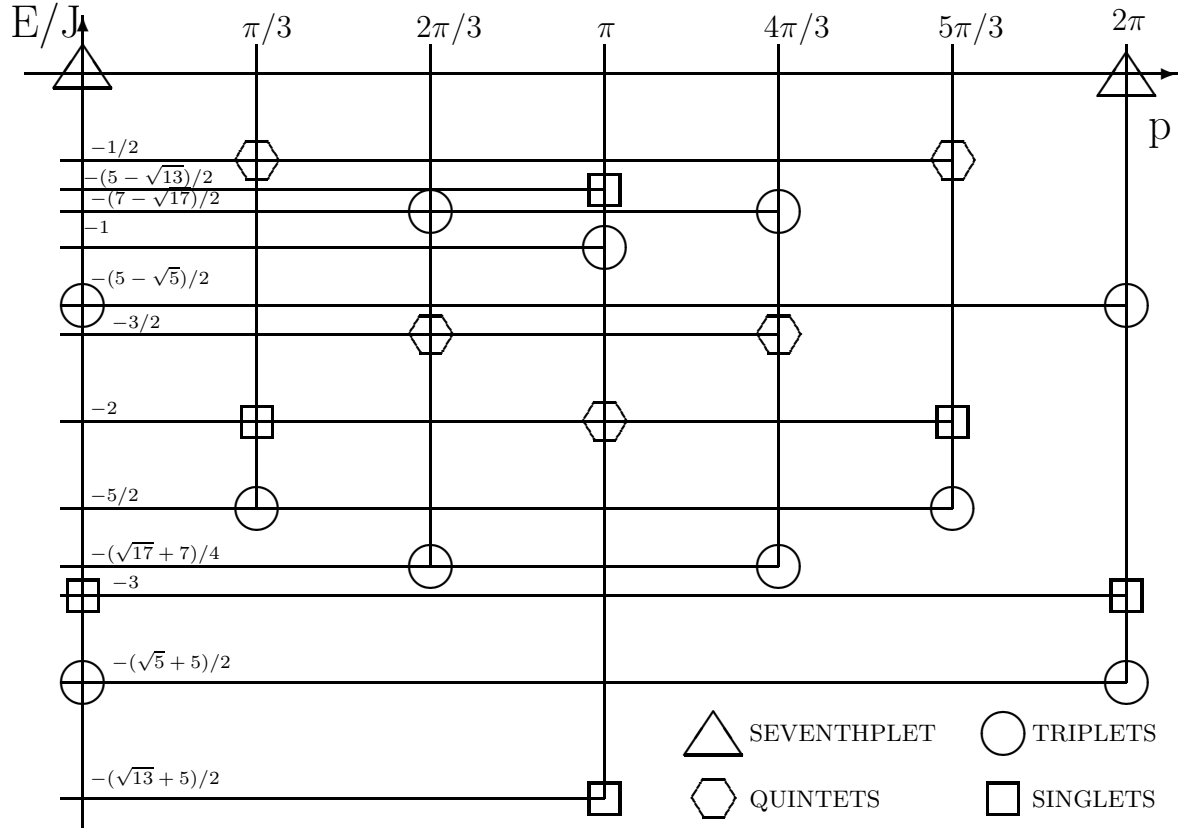


Figure 3.3: Six sites chain spectrum

By direct diagonalization one gets

$$\alpha = -0.412773 \quad (3.149)$$

$$\beta = 0.344301 \quad (3.150)$$

$$\gamma = 0.226109 \quad (3.151)$$

$$\delta = -0.087227 \quad (3.152)$$

$$\epsilon = 0.136945 \quad (3.153)$$

$$\zeta = 0.018754 \quad (3.154)$$

$$\mathcal{N} = 2 + 16\alpha^2 + 8\beta^2 + 4\gamma^2 + 16\delta^2 + 16\epsilon^2 + 8\zeta^2 = 6.30356 \quad (3.155)$$

The energy of the ground state is

$$E_{g.s.} = -5.65109J \quad (3.156)$$

Eq.(3.156) differs only by 1.8% from the thermodynamic limit expression $E_{g.s.} = -8 \ln 2 = -5.54518$. Moreover also the correlation function of distance 2 Eq.(3.158) computed for the 8 sites chain is $G(2) = 0.1957N$, value which is 7% higher than the exact answer Eq.(3.159).

In the analysis of finite size systems I were able to find the coefficient β of the first set of states containing $N - 2$ domain walls in the ground state. These states are obtained interchanging two adjacent spins in the Néel states. The β is for a generic chain of N -sites

$$\beta = \frac{N + 2E_{g.s.}}{N} = 1 - 2 \ln 2 \quad (3.157)$$

3.3.2 Spin-spin correlators

The explicit computation of spin-spin correlations is far from being trivial since the correlator $G(r) = \langle g.s. | \vec{S}_0 \cdot \vec{S}_r | g.s. \rangle$ is not known for arbitrary lattice separations r . For $r = 2$ it was computed by M. Takahashi [42] in his perturbative analysis of the half filled Hubbard model in one dimension. For $r > 2$ no exact numerical values of $G(r)$ are known. In [52] were given two representations of $G(r)$, while in [53, 54] the exact asymptotic ($r \rightarrow \infty$) expression of $G(r)$ was derived.

In order to explicitly compute the second order energies Eq.(5.62) and Eq.(5.63) one has to evaluate the correlation function

$$G(2) = \frac{1}{N} \sum_{x=1}^N \langle g.s. | \vec{S}_x \cdot \vec{S}_{x+2} | g.s. \rangle \quad (3.158)$$

which has been exactly computed in [42] and is given by

$$G(2) = \frac{1}{4}(1 - 16 \ln 2 + 9\zeta(3)) = 0.1820 \quad . \quad (3.159)$$

In the following I shall show how the knowledge of this correlator allows one to compute explicitly the first three “emptiness formation probabilities”, used in Ref. [52] in the study of the Heisenberg chain correlators, $G(r)$. The isotropy of the Heisenberg model implies that

$$\sum_{x=1}^N \langle g.s. | \vec{S}_x \cdot \vec{S}_{x+2} | g.s. \rangle = 3 \sum_{x=1}^N \langle g.s. | S_x^3 \cdot S_{x+2}^3 | g.s. \rangle \quad . \quad (3.160)$$

Let us introduce the probability P_3 for finding three adjacent spins in a given position in the Heisenberg antiferromagnetic vacuum. Taking advantage of the isotropy of the Heisenberg model ground state and of its translational invariance, it is easy to see that the correlator (3.160) can be written in terms of the P_3 's as

$$\sum_{x=1}^N \langle g.s. | S_x^3 \cdot S_{x+2}^3 | g.s. \rangle = N \frac{1}{4} 2 (P_3(\uparrow\uparrow\uparrow) + P_3(\uparrow\downarrow\uparrow) - P_3(\uparrow\uparrow\downarrow) - P_3(\downarrow\uparrow\uparrow)) \quad . \quad (3.161)$$

The factor 2 appears in (3.161) due again to the isotropy of the Heisenberg model: the probability of a configuration and of the configuration rotated by π around the chain axis, are the same.

In [52] the so called “emptiness formation probability” $P(x)$ was introduced.

$$P(x) = \langle g.s. | \prod_{j=1}^x P_j | g.s. \rangle \quad , \quad (3.162)$$

where

$$P_j = \frac{1}{2}(\sigma_j^3 + 1) \quad (3.163)$$

and σ_j^3 is the Pauli matrix. $P(x)$ determines the probability of finding x adjacent spins up in the antiferromagnetic vacuum. One gets

$$P(\uparrow\uparrow\uparrow) = P(3) \quad (3.164)$$

$$P(\uparrow\downarrow\uparrow) = P(1) - 2P(2) + P(3) \quad (3.165)$$

$$P(\downarrow\uparrow\uparrow) = P(\uparrow\uparrow\downarrow) = P(2) - P(3) \quad (3.166)$$

so that Eq.(3.158) reads

$$G(2) = 2P(3) - 2P(2) + \frac{1}{2}P(1) \quad . \quad (3.167)$$

Using the exact value the correlator $G(2)$ computed in [42] from (3.167) and from the known values of $P(2)$ and $P(1)$ given in [52]

$$P(1) = \frac{1}{2} \quad (3.168)$$

$$P(2) = \frac{1}{3}(1 - \ln 2) \quad (3.169)$$

$$(3.170)$$

one gets

$$P(3) = \frac{1}{3}(1 - 7 \ln 2) + \frac{9}{8}\zeta(3) \quad (3.171)$$

For the general emptiness formation probability $P(x)$ of the antiferromagnetic Heisenberg chain, an integral representation was given in [52], but, to my knowledge, the exact value of $P(3)$ (3.171) was not known.

I illustrate now the computation of a spin-spin correlator which appears in the mass spectrum of the two-flavor lattice Schwinger model

$$\begin{aligned} \langle g.s. | \vec{V} \cdot \vec{V} | g.s. \rangle &= \sum_{x,y=1}^N \langle g.s. | (\vec{S}_x \cdot \vec{S}_y) (\vec{S}_{x+1} \cdot \vec{S}_{y+1}) | g.s. \rangle \\ &- \langle g.s. | (\vec{S}_x \cdot \vec{S}_{y+1}) (\vec{S}_{x+1} \cdot \vec{S}_y) | g.s. \rangle - \sum_{x=1}^N \langle g.s. | \vec{S}_x \cdot \vec{S}_{x+1} | g.s. \rangle \quad (3.172) \end{aligned}$$

It is possible to extract a numerical value from Eq.(3.172) only within the random phase approximation [42, 55]. For this purpose it is first convenient to rewrite the unconstrained sum over the sites x and y as a sum where all the four spins involved in the VEV's lie on different sites,

$$\begin{aligned} \langle g.s. | \vec{V} \cdot \vec{V} | g.s. \rangle &= \sum_{\substack{y \neq x \\ y \neq x \pm 1}} \langle g.s. | (\vec{S}_x \cdot \vec{S}_y) (\vec{S}_{x+1} \cdot \vec{S}_{y+1}) | g.s. \rangle \\ &- \langle g.s. | (\vec{S}_x \cdot \vec{S}_{y+1}) (\vec{S}_{x+1} \cdot \vec{S}_y) | g.s. \rangle + \frac{3}{8}N \\ &- \frac{1}{2} \sum_{x=1}^N \langle g.s. | \vec{S}_x \cdot \vec{S}_{x+1} | g.s. \rangle - \sum_{x=1}^N \langle g.s. | \vec{S}_x \cdot \vec{S}_{x+2} | g.s. \rangle \quad (3.173) \end{aligned}$$

and then factorize the four spin operators in Eq.(3.173) as

$$\begin{aligned} \langle g.s. | \vec{V} \cdot \vec{V} | g.s. \rangle &= N \sum_{r=2}^{\infty} (\langle g.s. | \vec{S}_0 \cdot \vec{S}_r | g.s. \rangle^2 - \langle g.s. | \vec{S}_0 \cdot \vec{S}_{r+1} | g.s. \rangle \langle g.s. | \vec{S}_1 \cdot \vec{S}_r | g.s. \rangle) \\ &+ \frac{3}{8}N - \frac{1}{2} \sum_{x=1}^N \langle g.s. | \vec{S}_x \cdot \vec{S}_{x+1} | g.s. \rangle - \sum_{x=1}^N \langle g.s. | \vec{S}_x \cdot \vec{S}_{x+2} | g.s. \rangle \quad (3.174) \end{aligned}$$

Of course, Eq.(3.174) provides an answer larger than the exact result; terms such as $\langle (\dots)(\dots) \rangle$ yield negative contributions which are eliminated once one factorizes them in the form $\langle (\dots) \rangle \langle (\dots) \rangle$. This is easily checked also by direct computation on finite size systems.

The spin-spin correlation functions $G(r)$ are exactly known for $r = 1, 2$. For the spin-spin correlation functions $G(r)$ up to a distance of $r = 30$ the results are reported in table (3.7) [53, 56].

For $r > 30$, one may write [53]

Table 3.7: Spin-spin correlation functions

r	$G(r)$	r	$G(r)$
1	-0.4431	16	0.0305
2	0.1821	17	-0.0296
3	-0.1510	18	0.0274
4	0.1038	19	-0.0267
5	-0.0925	20	0.0249
6	0.0731	21	-0.0242
7	-0.0671	22	0.0228
8	0.0567	23	-0.0223
9	-0.0532	24	0.0211
10	0.0465	25	-0.0206
11	-0.0442	26	0.0196
12	0.0395	27	-0.0193
13	-0.0379	28	0.0183
14	0.0344	29	-0.0181
15	-0.0332	30	0.0172

$$G(r) = \frac{3}{4} \sqrt{\frac{2}{\pi^3}} \frac{1}{r \sqrt{g(r)}} \left[1 - \frac{3}{16} g(r)^2 + \frac{156\zeta(3) - 73}{384} g(r)^3 + O(g(r)^4) \right] - \frac{0.4}{2r} ((-1)^r + 1 + O(g(r)) + O(\frac{1}{r^2})) \quad (3.175)$$

with $g(r)$ satisfying

$$g(r) = \frac{1}{C(r)} \left(1 + \frac{1}{2} g(r) \ln(g(r)) \right) \quad (3.176)$$

and

$$C(r) = \ln(2\sqrt{2\pi} e^{\gamma+1} r) \quad (3.177)$$

Eq.(3.176) may be solved by iteration. To the lowest order in $\frac{1}{C}$ one finds

$$g(r) \approx \frac{1}{C(r)} - \frac{1}{C(r)^2} \ln C(r) \quad (3.178)$$

Inserting (3.178) in Eq.(3.175) leads to

$$G(r) \approx \sqrt{2}\pi^3 \frac{1}{r} \sqrt{C(r)} \left[1 + \frac{1}{4C(r)} \ln C(r) \right] + O\left(\frac{1}{C(r)^2}\right) \quad (3.179)$$

Inserting Eq.(3.179) in (3.174), one finally gets

$$\langle g.s. | \vec{V} \cdot \vec{V} | g.s. \rangle = 0.3816N \quad (3.180)$$

Last, I report the following exact three spin correlators that have been used in the determination of the mass spectrum of the two-flavor lattice Schwinger model

$$\langle g.s. | \sum_{x=1}^N S_x^3 S_{x+1}^3 S_{x+2}^3 | g.s. \rangle = 0 \quad (3.181)$$

$$\langle g.s. | \sum_{x=1}^N S_x^+ S_{x+1}^- S_{x+2}^3 | g.s. \rangle = 0 \quad (3.182)$$

$$\langle g.s. | \sum_{x=1}^N S_x^- S_{x+1}^+ S_{x+2}^3 | g.s. \rangle = 0 \quad (3.183)$$

$$\langle g.s. | \sum_{x=1}^N S_x^+ S_{x+1}^3 S_{x+2}^- | g.s. \rangle = 0 \quad (3.184)$$

$$\langle g.s. | \sum_{x=1}^N S_x^- S_{x+1}^3 S_{x+2}^+ | g.s. \rangle = 0 \quad (3.185)$$

So, on a spin singlet, not only the VEV of $\sum_{x=1}^N S_x^3$ is zero, but also every VEV with an odd number of S^3 .

3.4 $SU(\mathcal{N})$ quantum antiferromagnetic chains

It is my purpose to introduce spin-1/2 antiferromagnetic Heisenberg chains where “spins” are generators of the $SU(\mathcal{N})$ group. In the limit $\mathcal{N} = 2$ one has the usual antiferromagnetic Heisenberg chain discussed in the previous section. An $U(\mathcal{N})$ spin-1/2 quantum antiferromagnetic chain is described by the Hamiltonian

$$H_J^{U(\mathcal{N})} = J \sum_{x=1}^N S_{ab}(x) S_{ba}(x+1) \quad (3.186)$$

where $S_{ab}(x)$ $a, b = 1, \dots, \mathcal{N}$ are the generators of $U(\mathcal{N})$ satisfying the Lie algebra

$$[S_{ab}(x), S_{cd}(y)] = (S_{ad}(x)\delta_{bc} - S_{cb}(x)\delta_{ad})\delta_{xy} \quad (3.187)$$

and they can be conventionally represented by fermion bilinear operators

$$S_{ab}(x) = \psi_{ax}^\dagger \psi_{bx} - \frac{\delta_{ab}}{2} \quad (3.188)$$

The representation of the algebra on each site is fixed by specifying the fermion number occupation

$$\rho(x) = \sum_{a=1}^{\mathcal{N}} S_{aa}(x) \quad (3.189)$$

By fulfilling the global neutrality condition $\sum_{x=1}^N \rho(x) = 0$, one may choose

$$\sum_{a=1}^{\mathcal{N}} \psi_{ax}^\dagger \psi_{ax} = \begin{cases} m & x \text{ even} \\ \mathcal{N} - m & x \text{ odd} \end{cases} \quad (3.190)$$

or viceversa the opposite choice for x even-odd. Eq.(3.190) restricts on each site the Hilbert space to a representation with Young tableau of m rows for x even and $\mathcal{N} - m$ rows for x odd. For each site x $\rho(x)$ is the generator of the $U(1)$ subgroup of $U(\mathcal{N})$.

Let us use the basis $T^\alpha = (T^\alpha)^*$, $\alpha = 1, \dots, \mathcal{N}^2 - 1$, of the Lie algebra of $SU(\mathcal{N})$ in the fundamental representation such that $tr(T^\alpha T^\beta) = \delta^{\alpha\beta}/2$ and $[T^\alpha, T^\beta] = i f^{\alpha\beta\gamma} T^\gamma$, where $f^{\alpha\beta\gamma}$ are the structure constants. By means of

$$T_{ab}^\alpha T_{cd}^\alpha = \frac{1}{2} \delta_{ad} \delta_{bc} - \frac{1}{2\mathcal{N}} \delta_{ab} \delta_{cd} \quad (3.191)$$

and redefining the group generators

$$S_x^\alpha = \psi_{ax}^\dagger T_{ab}^\alpha \psi_{bx} \quad (3.192)$$

one can rewrite the Hamiltonian (3.186) as

$$H_J^{U(\mathcal{N})} = J \sum_{x=1}^N \rho(x)\rho(x+1) + H_J^{SU(\mathcal{N})} \quad (3.193)$$

where

$$H_J^{SU(\mathcal{N})} = J \sum_{x=1}^N S_x^\alpha S_{x+1}^\alpha \quad (3.194)$$

is the Hamiltonian of an $SU(\mathcal{N})$ quantum antiferromagnet. From Eq.(3.193) it is clear that by fixing $\rho(x)$ $H_J^{U(\mathcal{N})}$ is reduced to $H_J^{SU(\mathcal{N})}$.

The representations of the $SU(\mathcal{N})$ spins relevant for the relationship of the spin Hamiltonians (3.194) with the Schwinger models are different when \mathcal{N} is even or odd. When \mathcal{N} is even I shall consider the representation on each site with Young tableau of one column and $\mathcal{N}/2$ rows so that $\rho(x) = 0$. When \mathcal{N} is odd I shall consider on one sublattice the representation with Young tableau of one column and $(\mathcal{N} + 1)/2$ rows and of one column and $(\mathcal{N} - 1)/2$ rows on the other sublattice.

As an explicit example let us consider the case $\mathcal{N} = 3$. The generators T^α of the $SU(3)$ group in Eq.(3.192) are the Gell Mann matrices. By denoting u, d and s the three flavors, the eight spin operators S_x^α read

$$S_x^1 = \psi_{ux}^\dagger \psi_{dx} + \psi_{dx}^\dagger \psi_{ux} \quad (3.195)$$

$$S_x^2 = -i\psi_{ux}^\dagger \psi_{dx} + i\psi_{dx}^\dagger \psi_{ux} \quad (3.196)$$

$$S_x^3 = \psi_{ux}^\dagger \psi_{ux} - \psi_{dx}^\dagger \psi_{dx} \quad (3.197)$$

$$S_x^4 = \psi_{ux}^\dagger \psi_{sx} + \psi_{sx}^\dagger \psi_{ux} \quad (3.198)$$

$$S_x^5 = -i\psi_{ux}^\dagger \psi_{sx} + i\psi_{sx}^\dagger \psi_{ux} \quad (3.199)$$

$$S_x^6 = \psi_{dx}^\dagger \psi_{sx} + \psi_{sx}^\dagger \psi_{dx} \quad (3.200)$$

$$S_x^7 = -i\psi_{dx}^\dagger \psi_{sx} + i\psi_{sx}^\dagger \psi_{dx} \quad (3.201)$$

$$S_x^8 = \frac{1}{\sqrt{3}}(\psi_{ux}^\dagger \psi_{ux} + \psi_{dx}^\dagger \psi_{dx} - 2\psi_{sx}^\dagger \psi_{sx}) \quad (3.202)$$

Let us find the ground state of the Hamiltonian (3.194) for a chain of two sites. Taking the representations with one particle on site 1 and two particles on site 2, the ground state with energy $E_{g.s.} = -16J/3$ reads

$$|g.s. \rangle = \frac{1}{\sqrt{3}}(|u \begin{smallmatrix} d \\ s \end{smallmatrix} \rangle - |d \begin{smallmatrix} u \\ s \end{smallmatrix} \rangle + |s \begin{smallmatrix} u \\ d \end{smallmatrix} \rangle) \quad (3.203)$$

The state (3.203) is a singlet of $SU(3)$, *i.e.* it is annihilated by the Casimir $\vec{S}^2 = (\vec{S}_1 + \vec{S}_2)^2 = \sum_{\alpha=1}^8 [(S_1^\alpha)^2 + (S_2^\alpha)^2 + 2S_1^\alpha S_2^\alpha]$. If one chooses the representation with two particles on site 1 and one particle on site 2, the ground state degenerate with (3.203) is

$$|g.s. \rangle' = \frac{1}{\sqrt{3}}(| \begin{smallmatrix} d \\ s \end{smallmatrix} u \rangle - | \begin{smallmatrix} u \\ s \end{smallmatrix} d \rangle + | \begin{smallmatrix} u \\ d \end{smallmatrix} s \rangle) \quad (3.204)$$

Diagonalizing the translation operator \hat{T} with the Hamiltonian (3.194), one gets two degenerate ground states

$$|G.S. \rangle^\pm = \frac{|g.s. \rangle \pm |g.s. \rangle'}{\sqrt{2}} \quad (3.205)$$

In Eq.(3.205) the linear combination with the $+$ has momentum zero and the one with the $-$ has momentum π . By studying this very simple example, one can infer that the thermodynamic limit $N \rightarrow \infty$ analysis for a generic $SU(\mathcal{N})$ chain is very involved.

Unfortunately, no analysis with a level of completeness such as the one given in [30] for the $SU(2)$ case does exist for a generic symmetry group $SU(\mathcal{N})$ with spins in the representation in which I am interested. In [57] $SU(\mathcal{N})$ antiferromagnetic models were solved for a particular spin representation such that the Hamiltonian (3.194) becomes

$$H_J^{SU(\mathcal{N})} = J \sum_{x=1}^N P_{xx+1} \quad (3.206)$$

with P_{xx+1} the operator that permutes whatever objects occupy sites x and $x + 1$. The spectrum of Eq.(3.206) was shown to exhibit massless excitations.

A large \mathcal{N} expansion approach has been performed in [58] for an $SU(\mathcal{N})$ antiferromagnetic chain characterized by spins living in a representation with Young tableaux of one row on one sublattice and $\mathcal{N} - 1$ rows on the other sublattice. In the case of Young tableaux of one column it was found that the ground state is twofold degenerate and breaks translational and parity symmetry. Moreover the elementary excitations are massive non relativistic solitons in the large \mathcal{N} limit with a mass of $O(\mathcal{N})$.

In [59] the Lieb-Shultz-Mattis theorem [60] was generalized to $SU(\mathcal{N})$ spin chains. The theorem proves that a half-integer-S spin chain with essentially any reasonably local Hamiltonian respecting translational and rotational symmetry either has zero gap or else has degenerate ground states spontaneously breaking translational and parity invariance. In [60] it was proved the existence of a unique ground state of the $SU(\mathcal{N})$ chains where \mathcal{N} is even for spins in the antisymmetric \mathcal{N} tensor representation. Under the assumption of a unique ground state which must be a $SU(\mathcal{N})$ singlet, an infinitesimal energy gap was found for all the representations of $SU(\mathcal{N})$ whose Young tableaux contain a number of boxes not divisible by \mathcal{N} . Of course the degeneracy of the ground state trivially implies a zero gap.

Using the Lieb-Shultz-Mattis I can state that when \mathcal{N} is even the ground state of the Hamiltonian (3.194) is unique and there are gapless excitations for the spin representation with a Young tableau of one column and $\mathcal{N}/2$ rows. When \mathcal{N} is odd the ground state is twofold degenerate, as I illustrated with the simple example of the two site $SU(3)$ chain. It is doubtful if there exist gapless excitations in this case and at present time I am investigating this problem.

Chapter 4

The one-flavor lattice Schwinger model

In this chapter I study the one-flavor lattice Schwinger model in the strong coupling limit using staggered fermions and the hamiltonian approach to lattice gauge theories [61]. Even though the continuous axial symmetry is broken explicitly by the staggered fermions, the discrete axial symmetry remains and appears in the lattice theory as a translation by one site. In the continuum gauge model the chiral symmetry is broken by the anomaly. An interesting issue which arises in the lattice regularization of gauge theories is how the lattice theory produces the effects of the axial anomaly. Lattice field theory are manifestly gauge invariant by construction and therefore, to produce continuum theories, they must find a way to violate axial current conservation. Normally, in lattice gauge theories axial anomalies are either cancelled by fermion doubling or else the lattice regularization breaks the axial symmetry explicitly. The lattice Schwinger model in the hamiltonian formalism with one species of staggered fermions represents the unique example where neither of these occur. The effects of the anomaly are not cancelled by doubling since the continuum limit of (1+1)-dimensional staggered fermions produce exactly a Dirac fermion which is the matter content of the model. Furthermore, even if the continuum axial symmetry is explicitly broken, the remaining discrete axial symmetry must be spontaneously broken. The mass operator $\bar{\psi}\psi$ is odd under discrete axial transformations, if this symmetry is unbroken then $\langle \bar{\psi}\psi \rangle = 0$. However, in the continuum theory it is known that [62],

$$\langle \bar{\psi}(x)\psi(x) \rangle = -\frac{e^\gamma}{2\pi} \frac{e_c}{\sqrt{\pi}} . \quad (4.1)$$

where $\gamma = 0.577\dots$ is the Euler constant. The expectation value in Eq.(4.1) is the chiral condensate. ¹ I shall show that the chiral condensate (4.1) is non-zero also on the lattice and the discrete axial symmetry is indeed spontaneously broken. In addition to the analysis of the chiral symmetry breaking pattern on the lattice, by performing a strong coupling expansion around a gauge invariant ground state I shall derive results converging more rapidly to the continuum than the results provided in [63]. The one-flavor Schwinger model has also been used as an example of the fact that quantum link models may reproduce the physics of conventional hamiltonian lattice gauge theories [65].

¹It is worth to stress that the sign of the chiral condensate in Eq.(4.1) is just a convention. The chiral condensate has always the opposite sign of the fermion mass m that appears in the Lagrangian of the theory: it is the order parameter for a spontaneous symmetry breaking of the chiral symmetry. The chiral condensate is the analogous of the magnetization for a spin model and the mass m plays the role of the magnetic field. So even if one is studying a massless model, in order to decide the sign of the chiral condensate, one has to consider a small mass term m that then one sends to zero. The minus sign which appears in Eq.(4.1) is due to the fact that one considers the $m \rightarrow 0^+$ limit in the Schwinger model Lagrangian.

4.1 Definition of the model

The continuum Schwinger model [28, 64] is the prototypical example of a solvable model where the anomaly occurs. It is 1+1-dimensional electrodynamics with a single charged massless Dirac spinor field. The action is

$$S = \int d^2x (\bar{\psi}(i\gamma_\mu \partial^\mu + \gamma_\mu A^\mu)\psi - \frac{1}{4e_c^2} F_{\mu\nu} F^{\mu\nu}) \quad (4.2)$$

It is invariant under gauge transformations,

$$\psi(x) \longrightarrow e^{i\theta(x)}\psi(x), \psi^\dagger(x) \longrightarrow \psi^\dagger(x)e^{-i\theta(x)} \quad (4.3)$$

$$A_\mu \longrightarrow A_\mu + \partial_\mu \theta(x) \quad (4.4)$$

and, formally, under the axial phase rotation,

$$\psi(x) \longrightarrow e^{i\gamma_5 \alpha}\psi(x), \psi^\dagger(x) \longrightarrow \psi^\dagger(x)e^{-i\gamma_5 \alpha} \quad (4.5)$$

(where $\gamma^5 = i\gamma^0\gamma^1$).

At the classical level the above symmetries lead to conservation laws for the vector and axial currents,

$$j^\mu(x) = \bar{\psi}(x)\gamma^\mu\psi(x), \quad j_5^\mu(x) = \bar{\psi}(x)\gamma^5\gamma^\mu\psi(x), \quad (4.6)$$

respectively. At the quantum level both currents cannot be simultaneously conserved. If the regularization is gauge invariant, so that the vector current is conserved, then the axial current obeys the anomaly equation [66]

$$\partial_\mu j_5^\mu(x) = \frac{e_c^2}{2\pi} \epsilon^{\mu\nu} F_{\mu\nu}(x). \quad (4.7)$$

Moreover, the correlation functions of the model do not exhibit axial symmetry.

There are only neutral particles in the spectrum of the Schwinger model; notably, the bound state boson created by the axial current operator,

$$\partial^\mu \phi(x) = \sqrt{\pi} j_5^\mu(x) \quad (4.8)$$

appears in the spectrum as a free pseudoscalar with mass $\frac{e_c}{\sqrt{\pi}}$.

In terms of the boson field, the action is

$$S = \int d^2x \left(\frac{1}{2} \partial_\mu \phi \partial^\mu \phi + \frac{e_c^2}{2\pi} \phi^2 \right) \quad (4.9)$$

and the correlation functions for the vector and axial currents are obtained from the correlation functions of derivatives of the boson fields. The coupling constant e_c has the dimension of a mass and the model is super-renormalizable.

Since the Schwinger model is solvable it has often been used as a field theory where methods of lattice gauge theory, particularly the strong coupling expansion can be tested and compared with exact results of the continuum model [63].

In this chapter, I shall revisit the lattice quantization of the Schwinger model. My main purpose is to demonstrate two results. One is to show how the effects of the anomaly appear through spontaneous symmetry breaking. The other is to demonstrate that a strong coupling expansion around a gauge, parity and charge conjugation invariant lattice ground state can produce results in good agreement with the continuum. My results turn out to be quite

different from those of previous strong coupling computations [63]. The difference arises from my careful treatment of the normal ordering of the charge density operator, which must be defined so as to be compatible with all of the discrete symmetries of the theory. The necessity of careful normal ordering of the charge operator was pointed out in [24]. My vacuum state, vacuum energy and energies of elementary excitations are different from those in [63, 67] and, as I shall show, they give a more accurate extrapolation to the continuum limit.

The Hamiltonian and gauge constraint of the continuum Schwinger model are

$$H = \int dx \left(\frac{e_c^2}{2} E^2(x) + \psi^\dagger(x) \alpha (i\partial_x + eA(x)) \psi(x) \right) \quad (4.10)$$

$$\partial_x E(x) + \psi^\dagger(x) \psi(x) \sim 0 \quad (4.11)$$

A lattice Hamiltonian and constraint which reduce to these in the continuum limit are:

$$H_S = \frac{e_L^2 a}{2} \sum_x E_x^2 - \frac{it}{2a} \sum_x (\psi_{x+1}^\dagger e^{iA_x} \psi_x - \psi_x^\dagger e^{-iA_x} \psi_{x+1}) \quad (4.12)$$

$$E_x - E_{x-1} + \psi_x^\dagger \psi_x - \frac{1}{2} \sim 0, \quad (4.13)$$

where the fermion fields are defined on the sites, $x = -\frac{N}{2}, -\frac{N}{2} + 1, \dots, \frac{N}{2}$, gauge and the electric fields, A_x and E_x , on the links $[x; x+1]$, N is an even integer and, when N is finite, I use periodic boundary conditions. When N is finite, the continuum limit is the Schwinger model on a circle [68, 62]. The coefficient t of the hopping term in (4.12) plays the role of the lattice light speed. In the naive continuum limit, $e_L = e_c$ and $t = 1$. However, I shall keep e_L and t as parameters which can be adjusted to fit the lattice values of quantities such as the mass gap and the chiral condensate to those which are known in the continuum.

The non vanishing (anti-)commutators for the lattice variables are

$$[A_x, E_y] = i\delta_{xy}, \quad \{\psi_x, \psi_y^\dagger\} = \delta_{xy} \quad (4.14)$$

The Hamiltonian and gauge constraint exhibit the discrete symmetries

- Parity P:

$$A_x \longrightarrow -A_{-x-1}, \quad E_x \longrightarrow -E_{-x-1}, \quad \psi_x \longrightarrow (-1)^x \psi_{-x}, \quad \psi_x^\dagger \longrightarrow (-1)^x \psi_{-x}^\dagger \quad (4.15)$$

- Discrete axial symmetry Γ :

$$A_x \longrightarrow A_{x+1}, \quad E_x \longrightarrow E_{x+1}, \quad \psi_x \longrightarrow \psi_{x+1}, \quad \psi_x^\dagger \longrightarrow \psi_{x+1}^\dagger \quad (4.16)$$

- Charge conjugation C:

$$A_x \longrightarrow -A_{x+1}, \quad E_x \longrightarrow -E_{x+1}, \quad \psi_x \longrightarrow \psi_{x+1}^\dagger, \quad \psi_x^\dagger \longrightarrow \psi_{x+1} \quad (4.17)$$

When $A_x = 0$, the spectrum of the hopping Hamiltonian is $\epsilon(pa) = t \sin pa$ ($p \in [0, \frac{2\pi}{a}]$). In the low energy limit it resembles a massless relativistic spectrum for excitations near the Fermi level. The two intersections of the energy band with the Fermi level provide the continuum right and left moving massless fermions. The electron ground state is invariant under charge conjugation only when the Fermi level is at $\epsilon(p_F) = 0$ (i.e. when exactly half of the fermion states are filled and $\sum_x \langle \rho(x) \rangle = 0$). In the remainder of this paper I consider only this case of half-filling.

One has two possible ways to put the spinors $\psi = \begin{pmatrix} \psi_1 \\ \psi_2 \end{pmatrix}$ on the lattice in the staggered fermion formalism. One can put upper components on even sites and lower components on odd sites or viceversa. The mass operator, which reduces to $\bar{\psi}\psi$ in the continuum limit is the staggered charge density

$$M(x) = \frac{(-1)^x}{a} (\psi_x^\dagger \psi_x - 1/2) \quad (4.18)$$

for the first choice of staggered fermions or

$$M(x) = \frac{(-1)^{x+1}}{a} (\psi_x^\dagger \psi_x - 1/2) \quad (4.19)$$

in the other case.

These operators (4.18)(4.19) are scalars under parity and are even under charge conjugation but change sign under a discrete axial transformation.

The lattice Schwinger model is equivalent to a one dimensional quantum Coulomb gas on the lattice. To see this one can fix the gauge, $A_x = A$ (Coulomb gauge). Eliminating the non-constant electric field and using the gauge constraint, one obtains the effective Hamiltonian

$$\begin{aligned} H_S &= H_u + H_p \equiv \left[\frac{e_L^2}{2N} E^2 + \frac{e_L^2 a}{2} \sum_{x,y} \rho(x) V(x-y) \rho(y) \right] + \\ &+ \left[-\frac{it}{2a} \sum_x (\psi_{x+1}^\dagger e^{iA} \psi_x - \psi_x^\dagger e^{-iA} \psi_{x+1}) \right], \end{aligned} \quad (4.20)$$

where the charge density is

$$\rho(x) = \psi_x^\dagger \psi_x - \frac{1}{2}, \quad (4.21)$$

and the potential

$$V(x-y) = \frac{1}{N} \sum_{n=1}^{N-1} e^{i2\pi n(x-y)/N} \frac{1}{4 \sin^2 \frac{\pi n}{N}} \quad (4.22)$$

is the Fourier transform of the inverse laplacian on the lattice for non zero momentum. The constant electric field is normalized so that $[A, E] = i$. The constant modes of the gauge field decouple in the thermodynamic limit $N \rightarrow \infty$. The gauge fixed Hamiltonian (4.20) can also be written as a quantum spin model. Consider the Jordan-Wigner transformation

$$\psi_x = \prod_{y < x} [2iS_3(y)] S^-(x), \quad \psi_x^\dagger = \prod_{y < x} [-2iS_3(y)] S^+(x), \quad \psi_x^\dagger \psi_x = S^3(x) + 1/2 \quad (4.23)$$

Then, the Hamiltonian is

$$H = \frac{t}{2a} \sum_x (e^{iA} S^+(x+1) S^-(x) + e^{-iA} S^-(x+1) S^+(x)) + \frac{e_L^2 a}{2} \sum_{x,y} S^3(x) V(x-y) S^3(y) + e_L^2 E^2 / 2N \quad (4.24)$$

For the moment, let us ignore the constant modes E and A . The first term in the Hamiltonian is the quantum x-y model which has a disordered ground state (of course, exact solution of this model is obtained by the inverse Jordan-Wigner transformation [60, 69]). The second is a long-ranged Ising interaction. I will prove in the next section that, in spite of the low dimensionality of this system, the latter term has a Néel ordered ground state. This is a result of the infinite range of the Coulomb interaction. When both terms are present in the Hamiltonian, they compete, the first one favoring disorder and the second one favoring order. Later, when I extrapolate my strong coupling results to the continuum limit, I shall assume that the ordered ground state persists for all positive values of the dimensionless constant

$e_L^2 a^2/t$. The strong coupling limit is where this constant is large and the ground state has Néel order. The continuum limit of the Schwinger model is found where this constant is small. I shall assume that the Néel order persists in that limit. ²

4.2 The low-lying excitation spectrum

I shall examine the Schwinger model in the strong coupling limit. To solve the lattice Schwinger model in the strong coupling expansion, it is necessary to find states which are annihilated by the generator of gauge transformations

$$\mathcal{G}_x = E_x - E_{x-1} + \psi_x^\dagger \psi_x - \frac{1}{2} \quad (4.25)$$

and, at the same time, are eigenstates of the unperturbed Hamiltonian

$$H_u = \frac{e_L^2}{2} \sum_x E_x^2. \quad (4.26)$$

I shall quantize the gauge fields in the functional Schrödinger picture where the wavefunctions are functions of the variables A_x and the electric field operators are defined as

$$E_x = \frac{1}{i} \frac{\delta}{\delta A_x}. \quad (4.27)$$

In [24] it was proved that there were two gauge invariant ground states of the system. In fact, when the number, N , of lattice sites is even the two states

$$|\psi\rangle = \prod_{x=\text{even}} \psi_x^\dagger |0\rangle e^{-i \sum_x A_x \frac{(-1)^x}{4}} \quad (4.28)$$

$$|\chi\rangle = \prod_{x=\text{odd}} \psi_x^\dagger |0\rangle e^{i \sum_x A_x \frac{(-1)^x}{4}} \quad (4.29)$$

are degenerate gauge invariant ground states of H_u . They are gauge invariant since are annihilated by the operator \mathcal{G}_x . To see that they are indeed ground states, note that when H_u acts on gauge invariant states, it is effectively the sum of two operators, the zero mode energy $e_L^2 E^2/2N$ where $E = \sum_x E_x/\sqrt{N}$ and the Coulomb energy

$$H_C = \frac{e_L^2 a}{2} \sum_{x,y} \rho(x) V(x-y) \rho(y) = \frac{e_L^2 a}{2N} \sum_{k \neq 0} \rho(-k) \frac{1}{4 \sin^2 \frac{k}{2}} \rho(k). \quad (4.30)$$

where I have used the Fourier transform

$$\psi_x^\dagger \psi_x - \frac{1}{2} = \frac{1}{N} \sum_p e^{ipx} \rho(p), \quad p = \frac{2\pi n}{N}, \quad n \in \left\{ -\frac{N}{2}, \dots, \frac{N}{2} - 1 \right\} \quad (4.31)$$

Furthermore, gauge invariant states have vanishing total charge,

$$\sum_x (\psi_x^\dagger \psi_x - \frac{1}{2}) = 0 \quad (4.32)$$

The Coulomb energy satisfies the bound

$$\begin{aligned} \frac{e_L^2 a}{2N} \sum_{k \neq 0} \rho(-k) \frac{1}{4 \sin^2 \frac{k}{2}} \rho(k) &\geq \frac{e_L^2 a}{2N} \sum_{k \neq 0} \rho(-k) \frac{1}{4} \rho(k) = \\ &= \frac{e_L^2 a}{8} \sum_x (\psi_x^\dagger \psi_x - \frac{1}{2})^2 = e_L^2 a N / 32 \end{aligned} \quad (4.33)$$

²If it did not persist, but there was a second order phase transition at some critical value of the constant to a disordered state, the continuum limit would be found at that phase transition.

(since $(\psi_x^\dagger \psi_x - \frac{1}{2})^2 = \frac{1}{4}$). The states $|\psi\rangle$ and $|\chi\rangle$ are eigenstates of the charge density with eigenvalues $\rho(k) = \pm \frac{N}{2} \delta k, \pi$. These charge densities saturate the lower bound for the Coulomb energy. Furthermore, $E|\psi\rangle = 0 = E|\chi\rangle$ so $|\psi\rangle$ and $|\chi\rangle$ minimize the energy of the zero mode. Therefore, they are degenerate ground states of H_u .

The ground states are invariant under parity and charge conjugation but they both break chiral symmetry, i.e. the symmetry under translations by one site. The invariance under parity is easy to see

$$P|\psi\rangle = \prod_{x=even} (-1)^x \psi_{-x}^\dagger e^{-i \sum_x -A_{-x-1} \frac{(-1)^x}{4}} |0\rangle = |\psi\rangle \quad (4.34)$$

and analogously

$$P|\chi\rangle = -|\chi\rangle \quad (4.35)$$

For what concerns charge conjugation one has

$$C|\psi\rangle = \prod_{x=even} C \psi_x^\dagger e^{-i \sum_x A_x \frac{(-1)^x}{4}} C^{-1} |0\rangle = \prod_{x=even} \psi_{x+1} e^{-i \sum_x A_x \frac{(-1)^x}{4}} C |0\rangle = |\psi\rangle \quad (4.36)$$

where the last equality is true since, being

$$\sum_x \langle 0 | \rho(x) | 0 \rangle = -\frac{N}{2} \quad (4.37)$$

$$\sum_x \langle 0 | C^{-1} \rho(x) C | 0 \rangle = \frac{N}{2} \quad (4.38)$$

one has

$$\prod_{x=even} \psi_x^\dagger |0\rangle = \prod_{x=even} \psi_{x+1} C |0\rangle \quad (4.39)$$

Analogously one finds

$$C|\chi\rangle = |\chi\rangle \quad (4.40)$$

Under discrete chiral symmetry one gets

$$\Gamma|\psi\rangle = |\chi\rangle \quad ; \quad \Gamma|\chi\rangle = |\psi\rangle \quad (4.41)$$

The order parameter of the chiral symmetry, the mass operator $M = \frac{1}{Na} \sum_x M(x)$, is diagonal in these states and has eigenvalue $\frac{1}{2}$.³ In order to have a chiral condensate of negative sign as in the continuum, one has to consider the mass operator $M'(x) = -M(x)$. It is interesting that the ground states are degenerate and are not invariant under chiral symmetry, even in finite volume and in one spatial dimension; it is possible due to the long-ranged nature of the Coulomb interaction [43]. The chiral symmetry is spontaneously broken in the infinite volume limit. It is essential that the number of sites of the lattice, N , is even.

Of course once perturbations from the hopping term in the fermion Hamiltonian are taken into account, when the volume is finite, there are high order terms (of order N) in the strong coupling perturbation theory which mix the ground states that are constructed by perturbing $|\psi\rangle$ and $|\chi\rangle$. The mixing amplitude is

$$\langle \chi | H_p \left(\frac{1}{E_0 - H_C} H_p \right)^{N-1} | \psi \rangle = -\frac{N^2}{2} \frac{|t|^N}{2^N} \frac{4^{N-1}}{e_L^{2(N-1)}} \frac{N!}{\left(\frac{N}{2}\right)!^2} \quad (4.42)$$

Since the amplitude (4.42) is negative and real, whatever the diagonal elements are, the state with lower energy is the state

$$\frac{1}{\sqrt{2}} (|\psi\rangle + |\chi\rangle) \quad (4.43)$$

³One has to consider $M(x)$ given by Eq.(4.18) when applying it to $|\psi\rangle$ and $M(x)$ given by Eq.(4.19) when applying it to $|\chi\rangle$.

This is an eigenstate of the discrete axial transformation, with eigenvalue 1. Thus the true ground state is chirally symmetric.

In order to avoid this restoration of the symmetry, it is necessary to take the infinite N limit so that the two ground states are not mixed to any finite order of perturbation theory. Thus, in the perturbative expansion one only has to consider diagonal matrix elements and, consequently, perturbation theory for non-degenerate-states. I shall then choose as unperturbed ground state $|\psi\rangle$. The results concerning the energies would have been the same had I chosen $|\chi\rangle$.

Excitations are created by the operators

$$\psi_j^\dagger e^{i\sum_{x=i}^j A_x} \psi_i \quad (4.44)$$

and have energy $\frac{e_L^2}{2}|i-j|$ greater than the ground state energy. A single electron, in order to have a gauge invariant state, must be attached to a line of electric flux which goes from the electron to infinity. This is not allowed at all in a finite volume with periodic boundary conditions and on the infinite lattice, the string of electric flux would have infinite energy. Thus electric charges are confined and the string tension is given by the electric charge $\frac{e_L^2}{2}$.

Let us now start the perturbative computation of the excitations mass gap. I shall work in the Coulomb gauge $\nabla A = 0$, so that A is x -independent and the ground states are

$$|\psi\rangle = \prod_{x=even} \psi_x^\dagger |0\rangle \quad (4.45)$$

$$|\chi\rangle = \prod_{x=odd} \psi_x^\dagger |0\rangle. \quad (4.46)$$

The Coulomb potential reads

$$V(x-y) = \frac{1}{N} \sum_{k \neq 0} \frac{1}{4 \sin^2 \frac{k}{2}} e^{ik(x-y)} = \frac{1}{2N}(x-y)^2 - \frac{1}{2}|x-y| + \frac{1}{12N}(N^2-1). \quad (4.47)$$

The Schwinger Hamiltonian, rescaled by the factor $e_L^2 a$, may then be written as

$$H = H_0 + \epsilon H_h = \frac{1}{e_L^2 a} (H_C + H_p) \quad (4.48)$$

with

$$H_0 = \sum_{x>y} \left[\frac{(x-y)^2}{2N} - \frac{(x-y)}{2} \right] \rho(x) \rho(y) \quad (4.49)$$

$$H_h = -i \sum_x (\psi_{x+1}^\dagger e^{iA} \psi_x - \psi_x^\dagger e^{-iA} \psi_{x+1}) = -i(R-L) \quad (4.50)$$

and

$$\epsilon = \frac{t}{2e_L^2 a^2}. \quad (4.51)$$

To the fourth order in ϵ the perturbative expansion for the energy is given by⁴

$$E_\psi = E_\psi^{(0)} + \epsilon^2 E_\psi^{(2)} + \epsilon^4 E_\psi^{(4)} \quad (4.52)$$

⁴ Let us observe that for the ground state perturbative expansion the relative minus sign in the hopping Hamiltonian is irrelevant whereas it will play an important role in the calculation of the excited state energy. This is easily seen if one notices that at the second order in ϵ one gets

$$\begin{aligned} E_\psi^{(2)} &= \langle \psi | (L-R) \frac{\Pi_\psi}{E_\psi^{(0)} - H_0} (R-L) | \psi \rangle = \\ &= \langle \psi | L \frac{\Pi_\psi}{E_\psi^{(0)} - H_0} R | \psi \rangle + \langle \psi | R \frac{\Pi_\psi}{E_\psi^{(0)} - H_0} L | \psi \rangle \end{aligned}$$

where

$$E_\psi^{(0)} = \langle \psi | H_0 | \psi \rangle \quad (4.53)$$

$$E_\psi^{(2)} = \langle \psi | H_h^\dagger \frac{\Pi_\psi}{E_\psi^{(0)} - H_0} H_h | \psi \rangle \quad (4.54)$$

$$\begin{aligned} E_\psi^{(4)} = & \langle \psi | H_h^\dagger \frac{\Pi_\psi}{E_\psi^{(0)} - H_0} H_h^\dagger \frac{\Pi_\psi}{E_\psi^{(0)} - H_0} H_h \frac{\Pi_\psi}{E_\psi^{(0)} - H_0} H_h | \psi \rangle + \\ & - \langle \psi | H_h^\dagger \frac{\Pi_\psi}{E_\psi^{(0)} - H_0} H_h | \psi \rangle \langle \psi | H_h^\dagger \frac{\Pi_\psi}{(E_\psi^{(0)} - H_0)^2} H_h | \psi \rangle \end{aligned} \quad (4.55)$$

and $1 - \Pi_\psi$ is a projection operator which projects a generic state $|s\rangle$ on $|\psi\rangle$

$$(1 - \Pi_\psi)|s\rangle = |\psi\rangle . \quad (4.56)$$

The phases e^{iA} in the hopping Hamiltonian are irrelevant until one reaches the N^{th} order in the perturbative expansion. As a matter of fact, only at this order the transverse electric field becomes important. By direct evaluation one gets

$$E_\psi^{(0)} = \frac{N}{32} \quad (4.57)$$

$$E_\psi^{(2)} = -4N \quad (4.58)$$

$$E_\psi^{(4)} = 192N \quad (4.59)$$

$$E_\psi = \frac{N}{32} - 4N\epsilon^2 + 192N\epsilon^4. \quad (4.60)$$

Next I compute the energies of the low-lying excitations to the same order in the perturbative expansion. The lowest-lying excitations are degenerate and are created by the operators

$$L(x) = \psi_x^\dagger e^{iA} \psi_{x+1} \quad (4.61)$$

$$R(x) = \psi_{x+1}^\dagger e^{-iA} \psi_x \quad (4.62)$$

which move a particle one lattice spacing to the left and right respectively. When they act on the vacuum $|\psi\rangle$ they create the two states

$$|x, R\rangle \equiv R(x)|\psi\rangle = \psi_{x+1}^\dagger e^{-iA} \psi_x |\psi\rangle \quad (4.63)$$

$$|x, L\rangle \equiv L(x)|\psi\rangle = \psi_x^\dagger e^{iA} \psi_{x+1} |\psi\rangle \quad (4.64)$$

which are degenerate in energy (see Eq.(4.92)). In order to resolve the degeneracy of these two states, one must find the first nontrivial order of the perturbative expansion in which the two states are mixed; this turns out to be the second order. It is easy to show that the second order of perturbative expansion is diagonal in the two states which are created by the parity odd and even operators

$$H_-(x) \equiv R(x) + L(x) \quad (4.65)$$

$$H_+(x) \equiv R(x) - L(x) . \quad (4.66)$$

In fact

$$PH_\pm(x) = \pm H_\pm(-x) . \quad (4.67)$$

The parity odd operator creates the state with lower energy. Thus, it is this the state which will have finite energy gap in the continuum limit and which will correspond to the pseudoscalar boson of the continuum Schwinger model. In the continuum one gets this

massive excitation by applying the vector flux $j^1 = j_5^0$ to the vacuum. The excitation created by H_+ is the scalar excitation which in the continuum limit decouples from the spectrum. Since one is interested in the masses of these excitations, one has to compute their energies at zero momentum.

On the lattice the construction of the pseudoscalar excitation at zero momentum is provided by

$$\begin{aligned} |\theta\rangle &\equiv \frac{1}{\sqrt{N}} \sum_{x=1}^N |\theta(x)\rangle = \frac{1}{\sqrt{N}} \sum_{x=1}^N H_-(x) |\psi\rangle = \frac{1}{\sqrt{N}} \sum_{x=1}^N (\psi_x^\dagger e^{iA} \psi_{x+1} + \psi_{x+1}^\dagger e^{-iA} \psi_x) |\psi\rangle = \\ &= \frac{1}{\sqrt{N}} \sum_{x=1}^N j^1(x) |\psi\rangle = \frac{1}{\sqrt{N}} \sum_{x=1}^N j_5^0(x) |\psi\rangle. \end{aligned} \quad (4.68)$$

One could also consider the scalar massive excitation

$$\begin{aligned} |\varphi\rangle &\equiv \frac{1}{\sqrt{N}} \sum_{x=1}^N |\varphi(x)\rangle = \frac{1}{\sqrt{N}} \sum_{x=1}^N H_+(x) |\psi\rangle = \\ &= \frac{1}{\sqrt{N}} \sum_{x=1}^N (\psi_x^\dagger e^{iA} \psi_{x+1} - \psi_{x+1}^\dagger e^{-iA} \psi_x) |\psi\rangle = \frac{1}{\sqrt{N}} \sum_{x=1}^N j^5(x) |\psi\rangle; \end{aligned} \quad (4.69)$$

The states $|\theta\rangle$ and $|\varphi\rangle$ are characterized by a dimer-antidimer configuration; that is by a pair of particles followed or preceded by a pair of antiparticles.

The energy of the state $|\theta\rangle$, at the second order in ϵ , is given by

$$E_\theta^{(2)} = \sum_{x,y} \frac{1}{N} \langle \theta(y) | (L - R) \Lambda_\theta (R - L) | \theta(x) \rangle \quad (4.70)$$

where

$$\Lambda_\theta = \frac{\Pi_\theta}{E_\theta^{(0)} - H_0} \quad (4.71)$$

with $E_\theta^{(0)} = E_\psi^{(0)} + \Delta$, $\Delta = \frac{1}{4}$ and $1 - \Pi_\theta$ a projection operator onto $|\theta\rangle$. A state obtained by applying the hopping Hamiltonian to the state $|\theta\rangle$ has a dimer-antidimer pair; as a consequence its energy will be raised of 2Δ with respect to $E_\psi^{(0)}$.⁵ The computation of $E_\theta^{(2)}$ (see section (4.2.2)) leads to

$$E_\theta^{(2)} = -\frac{1}{\Delta} N + \frac{2}{\Delta} = -4N + 8 \quad (4.72)$$

and

$$\langle \theta | H_h^\dagger \Lambda_\theta^2 H_h | \theta \rangle = \frac{N}{\Delta^2} - \frac{2}{\Delta^2} = 16N - 32. \quad (4.73)$$

Next one should compute

$$\begin{aligned} E_\theta^{(4)} &= \frac{1}{N} \sum_{x,y} \langle \theta(y) | H_h^\dagger \Lambda_\theta H_h^\dagger \Lambda_\theta H_h \Lambda_\theta H_h | \theta(x) \rangle + \\ &- \frac{1}{N^2} \sum_{x,y} \langle \theta(y) | H_h^\dagger \Lambda_\theta H_h | \theta(x) \rangle \sum_{x,y} \langle \theta(y) | H_h^\dagger \Lambda_\theta^2 H_h | \theta(x) \rangle. \end{aligned} \quad (4.74)$$

⁵One must be careful in applying one more time the hopping Hamiltonian. Since the Coulomb Hamiltonian and the hopping Hamiltonian do not commute (see section (4.2.2)), there is a state created by applying two times the hopping Hamiltonian to the state $|\theta\rangle$ which has not a gap of 3Δ with respect to the ground state, but it has a gap of 5Δ -characterized by three particles followed or preceded by three antiparticles, that is, it is created by applying L^3 or R^3 to the ground state.

Using the matrix elements given in paragraph (4.2.2), one gets

$$E_\theta^{(4)} = \frac{3}{\Delta^3}N - \frac{9}{\Delta^3} = 192N - 576 . \quad (4.75)$$

The pseudoscalar excitation energy, to the fourth order in ϵ , is then given by

$$E_\theta = \left(\frac{N}{32} + \frac{1}{4}\right) + (-4N + 8)\epsilon^2 + (192N - 576)\epsilon^4 . \quad (4.76)$$

Using again the matrix element given in appendix C, one easily obtains the energy E_φ of the state $|\varphi\rangle$, *i.e.*

$$E_\varphi = \left(\frac{N}{32} + \frac{1}{4}\right) + (-4N + 24)\epsilon^2 + (192N - 1600)\epsilon^4 . \quad (4.77)$$

Taking the difference between E_θ (E_φ) and E_ψ , one gets the masses of the pseudoscalar and scalar excitations,

$$\frac{m^P}{e_L^2 a} = \frac{1}{4} + 8\epsilon^2 - 576\epsilon^4 , \quad (4.78)$$

$$\frac{m^S}{e_L^2 a} = \frac{1}{4} + 24\epsilon^2 - 1600\epsilon^4 . \quad (4.79)$$

Eqs.(4.78,4.79) provide the behavior of m^P and m^S for small values of $z = \epsilon^2 = \frac{t^2}{4e_L^2 a^4}$.

As expected from the continuum theory, the pseudoscalar particle mass is smaller than the scalar particle mass. Furthermore, since both quantities are intensive, there is no N dependence in Eqs.(4.78,4.79).

Now let us compute the dispersion relation of the pseudoscalar and scalar excitations to the fourth order in perturbation theory.

At the zero-th order one has no momentum dependence in the lattice pseudoscalar excitation since

$$E_\theta^{(0)}(p) = \frac{1}{N} \sum_{x,y} \langle \theta(y) | H_0 | \theta(x) \rangle e^{ip(x-y)} = \frac{N}{32} + \Delta = \frac{N}{32} + \frac{1}{4} . \quad (4.80)$$

The momentum dependence starts only at the second order in ϵ , where one gets

$$E_\theta^{(2)}(p) = \frac{1}{N} \sum_{x,y} \langle \theta(y) | H_h^\dagger \Lambda_\theta H_h | \theta(x) \rangle e^{ip(x-y)} . \quad (4.81)$$

Using the matrix elements given in paragraph (4.2.2), one has

$$E_\theta^{(2)}(p) = -\frac{1}{\Delta}(N - 4) - \frac{2}{\Delta} \cos pa = -4N + 16 - 8 \cos pa . \quad (4.82)$$

The dispersion relation, at the fourth order in perturbation theory, reads

$$E_\theta^{(4)}(p) = \frac{1}{N} \sum_{x,y} \langle \theta(y) | H_h^\dagger \Lambda_\theta H_h^\dagger \Lambda_\theta H_h \Lambda_\theta H_h | \theta(x) \rangle e^{ip(x-y)} + \\ - \frac{1}{N^2} \sum_{x,y} \langle \theta(y) | H_h^\dagger \Lambda_\theta H_h | \theta(x) \rangle e^{ip(x-y)} \sum_{x,y} \langle \theta(y) | H_h^\dagger \Lambda_\theta^2 H_h | \theta(x) \rangle e^{ip(x-y)} \quad (4.83)$$

and leads to

$$\begin{aligned} E_\theta^{(4)}(p) &= \frac{3}{\Delta^3}N - \frac{1}{2\Delta^3}\cos 2pa + \frac{4}{\Delta^3}(2\cos pa - \cos^2 pa) - \frac{25}{2}\frac{1}{\Delta^3} = \\ &= 192N - 32\cos 2pa + 256(2\cos pa - \cos^2 pa) - 800 . \end{aligned} \quad (4.84)$$

Using Eqs.(4.80), (4.81) and (4.84), the dispersion relation of the lattice pseudoscalar excitation is given by

$$\begin{aligned} E_\theta(p) &= E_\theta^{(0)}(p) + \epsilon^2 E_\theta^{(2)}(p) + \epsilon^4 E_\theta^{(4)}(p) + \dots = \\ &= E_\theta(0) + \frac{2}{\Delta}(1 - \cos pa)\epsilon^2 + \left[\frac{1}{2\Delta^3}(1 - \cos 2pa) - \frac{4}{\Delta^3}(1 - \cos pa)^2\right]\epsilon^4 = \\ &= E_\theta(0) + 8(1 - \cos pa)\epsilon^2 + [32(1 - \cos 2pa) - 256(1 - \cos pa)^2]\epsilon^4. \end{aligned} \quad (4.85)$$

Performing a small momentum expansion, one gets

$$E_\theta(p) = E_\theta(0) + (4\epsilon^2 + 64\epsilon^4)(pa)^2 + \dots \quad (4.86)$$

The same procedure yields

$$\begin{aligned} E_\varphi(p) &= E_\varphi^{(0)}(p) + \epsilon^2 E_\varphi^{(2)}(p) + \epsilon^4 E_\varphi^{(4)}(p) + \dots = \\ &= E_\theta(0) - \frac{2}{\Delta}(1 - \cos pa)\epsilon^2 + \left[\frac{1}{2\Delta^3}(1 - \cos 2pa) + \frac{16}{\Delta^3} - \frac{4}{\Delta^3}(1 + \cos pa)^2\right]\epsilon^4 = \\ &= E_\theta(0) - 8(1 - \cos pa)\epsilon^2 + [32(1 - \cos 2pa) + 1024 - 256(1 + \cos pa)^2]\epsilon^4. \end{aligned} \quad (4.87)$$

which, for small momentum gives

$$E_\varphi(p) = E_\varphi(0) + (-4\epsilon^2 + 72\epsilon^4)(pa)^2 + \dots \quad (4.88)$$

The p^2 terms are consistent with the bosonic nature of the excitations.

Eq.(4.86) and Eq.(4.88) give us the masses of the pseudoscalar and scalar excitations from the curvature of the energy momentum relation

$$\frac{1}{2m_*^P e_L^2 a^3} = (4\epsilon^2 + 64\epsilon^4) \quad (4.89)$$

$$\frac{1}{2m_*^S e_L^2 a^3} = (-4\epsilon^2 + 72\epsilon^4) \quad (4.90)$$

4.2.1 Unperturbed energies of the dimer states

In this section the energies of the excitations generated by applying the hopping Hamiltonian H_h to the ground state $|\psi\rangle$, are evaluated. The action of H_h on the state $|\psi\rangle$ generates a dimer-antidimer pair. All the states with one dimer-antidimer pair, and with two dimer-antidimer pairs (obtained applying H_h twice), have the same energy gap with respect to the ground state. However, not all the states obtained applying $(H_h)^n$, with $n \geq 3$, to $|\psi\rangle$ have the same energy. There are, for example, two possible energies, corresponding to a gap of $3\Delta = 3e_L^2 a/4$ and 5Δ , for the states with three dimer-antidimer pairs.

The states with a dimer-antidimer pair are given by

$$|S_{R,L}^1\rangle = H_{R,L}(y)|\psi\rangle . \quad (4.91)$$

Applying on these states the unperturbed Hamiltonian one gets

$$\begin{aligned} H_u |S_{R,L}^1 \rangle &= H_{R,L}(y) \frac{e_L^2 a}{2} \sum_x (E_x \pm \delta_{xy})^2 |\psi \rangle = \\ &= [E_\psi^0 + \frac{e_L^2 a}{2} \sum_x (-\frac{(-1)^x}{2} \delta_{xy} + \delta_{xy})] |S_{R,L}^1 \rangle \end{aligned} \quad (4.92)$$

where y must be even if one applies R and must be odd if one applies L . One thus sees that all the states $|S_{R,L}^1 \rangle$ have a mass gap of Δ .

The states with two dimer-antidimer pairs are given by

$$|S_{(R,L)(R,L)}^2 \rangle = H_{R,L}(z) H_{R,L}(y) |\psi \rangle \quad (4.93)$$

$$H_u |S_{(R,L)(R,L)}^2 \rangle = \frac{e_L^2 a}{2} H_{R,L}(z) H_{R,L}(y) \sum_x (E_x \pm \delta_{xz} \pm \delta_{xy})^2 |\psi \rangle \quad (4.94)$$

It is easy to show that all these states have an energy gap of 2Δ .

Based on Eq.(4.92) and Eq.(4.94) one might expect that the states with three dimer-antidimer pairs have an energy gap of 3Δ . This is actually true for all the states of this type except for the 2 states with three particles followed or preceded by three antiparticles. These states have an energy gap of 5Δ . If one considers the state

$$|S_{RRR}^3 \rangle = R(w)R(z)R(y)|\psi \rangle, \quad (4.95)$$

one easily obtains that

$$\begin{aligned} H_u |S_{RRR}^3 \rangle &= \frac{e_L^2 a}{2} R(w)R(z)R(y) \sum_x (E_x + \delta_{xw} + \delta_{xz} + \delta_{xy})^2 |\psi \rangle = \\ &= [E_\psi^0 + \frac{e_L^2 a}{2} \sum_x (-\frac{(-1)^x}{2} \delta_{xw} - \frac{(-1)^x}{2} \delta_{xz} - \frac{(-1)^x}{2} \delta_{xy} + \\ &+ 2\delta_{xw}\delta_{xz} + 2\delta_{xw}\delta_{xy} + 2\delta_{xz}\delta_{xy} + \\ &+ \delta_{xw} + \delta_{xz} + \delta_{xy})] |S_{RRR}^3 \rangle \end{aligned} \quad (4.96)$$

To generate a state with three antiparticles followed by three particles, one must have

$$z = y - 2 \quad (4.97)$$

$$w = y - 1 \quad (4.98)$$

The energy gap for this state is 5Δ . The same result is obtained for the state $|S_{LLL}^3 \rangle = L(w)L(z)L(y)|\psi \rangle$ with $z = y + 3$ and $w = y + 2$, which contains three particles followed by three antiparticles.

The reason for these different behaviours, lies on the fact that the commutation relation between H_0 and H_h is

$$[H_0, H_h] = \frac{e_L^2 a}{4} H_h + \frac{e_L^2 t}{8} (\sum_{j \geq k} - \sum_{k \geq j}) (\psi_{k+1}^\dagger e^{iA} \psi_k - \psi_k^\dagger e^{-iA} \psi_{k+1}) \rho_j \quad (4.99)$$

If the second term in the r.h.s. was absent, all the states with n dimer-antidimer pairs would have an energy gap of $n\Delta$.

4.2.2 Perturbative matrix elements

In paragraph I provide the matrix elements needed in the strong coupling expansion expression of the mass gap. The six matrix elements that arise in the computation of the second

order bosonic excitation energies, are

$$\begin{aligned} M_1 &= \langle \psi | R(y) R \Lambda_\theta L L(x) | \psi \rangle = \\ &= -\frac{1}{\Delta} \left(\frac{N}{2} - 1 \right) \delta_{xy} - \frac{1}{\Delta} (1 - \delta_{xy}) \end{aligned} \quad (4.100)$$

$$\begin{aligned} M_2 &= \langle \psi | L(y) L \Lambda_\theta R R(x) | \psi \rangle = \\ &= -\frac{1}{\Delta} \left(\frac{N}{2} - 1 \right) \delta_{xy} - \frac{1}{\Delta} (1 - \delta_{xy}) \end{aligned} \quad (4.101)$$

$$\begin{aligned} M_3 &= \langle \psi | R(y) L \Lambda_\theta R L(x) | \psi \rangle = \\ &= -\frac{1}{\Delta} \left(\frac{N}{2} - 3 \right) \delta_{xy} + \frac{1}{\Delta} (1 - \delta_{xy}) \end{aligned} \quad (4.102)$$

$$\begin{aligned} M_4 &= \langle \psi | L(y) R \Lambda_\theta L R(x) | \psi \rangle = \\ &= -\frac{1}{\Delta} \left(\frac{N}{2} - 3 \right) \delta_{xy} + \frac{1}{\Delta} (1 - \delta_{xy}) \end{aligned} \quad (4.103)$$

$$\begin{aligned} M_5 &= -\langle \psi | R(y) L \Lambda_\theta L R(x) | \psi \rangle = \\ &= -\frac{1}{\Delta} (\delta_{y,x-1} + \delta_{y,x+1}) \end{aligned} \quad (4.104)$$

$$\begin{aligned} M_6 &= -\langle \psi | L(y) R \Lambda_\theta R L(x) | \psi \rangle = \\ &= -\frac{1}{\Delta} (\delta_{y,x-1} + \delta_{y,x+1}) \end{aligned} \quad (4.105)$$

where M_1 and M_3 are defined for x and y odd, M_2 and M_4 for x and y even, M_5 for x even and y odd, and M_6 for x odd and y even.

To compute the fourth order energy gap one needs also the matrix elements M'_i , $i = 1, \dots, 6$ obtained by replacing Λ_θ with Λ_θ^2 in M_i

$$M'_1 = M'_2 = M'_3 = M'_4 = \frac{1}{\Delta^2} \left(\frac{N}{2} - 1 \right) \delta_{xy} + \frac{1}{\Delta^2} (1 - \delta_{xy}) \quad (4.106)$$

$$M'_5 = M'_6 = -\frac{1}{\Delta^2} (\delta_{y,x-1} + \delta_{y,x+1}) - \frac{2}{\Delta^2} (1 - \delta_{y,x-1} - \delta_{y,x+1}) \quad (4.107)$$

with the same constraints on x and y as before.

One must then evaluate the twenty matrix elements arising when three H_R and three H_L are combined in all possible ways in the expression in the first line of Eq.(4.74)

$$\langle \theta(y) | (L - R) \Lambda_\theta (L - R) \Lambda_\theta (R - L) \Lambda_\theta (R - L) | \theta(x) \rangle \quad (4.108)$$

Since hermiticity of the Hamiltonian requires that the elements obtained changing R with L are equal one has only to compute the ten matrix elements,

$$M''_1 = \frac{1}{N} \sum_{x,y} M''_1(x,y) = \frac{1}{N} \sum_{x,y} \langle \psi | R(y) R \Lambda_\theta R \Lambda_\theta L \Lambda_\theta L L(x) | \psi \rangle \quad (4.109)$$

$$M''_2 = \frac{1}{N} \sum_{x,y} M''_2(x,y) = \frac{1}{N} \sum_{x,y} \langle \psi | R(y) L \Lambda_\theta L \Lambda_\theta R \Lambda_\theta R L(x) | \psi \rangle \quad (4.110)$$

$$M''_3 = \frac{1}{N} \sum_{x,y} M''_3(x,y) = \frac{1}{N} \sum_{x,y} \langle \psi | R(y) R \Lambda_\theta L \Lambda_\theta R \Lambda_\theta L L(x) | \psi \rangle \quad (4.111)$$

$$M''_4 = \frac{1}{N} \sum_{x,y} M''_4(x,y) = \frac{1}{N} \sum_{x,y} \langle \psi | R(y) R \Lambda_\theta L \Lambda_\theta L \Lambda_\theta R L(x) | \psi \rangle \quad (4.112)$$

$$M''_5 = \frac{1}{N} \sum_{x,y} M''_5(x,y) = \frac{1}{N} \sum_{x,y} \langle \psi | R(y) L \Lambda_\theta R \Lambda_\theta R \Lambda_\theta L L(x) | \psi \rangle \quad (4.113)$$

$$M''_6 = \frac{1}{N} \sum_{x,y} M''_6(x,y) = \frac{1}{N} \sum_{x,y} \langle \psi | R(y) L \Lambda_\theta R \Lambda_\theta L \Lambda_\theta R L(x) | \psi \rangle \quad (4.114)$$

$$M_7'' = \frac{1}{N} \sum_{x,y} M_7''(x,y) = -\frac{1}{N} \sum_{x,y} \langle \psi | R(y) R \Lambda_\theta L \Lambda_\theta L \Lambda_\theta L R(x) | \psi \rangle \quad (4.115)$$

$$M_8'' = \frac{1}{N} \sum_{x,y} M_8''(x,y) = -\frac{1}{N} \sum_{x,y} \langle \psi | R(y) L \Lambda_\theta R \Lambda_\theta L \Lambda_\theta L R(x) | \psi \rangle \quad (4.116)$$

$$M_9'' = \frac{1}{N} \sum_{x,y} M_9''(x,y) = -\frac{1}{N} \sum_{x,y} \langle \psi | R(y) L \Lambda_\theta L \Lambda_\theta R \Lambda_\theta L R(x) | \psi \rangle \quad (4.117)$$

$$M_{10}'' = \frac{1}{N} \sum_{x,y} M_{10}''(x,y) = -\frac{1}{N} \sum_{x,y} \langle \psi | R(y) L \Lambda_\theta L \Lambda_\theta L \Lambda_\theta R R(x) | \psi \rangle \quad (4.118)$$

where $M_1''(x,y), \dots, M_6''(x,y)$ are defined for x and y odd, $M_7''(x,y), \dots, M_{10}''(x,y)$ are defined for x even and y odd. The results are

$$\begin{aligned} M_1''(x,y) &= -\frac{1}{2\Delta^3} \delta_{x,y} - \frac{1}{4\Delta^3} (N-2)(N-4) \delta_{x,y} + \\ &\quad - \frac{1}{4\Delta^3} (\delta_{y,x+2} + \delta_{y,x-2}) - \frac{1}{\Delta^3} (N-4)(1 - \delta_{x,y}) \end{aligned} \quad (4.119)$$

$$M_2''(x,y) = -\frac{1}{4\Delta^3} (N-4)(N-6) \delta_{x,y} \quad (4.120)$$

$$\begin{aligned} M_3''(x,y) &= M_4''(x,y) = M_5''(x,y) = M_6''(x,y) = -\frac{1}{8\Delta^3} (N-4)(N-6) \delta_{x,y} + \\ &\quad - \frac{1}{4\Delta^3} (N-6) (\delta_{y,x+2} + \delta_{y,y-2}) - \frac{1}{4\Delta^3} (1 - \delta_{x,y} - \delta_{y,x+2} - \delta_{y,x-2}) \end{aligned} \quad (4.121)$$

$$\begin{aligned} M_7''(x,y) &= M_8''(x,y) = M_9''(x,y) = M_{10}''(x,y) = \\ &= \frac{1}{2\Delta^3} (N-6) (1 - \delta_{y,x-1} - \delta_{y,x+1}) \end{aligned} \quad (4.122)$$

and

$$M_1'' = -\frac{1}{2\Delta^3} - \frac{3}{8\Delta^3} (N-2)(N-4) \quad (4.123)$$

$$M_2'' = M_3'' = M_4'' = M_5'' = M_6'' = -\frac{1}{8\Delta^3} (N-4)(N-6) \quad (4.124)$$

$$M_7'' = M_8'' = M_9'' = M_{10}'' = +\frac{1}{8\Delta^3} (N-4)(N-6) \quad (4.125)$$

4.3 The chiral condensate

In the continuum Schwinger model, the phenomenon of dynamical symmetry breaking of the chiral symmetry, is due to the anomaly. The order parameter is the mass operator $M(x) = \bar{\psi}(x)\psi(x)$ which acquires a non zero vacuum expectation value, giving rise to the chiral condensate [62]

$$\chi_c = \langle \bar{\psi}(x)\psi(x) \rangle = -\frac{e^\gamma}{2\pi} m_c = -\frac{e^\gamma}{2\pi} \frac{e_c}{\sqrt{\pi}}. \quad (4.126)$$

In this section I compute the lattice chiral condensate to the fourth order in perturbation theory. In the staggered fermion formalism (having put particles on even sites and antiparticles on odd sites), one has

$$\bar{\psi}(x)\psi(x) \longrightarrow \frac{(-1)^x}{a} (\psi_x^\dagger \psi_x - \frac{1}{2}) \quad (4.127)$$

The lattice chiral condensate may be obtained by considering the mass operator

$$M = -\frac{1}{Na} \sum_{x=1}^N (-1)^x \psi_x^\dagger \psi_x \quad (4.128)$$

where the extra minus sign is there to give the same sign to the lattice and continuum chiral condensates (see footnote 1 of this chapter), and evaluating the expectation value of (4.128) on the perturbed states $|p_\psi\rangle$ generated by applying H_h to $|\psi\rangle$. One has

$$|p_\psi\rangle = |\psi\rangle + \epsilon|p_\psi^1\rangle + \epsilon^2|p_\psi^2\rangle \quad (4.129)$$

where

$$|p_\psi^1\rangle = -\frac{1}{\Delta}H_h|\psi\rangle \quad (4.130)$$

$$|p_\psi^2\rangle = \frac{\Pi_\psi}{2\Delta^2}H_hH_h|\psi\rangle. \quad (4.131)$$

The lattice chiral condensate is then given by

$$\chi_L = \frac{\langle p_\psi|M|p_\psi\rangle}{\langle p_\psi|p_\psi\rangle} = \frac{\langle \psi|M|\psi\rangle + \epsilon^2 \langle p_\psi^1|M|p_\psi^1\rangle + \epsilon^4 \langle p_\psi^2|M|p_\psi^2\rangle}{\langle \psi|\psi\rangle + \epsilon^2 \langle p_\psi^1|p_\psi^1\rangle + \epsilon^4 \langle p_\psi^2|p_\psi^2\rangle}. \quad (4.132)$$

One gets the following expressions for the wave functions

$$\langle \psi|\psi\rangle = 1 \quad (4.133)$$

$$\langle p_\psi^1|p_\psi^1\rangle = \frac{N}{\Delta^2} \quad (4.134)$$

$$\langle p_\psi^2|p_\psi^2\rangle = \frac{N(N-3)}{2\Delta^4} \quad (4.135)$$

and for the M operator

$$\langle \psi|M|\psi\rangle = -\frac{1}{2a} \quad (4.136)$$

$$\langle p_\psi^1|M|p_\psi^1\rangle = -\frac{1}{\Delta^2 a} \left(\frac{N}{2} - 2\right) \quad (4.137)$$

$$\langle p_\psi^2|M|p_\psi^2\rangle = -\frac{1}{4\Delta^4 a} \left(\frac{N}{2} - 4\right) \cdot 2 \cdot (N-3). \quad (4.138)$$

To the fourth order in ϵ , the lattice chiral condensate is given by

$$\chi_L = -\frac{1}{a} \left(\frac{1}{2} - \frac{2}{\Delta^2} \epsilon^2 + \frac{6}{\Delta^4} \epsilon^4\right) = -\frac{1}{a} \left(\frac{1}{2} - 32\epsilon^2 + 1536\epsilon^4\right). \quad (4.139)$$

4.4 Lattice versus continuum

In this section I want to extract some physics from the lattice results I obtained; to do this, one should compare the answer of the strong coupling analysis of the lattice theory with the exact results of the continuum model. For this purpose one should extrapolate the strong coupling expansion derived under the assumption that the parameter $z = \frac{t^2}{4e_L^4 a^4} \ll 1$ to the region in which $z \gg 1$; this region corresponds to the continuum theory since $e_L^4 a^4 \rightarrow 0$, $z \rightarrow \infty$. To make this extrapolation possible, it is customary [29] to make use of Padé approximants, which allow to extrapolate a series expansion beyond the convergence radius. Strong coupling perturbation theory improved with Padé approximants should be compared with the continuum theory.

As we shall see, the gauge invariant strong coupling expansion here proposed, provides a very accurate estimate of the observables of the continuum theory, already at the second order in powers of z . This strongly suggests that, expanding around the gauge, parity and charge conjugation invariant ground state $|\psi\rangle$, leads to a perturbative series converging to the continuum theory faster than the one used in [63, 67].

Let us first compute the ratio between the continuum value of the meson mass $m_c = e_c/\sqrt{\pi}$ and the lattice coupling constant e_L , by equating the lattice chiral condensate (4.139), to its continuum counterpart (4.126)

$$\frac{1}{a} \left(\frac{1}{2} - 32z + 1536z^2 \right) = \frac{e^\gamma}{2\pi} m_c . \quad (4.140)$$

Of course, Eq.(4.140) is true only when Padé approximants are used, since - as it stands - the l.h.s. holds only for $z \ll 1$, while the r.h.s. provides the value of the chiral condensate to be obtained when $z \simeq \infty$. Using the relation

$$a = \left(\frac{t^2}{4z} \right)^{\frac{1}{4}} \frac{1}{e_L} \quad (4.141)$$

one gets from (4.140)

$$\frac{m_c}{e_L} = \left(\frac{4z}{t^2} \right)^{\frac{1}{4}} \frac{2\pi}{e^\gamma} \left(\frac{1}{2} - 32z + 1536z^2 \right) \quad (4.142)$$

As in Ref. [63], due to the factor $z^{\frac{1}{4}}$, the fourth power of (4.142) should be considered in order to construct a non-diagonal Padé approximant. Since the strong coupling expansion has been carried out up to second order in z , one is allowed to construct only the $[0, 1]$ Padé approximant for the polynomial written in (4.142). One gets

$$\left(\frac{m_c}{e_L} \right)^4 = \frac{1}{4t^2} \left(\frac{2\pi}{e^\gamma} \right)^4 \frac{z}{1 + 256z} \quad (4.143)$$

Taking the continuum limit $z \rightarrow \infty$ one has

$$\left(\frac{m_c}{e_L} \right)^4 = \frac{\pi^4}{64e^{4\gamma}} \frac{1}{t^2} \quad (4.144)$$

Next let us compute the same ratio by equating the pseudoscalar mass gap given in (4.78) to its continuum counterpart m_c

$$e_L^2 a \left(\frac{1}{4} + 8z - 576z^2 \right) = m_c . \quad (4.145)$$

Again Eq.(4.145) is true only when Padé approximants are used.

Dividing both sides of Eq.(4.145) by e_L and taking into account that

$$e_L a = \left(\frac{t^2}{4z} \right)^{\frac{1}{4}}, \quad (4.146)$$

one gets

$$\frac{m_c}{e_L} = \left(\frac{t^2}{4z} \right)^{\frac{1}{4}} \left(\frac{1}{4} + 8z - 576z^2 \right), \quad (4.147)$$

Taking the fourth power, as I did for the chiral condensate equation, and constructing the $[1, 0]$ Padé approximant for the r.h.s. of Eq.(4.147) one gets

$$\left(\frac{m_c}{e_L} \right)^4 = \frac{t^2}{4z} \left(\frac{1}{256} + \frac{z}{2} \right) \quad (4.148)$$

One may now take the limit $z \rightarrow \infty$, obtaining

$$\left(\frac{m_c}{e_L} \right)^4 = \frac{t^2}{8} . \quad (4.149)$$

Equating Eq.(4.144) and Eq.(4.149) one gets an equation for t which gives

$$t = \frac{\pi}{8^{\frac{1}{4}} e^\gamma} = 1.049 \quad (4.150)$$

which lies 4.9% above the exact value. It is comforting to see that the lattice theory gives a light velocity very close to (but greater than) 1. Putting this value of t in Eq.(4.144) or Eq.(4.149) one has

$$\frac{m_c}{e_L} = 0.609 \quad (4.151)$$

which lies 7.9% above the exact value $\frac{1}{\sqrt{\pi}}$.

It is worth to stress that I can reproduce very well the continuum results, even if I use just first order (in z) results of the strong coupling perturbation theory.

A second way [63] to extrapolate the polinomial in (4.142) is to equate it to the ratio

$$\frac{(1+bz)^x}{(1+az)^{x+\frac{1}{4}}} = 1 - 64z + 3072z^2 \quad (4.152)$$

so that one can take the limit $z \rightarrow \infty$ in (4.142). Setting $t = 1$ one gets

$$\frac{m_c}{e_L} = \frac{\sqrt{2\pi}}{e^\gamma} \frac{b^x}{a^{x+\frac{1}{4}}} \quad (4.153)$$

It is worth to say that this extrapolation works for a large range of values of the parameter x between 0 and 6 giving an answer that lies between 6.9% below and 10% above the exact answer. In particular for $x = 1$ one gets $\frac{m_c}{e_L} = 0.596$ which lies 5.6% above the exact value. For $x = \frac{3}{4}$ one gets $\frac{m_c}{e_L} = 0.593$ wich differs from the continuum value of the 5.1%. For $x = \frac{1}{10}$ one has only 0.7% of error. In the same way one can extrapolate the polinomial in (4.147)

$$\frac{(1+bz)^{x+\frac{1}{4}}}{(1+az)^x} = 1 + 32z - 2304z^2 \quad (4.154)$$

so that one can then take the limit $z \rightarrow \infty$ in (4.147). Setting $t = 1$ one gets

$$\frac{m_c}{e_L} = \frac{1}{4^{\frac{5}{4}}} (b)^{x+\frac{1}{4}} \frac{1}{a^x} \quad (4.155)$$

for $x = 1$ one gets $\frac{m_c}{e_L} = 0.617$ which lies 9% above the exact value, against the 30% error of ref.[63]. For $x = 0.5$ one has $\frac{m_c}{e_L} = 0.595$ which lies only 5.4% above the exact answer.

In the continuum Schwinger model the ratio between the masses of the scalar and the pseudoscalar particles, m^S/m^P , equals 2, since m^S is the lowest eigenvalue of the continuum mass spectrum, which starts at $2m^P$ [63]. I shall now evaluate this ratio using the lattice expression of m^P and m^S (4.78,4.79). m^S/m^P is given by

$$\frac{m^S}{m^P} = \frac{\frac{1}{4} + 24z - 1600z^2}{\frac{1}{4} + 8z - 576z^2} \quad (4.156)$$

Expanding the r.h.s. of (4.156) in power series of z

$$\frac{m^S}{m^P} = 1 + 64z - 6144z^2 \quad , \quad (4.157)$$

one may perform the [1, 1] Padé approximant

$$\frac{m^S}{m^P} = \frac{1 + 160z}{1 + 96z} \quad (4.158)$$

For $z \rightarrow \infty$

$$\frac{m^S}{m^P} = 1.67 \quad (4.159)$$

which lies 16% below the continuum value. My result coincides with the one obtained in [63] at the same order in the perturbative expansion.

Taking the $[1, 1]$ Padé approximants of Eq.(4.89) and Eq.(4.90) one can compute in an independent way the ratio between the masses of the scalar and pseudoscalar particles

$$\frac{m_*^S}{m_*^P} = -\frac{1 + 18z}{1 - 16z} \quad (4.160)$$

For $z \rightarrow \infty$

$$\frac{m_*^S}{m_*^P} = 1.125 \quad (4.161)$$

which lies 43% below the exact value. This means that one should go to the next order in perturbation theory in Eq.(4.89) and Eq.(4.90) to reproduce better the continuum limit, since in Eq.(4.89) and Eq.(4.90) one has no zeroth order term. Another test (also suggested in [63]) to check the validity of the lattice computations, may be performed by computing the quantity

$$D = \frac{z^{3/4}}{m^P} \frac{d}{dz} (z^{1/4} m^P) = \frac{1}{4} + \frac{z}{m^P} \frac{dm^P}{dz} . \quad (4.162)$$

This should equal $1/4$ if the lattice theory has to reproduce the continuum result.

Using (4.78) one gets

$$D = z \frac{8 - 1152z}{1/4 + 8z} \simeq 32z(1 - 176z) . \quad (4.163)$$

Constructing the $[0, 1]$ Padé approximant and taking the $z \rightarrow \infty$ limit, one has

$$D = z \frac{32}{1 + 176z} \xrightarrow{z \rightarrow \infty} = \frac{2}{11} = 0.182 \quad (4.164)$$

which lies 27% below the desired 0.25. This coincides with the result obtained in [63], using a strong coupling expansion up to the order z^4 . The agreement of my results with the continuum theory is very encouraging, since only terms up to the order z^2 have been used in the gauge invariant strong coupling expansion proposed in this paper.

4.5 Summary

The investigation, that has been exposed, is aimed at constructing an improved strong coupling expansion for the lattice Schwinger model. I showed that, gauge invariance together with the discrete symmetries of the model, force the ground state to be a Néel state. Moreover gauge invariance requires the ground state to have electric fields related to the charge density operator by the Gauss's law. Thus, for large e_L^2 , the ground state energy is of order e_L^2 rather than $\frac{1}{e_L}$ [63]; as a consequence, the strong coupling expansion here constructed provides a very accurate extrapolation to the continuum theory already at the second order in $z = \frac{t^2}{4e_L^4 a^4}$. Furthermore, the Coulomb energy of elementary excitations is also affected, since – besides the Coulomb self energy – there is also an interaction energy with the charge of the ground state.

The strongly coupled lattice Schwinger model is equivalent to a one-dimensional antiferromagnetic Ising spin chain with a Coulomb long range interaction, which admits the Néel state as an exact ground state. Due to this, in my approach, chiral symmetry is broken spontaneously in the lattice model already at zero-th order in z . I expect that chiral symmetry breaking should persist for all coupling, since the critical coupling for $D = 1$ should be at $e_L^2 = 0$. I conjecture that, for small e_L^2 , this behavior is a manifestation of a Peierls instability – the tendency of a one dimensional Fermi gas to form a gap at the Fermi surface. This happens with any infinitesimal interaction.

In the continuum theory the Schwinger model exhibits the Nambu-Goldstone phenomenon: global chiral symmetry is spontaneously broken, but no Goldstone boson appears in the spectrum since the local current is anomalous [66]. On the lattice there is no anomaly due to the Nielsen-Ninomiya theorem [27].

The present analysis shows that in the strong coupling limit, chiral symmetry is spontaneously broken at all orders, since the states $|\psi\rangle$ and $|\chi\rangle$ mix only at a perturbative order comparable with the volume of the system. Being chiral symmetry replaced by the discrete symmetry representing invariance under translations by one lattice site, effects related to the breaking of the chiral symmetry on the lattice should come from the coupling between the two sublattices. This is manifest in my strong coupling calculations.

Chapter 5

The two-flavor lattice Schwinger model

In this chapter I study the $SU(2)$ -flavor lattice Schwinger model in the hamiltonian formalism using staggered fermions. The existence of the continuum internal isospin symmetry makes the model much more interesting than the one-flavor case; the spectrum is extremely richer, exhibiting also massless excitations and the chiral symmetry breaking pattern is completely different from the one-flavor case. I shall demonstrate [39, 40] that the strong coupling limit of the two-flavor lattice Schwinger model is mapped onto an interesting quantum spin model – the one-dimensional spin-1/2 quantum Heisenberg antiferromagnet. The ground state of the antiferromagnetic chain has been known since many years [36] and its energy was computed in [37]; the complete spectrum has been determined by Faddeev and Takhtadzhyan [30] using the algebraic Bethe ansatz.

The two-flavor lattice Schwinger model with non-zero fermion mass m has been analysed in [70] in the limit of heavy fermions $m \gg e^2$; good agreement with the continuum theory has been found.

There are by now many hints at a correspondence between quantized gauge theories and quantum spin models, aimed at analyzing new phases relevant for condensed matter systems [16, 17, 18, 19, 20]. Recently Laughlin has argued that there is an analogy between the spectral data of gauge theories and strongly correlated electron systems [25]. Moreover, certain spin ladders have been shown to be related to the two-flavor Schwinger model [71].

The correspondence between the $SU(2)$ flavor Schwinger model and the quantum Heisenberg antiferromagnetic chain provides a concrete computational scheme in which the issue of the correspondence between quantized gauge theories and quantum spin models may be investigated. Because of dimensionality of the coupling constant in (1+1)-dimensions the infrared behavior is governed by the strong coupling limit, and it is tempting to conjecture the existence of an exact correspondence between the infrared limits of the Heisenberg and two-flavor Schwinger models. I shall derive [39, 40] results which support this conjecture. For example the gapless modes in the spectra have identical quantum numbers; within the accuracy of the strong coupling limit, the gapped mode of the two-flavor Schwinger model was also identified in the spectrum of the Heisenberg model.

In this chapter I present a complete study [40] of the strong coupling limit of the two-flavor lattice Schwinger model. I firstly compute explicitly the masses of the excitations to the second order in the strong coupling expansion; this computation needs the knowledge of

the spin-spin correlators of the quantum Heisenberg antiferromagnetic chain. The continuum massless two-flavor Schwinger model does exhibit neither an isoscalar $\langle \bar{\psi}\psi \rangle$ nor an isovector $\langle \bar{\psi}\sigma^a\psi \rangle$ chiral condensate, since this is forbidden by the Coleman theorem [43]. On the lattice I show that these fermion condensates are zero to all the orders in the strong coupling expansion. Moreover I find that the pertinent chiral condensate is $\langle \bar{\psi}_L^{(2)}\bar{\psi}_L^{(1)}\psi_R^{(1)}\psi_R^{(2)} \rangle$ and I compute its lattice expression up to the second order in the strong coupling expansion. It should be noticed that, in absence of gauge fields, the chiral condensate is zero, is different from zero only when the fermions are coupled to gauge fields. This can be viewed as the manifestation of the chiral anomaly in this model. I finally compare the lattice results with the ones of the continuum theory.

5.1 Definition of the model

The action of the 1 + 1-dimensional electrodynamics with two charged Dirac spinor fields is

$$S = \int d^2x \left[\sum_{a=1}^2 \bar{\psi}_a (i\gamma_\mu \partial^\mu + \gamma_\mu A^\mu) \psi_a - \frac{1}{4e_c^2} F_{\mu\nu} F^{\mu\nu} \right] \quad (5.1)$$

The theory has an internal $SU_L(2) \otimes SU_R(2)$ -flavor isospin symmetry; the Dirac fields are an isodoublet whereas the electromagnetic field is an isosinglet. It is well known that in 1 + 1 dimensions there is no spontaneous breakdown of continuous internal symmetries, unless there are anomalies or the Higgs phenomenon occurs. Neither mechanism is possible in the two-flavor Schwinger model for the $SU_L(2) \otimes SU_R(2)$ -symmetry: isovector currents do not develop anomalies and there are no gauge fields coupled to the isospin currents. The particles belong then to isospin multiplets. For what concerns the $U(1)$ gauge symmetry there is an Higgs phenomenon [66].

The action is invariant under the symmetry

$$SU_L(2) \otimes SU_R(2) \otimes U_V(1) \otimes U_A(1) \quad (5.2)$$

The group generators act on the fermion isodoublet to give

$$SU_L(2) : \psi_a(x) \longrightarrow (e^{i\theta_\alpha \frac{\sigma_\alpha}{2} P_L})_{ab} \psi_b(x), \quad \bar{\psi}_a(x) \longrightarrow \bar{\psi}_b(x) (e^{-i\theta_\alpha \frac{\sigma_\alpha}{2} P_R})_{ba} \quad (5.3)$$

$$SU_R(2) : \psi_a(x) \longrightarrow (e^{i\theta_\alpha \frac{\sigma_\alpha}{2} P_R})_{ab} \psi_b(x), \quad \bar{\psi}_a(x) \longrightarrow \bar{\psi}_b(x) (e^{-i\theta_\alpha \frac{\sigma_\alpha}{2} P_L})_{ba} \quad (5.4)$$

$$U_V(1) : \psi_a(x) \longrightarrow (e^{i\theta(x)\mathbf{1}})_{ab} \psi_b(x), \quad \psi_a^\dagger(x) \longrightarrow \psi_b^\dagger(x) (e^{-i\theta(x)\mathbf{1}})_{ba} \quad (5.5)$$

$$U_A(1) : \psi_a(x) \longrightarrow (e^{i\alpha\gamma_5\mathbf{1}})_{ab} \psi_b(x), \quad \psi_a^\dagger(x) \longrightarrow \psi_b^\dagger(x) (e^{-i\alpha\gamma_5\mathbf{1}})_{ba}, \quad (5.6)$$

where σ^α are the Pauli matrices, θ_α , $\theta(x)$ and α are real coefficients and

$$P_L = \frac{1}{2}(1 - \gamma_5), \quad P_R = \frac{1}{2}(1 + \gamma_5) \quad . \quad (5.7)$$

At the classical level the symmetries (5.3–5.6) lead to conservation laws for the isovector, vector and axial currents

$$j_\alpha^\mu(x)_R = \bar{\psi}_a(x) \gamma^\mu P_R \left(\frac{\sigma_\alpha}{2} \right)_{ab} \psi_b(x) \quad (5.8)$$

$$j_\alpha^\mu(x)_L = \bar{\psi}_a(x) \gamma^\mu P_L \left(\frac{\sigma_\alpha}{2} \right)_{ab} \psi_b(x) \quad (5.9)$$

$$j^\mu(x) = \bar{\psi}_a(x) \gamma^\mu \mathbf{1}_{ab} \psi_b(x) \quad (5.10)$$

$$j_5^\mu(x) = \bar{\psi}_a(x) \gamma^\mu \gamma^5 \mathbf{1}_{ab} \psi_b(x) \quad (5.11)$$

It is well known that at the quantum level the vector and axial currents cannot be simultaneously conserved, due to the anomaly phenomenon [26]. If the regularization is gauge

invariant, so that the vector current is conserved, then the axial current acquires the anomaly which breaks the $U_A(1)$ -symmetry

$$\partial_\mu j_5^\mu(x) = 2 \frac{e_c^2}{2\pi} \epsilon_{\mu\nu} F^{\mu\nu}(x) \quad (5.12)$$

The isoscalar and isovector chiral condensates are zero due to the Coleman theorem [43]; in fact, they would break not only the $U_A(1)$ symmetry of the action, but also the continuum internal symmetry $SU_L(2) \otimes SU_R(2)$ down to $SU_V(2)$. There is, however, a $SU_L(2) \otimes SU_R(2)$ invariant operator, which is non-invariant under the $U_A(1)$ -symmetry; it can acquire a non-vanishing VEV without violating Coleman's theorem and consequently may be regarded as a good order parameter for the $U_A(1)$ -breaking. Its expectation value is given by [72, 62]

$$\langle F \rangle \equiv \langle \bar{\psi}_L^{(2)} \bar{\psi}_L^{(1)} \psi_R^{(1)} \psi_R^{(2)} \rangle = \left(\frac{e^\gamma}{4\pi} \right)^2 \frac{2}{\pi} e_c^2 \quad . \quad (5.13)$$

It describes a process in which two right movers are annihilated and two left movers are created. Note that F , being quadrilinear in the fields, is actually invariant under chiral rotations of $\pi/2$, namely under the discrete axial symmetry

$$\psi_a(x) \rightarrow \gamma^5 \psi_a(x) \quad \bar{\psi}_a(x) \rightarrow -\bar{\psi}_a(x) \gamma^5 \quad . \quad (5.14)$$

As a consequence, this part of the chiral symmetry group is not broken by the non-vanishing VEV of F (5.13).

As we shall see in section (5.4), the lattice theory faithfully reproduces the pattern of symmetry breaking of the continuum theory; this happens even if on the lattice the $SU(2)$ -flavor symmetry is not protected by the Coleman theorem. The isoscalar and isovector chiral condensates are zero also on the lattice, whereas the operator F acquires a non-vanishing VEV due to the coupling of left and right movers induced by the gauge field. The continuous axial symmetry is broken explicitly by the staggered fermion, but the discrete axial symmetry (5.14) remains.

The action (5.1) may be presented in the usual abelian bosonized form [73]. Setting

$$: \bar{\psi}_a \gamma^\mu \psi_a := \frac{1}{\sqrt{\pi}} \epsilon^{\mu\nu} \partial_\nu \Phi_a \quad , \quad a = 1, 2 \quad , \quad (5.15)$$

the electric charge density and the action read

$$j_0 =: \psi_1^\dagger \psi_1 + \psi_2^\dagger \psi_2 := \frac{1}{\sqrt{\pi}} \partial_x (\Phi_1 + \Phi_2) \quad (5.16)$$

$$S = \int d^2x \left[\frac{1}{2} \partial_\mu \Phi_1 \partial^\mu \Phi_1 + \frac{1}{2} \partial_\mu \Phi_2 \partial^\mu \Phi_2 - \frac{e_c^2}{2\pi} (\Phi_1 + \Phi_2)^2 \right] \quad . \quad (5.17)$$

By changing the variables to

$$\Phi_+ = \frac{1}{\sqrt{2}} (\Phi_1 + \Phi_2) \quad (5.18)$$

$$\Phi_- = \frac{1}{\sqrt{2}} (\Phi_1 - \Phi_2) \quad , \quad (5.19)$$

one has

$$S = \int d^2x \left(\frac{1}{2} \partial_\mu \Phi_+ \partial^\mu \Phi_+ + \frac{1}{2} \partial_\mu \Phi_- \partial^\mu \Phi_- - \frac{e_c^2}{\pi} \Phi_+^2 \right) \quad . \quad (5.20)$$

The theory describes two scalar fields, one massive and one massless. Φ_+ is an isosinglet as evidenced from Eq.(5.16); its mass $m_S = \sqrt{\frac{2}{\pi}} e_c$ comes from the anomaly Eq.(5.12) [66]. Local electric charge conservation is spontaneously broken, but no Goldstone boson appears

because the Goldstone mode may be gauged away. Φ_- represents an isotriplet; it has rather involved nonlinear transformation properties under a general isospin transformation. All three isospin currents can be written in terms of Φ_- but only the third component has a simple representation in terms of Φ_- ; namely

$$\begin{aligned} j_\mu^3(x) &=:\bar{\psi}_a(x)\gamma_\mu\left(\frac{\sigma^3}{2}\right)_{ab}\psi_b(x):= \\ &= \frac{1}{2}:\bar{\psi}_1(x)\gamma_\mu\psi_1(x) - \bar{\psi}_2(x)\gamma_\mu\psi_2(x):= (2\pi)^{\frac{1}{2}}\epsilon^{\mu\nu}\partial_\nu\Phi_- \quad . \end{aligned} \quad (5.21)$$

The other two isospin currents $j_\mu^1(x)$ and $j_\mu^2(x)$ are nonlinear and nonlocal functions of Φ_- [73]; a more symmetrical treatment of the bosonized form of the isotriplet currents is available within the framework of non abelian bosonization [74]. For the multiflavor Schwinger model this approach has been carried out in [75], providing results in agreement with [73].

The excitations are most conveniently classified in terms of the quantum numbers of P -parity and G -parity; G -parity is related to the charge conjugation C by

$$G = e^{i\pi\frac{a^2}{2}}C \quad . \quad (5.22)$$

Φ_- is a G -even pseudoscalar, while Φ_+ is a G -odd pseudoscalar

$$\Phi_- \quad : \quad I^{PG} = 1^{-+} \quad (5.23)$$

$$\Phi_+ \quad : \quad I^{PG} = 0^{--} \quad . \quad (5.24)$$

The massive meson Φ_+ is stable by G conservation since the action (5.20) is invariant under $\Phi_+ \rightarrow -\Phi_+$.

In the massive $SU(2)$ Schwinger model – when the mass of the fermion m is small compared to e^2 (strong coupling) – Coleman [73] showed that - in addition to the triplet Φ_- ($I^{PG} = 1^{-+}$) the low-energy spectrum exhibits a singlet $I^{PG} = 0^{++}$ lying on top of the triplet Φ_- . In this limit the gauge theory is mapped to a sine-Gordon model and the low lying excitations are soliton-antisoliton states. When $m \rightarrow 0$, these soliton-antisoliton states become massless [76]; in this limit, the analysis of the many body wave functions, carried out in ref.[76], hints to the existence of a whole class of massless states with positive G -parity; P -parity however cannot be determined with the procedure developed in [76]. These are not the only excitations of the model: way up in mass there is the isosinglet $I^{PG} = 0^{--}$, (Φ_+), already discussed in ref. [73]. The model exhibits also triplets, whose mass – of order m_S or greater – stays finite [76]; among the triplets there is a G -even state ¹.

The Hamiltonian, gauge constraint and non-vanishing (anti-)commutators of the continuum two-flavor Schwinger model are

$$H = \int dx \quad \left[\frac{e^2}{2}E^2(x) + \sum_{a=1}^2 \psi_a^\dagger(x)\alpha(i\partial_x + eA(x))\psi_a(x) \right] \quad (5.25)$$

$$\partial_x E(x) + \sum_{a=1}^2 \psi_a^\dagger(x)\psi_a(x) \sim 0 \quad (5.26)$$

$$[A(x), E(y)] = i\delta(x-y), \quad \left\{ \psi_a(x), \psi_b^\dagger(y) \right\} = \delta_{ab}\delta(x-y) \quad . \quad (5.27)$$

A lattice Hamiltonian, constraint and (anti-) commutators reducing to (5.25,5.26,5.27) in the naive continuum limit are

$$\begin{aligned} H_S &= \frac{e^2 a}{2} \sum_{x=1}^N E_x^2 \quad - \quad \frac{it}{2a} \sum_{x=1}^N \sum_{a=1}^2 \left(\psi_{a,x+1}^\dagger e^{iA_x} \psi_{a,x} - \psi_{a,x}^\dagger e^{-iA_x} \psi_{a,x+1} \right) \\ E_x - E_{x-1} &+ \psi_{1,x}^\dagger \psi_{1,x} + \psi_{2,x}^\dagger \psi_{2,x} - 1 \sim 0 \quad , \quad (5.28) \\ [A_x, E_y] &= i\delta_{x,y} \quad , \quad \left\{ \psi_{a,x}, \psi_{b,y}^\dagger \right\} = \delta_{ab}\delta_{xy} \quad . \end{aligned}$$

¹K. Harada private communication.

The fermion fields are defined on the sites, $x = 1, \dots, N$, the gauge and electric fields, A_x and E_x , on the links $[x; x+1]$, N is an even integer and, when N is finite it is convenient to impose periodic boundary conditions. When N is finite, the continuum limit is the two-flavor Schwinger model on a circle [68]. The coefficient t of the hopping term in (5.28) plays the role of the lattice light speed. In the naive continuum limit, $e_L = e_c$ and $t = 1$.

The Hamiltonian and gauge constraint exhibit the discrete symmetries

- Parity P:

$$A_x \longrightarrow -A_{-x-1}, \quad E_x \longrightarrow -E_{-x-1}, \quad \psi_{a,x} \longrightarrow (-1)^x \psi_{a,-x}, \quad \psi_{a,x}^\dagger \longrightarrow (-1)^x \psi_{a,-x}^\dagger \quad (5.29)$$

- Discrete axial symmetry Γ :

$$A_x \longrightarrow A_{x+1}, \quad E_x \longrightarrow E_{x+1}, \quad \psi_{a,x} \longrightarrow \psi_{a,x+1}, \quad \psi_{a,x}^\dagger \longrightarrow \psi_{a,x+1}^\dagger \quad (5.30)$$

- Charge conjugation C:

$$A_x \longrightarrow -A_{x+1}, \quad E_x \longrightarrow -E_{x+1}, \quad \psi_{a,x} \longrightarrow \psi_{a,x+1}^\dagger, \quad \psi_{a,x}^\dagger \longrightarrow \psi_{a,x+1} \quad (5.31)$$

- G-parity:

$$\begin{aligned} A_x &\longrightarrow -A_{x+1}, \quad E_x \longrightarrow -E_{x+1} \\ \psi_{1,x} &\longrightarrow \psi_{2,x+1}^\dagger, \quad \psi_{1,x}^\dagger \longrightarrow \psi_{2,x+1} \\ \psi_{2,x} &\longrightarrow -\psi_{1,x+1}^\dagger, \quad \psi_{2,x}^\dagger \longrightarrow -\psi_{1,x+1} \end{aligned} \quad (5.32)$$

The lattice two-flavor Schwinger model is equivalent to a one dimensional quantum Coulomb gas on the lattice with two kinds of particles. To see this one can fix the gauge, $A_x = A$ (Coulomb gauge). Eliminating the non-constant electric field and using the gauge constraint, one obtains the effective Hamiltonian

$$\begin{aligned} H_S &= H_u + H_p \equiv \left[\frac{e_L^2}{2N} E^2 + \frac{e_L^2 a}{2} \sum_{x,y} \rho(x) V(x-y) \rho(y) \right] + \\ &+ \left[-\frac{it}{2a} \sum_x \sum_{a=1}^2 (\psi_{a,x+1}^\dagger e^{iA} \psi_{a,x} - \psi_{a,x}^\dagger e^{-iA} \psi_{a,x+1}) \right], \end{aligned} \quad (5.33)$$

where the charge density is

$$\rho(x) = \psi_{1,x}^\dagger \psi_{1,x} + \psi_{2,x}^\dagger \psi_{2,x} - 1, \quad (5.34)$$

and the potential

$$V(x-y) = \frac{1}{N} \sum_{n=1}^{N-1} e^{i2\pi n(x-y)/N} \frac{1}{4 \sin^2 \frac{\pi n}{N}} \quad (5.35)$$

is the Fourier transform of the inverse laplacian on the lattice for non zero momentum. The constant modes of the gauge field decouple in the thermodynamic limit $N \longrightarrow \infty$.

5.2 The strong coupling limit and the antiferromagnetic Heisenberg Hamiltonian

In the thermodynamic limit the Schwinger Hamiltonian (5.33), rescaled by the factor $e_L^2 a/2$, reads

$$H = H_0 + \epsilon H_h \quad (5.36)$$

with

$$H_0 = \sum_{x>y} \left[\frac{(x-y)^2}{N} - (x-y) \right] \rho(x)\rho(y) \quad , \quad (5.37)$$

$$H_h = -i(R-L) \quad (5.38)$$

and $\epsilon = t/e_L^2 a^2$. In Eq.(5.38) the right R and left L hopping operators are defined ($L = R^\dagger$) as

$$R = \sum_{x=1}^N R_x = \sum_{x=1}^N \sum_{a=1}^2 R_x^{(a)} = \sum_{x=1}^N \sum_{a=1}^2 \psi_{a,x+1}^\dagger e^{iA} \psi_{a,x} \quad . \quad (5.39)$$

On a periodic chain the commutation relation

$$[R, L] = 0 \quad (5.40)$$

is satisfied.

I shall consider the strong coupling perturbative expansion where the Coulomb Hamiltonian (5.37) is the unperturbed Hamiltonian and the hopping Hamiltonian (5.38) the perturbation. Due to Eq.(5.34) every configuration with one particle per site has zero energy, so that the ground state of the Coulomb Hamiltonian (5.37) is 2^N times degenerate. The degeneracy of the ground state can be removed only at the second perturbative order since the first order is trivially zero.

At the second order the lattice gauge theory is effectively described by the antiferromagnetic Heisenberg Hamiltonian. The vacuum energy – at order ϵ^2 – reads

$$E_0^{(2)} = \langle H_h^\dagger \frac{\Pi}{E_0^{(0)} - H_0} H_h \rangle \quad (5.41)$$

where the expectation values are defined on the degenerate subspace and Π is the operator projecting on a set orthogonal to the states with one particle per site. Due to the vanishing of the charge density on the ground states of H_0 , the commutator

$$[H_0, H_h] = H_h \quad (5.42)$$

holds on any linear combination of the degenerate ground states. Consequently, from Eq.(5.41) one finds

$$E_0^{(2)} = -2 \langle RL \rangle \quad . \quad (5.43)$$

On the ground state the combination RL can be written in terms of the Heisenberg Hamiltonian. By introducing the Schwinger spin operators

$$\vec{S}_x = \psi_{a,x}^\dagger \frac{\vec{\sigma}_{ab}}{2} \psi_{b,x} \quad (5.44)$$

the Heisenberg Hamiltonian H_J reads

$$\begin{aligned} H_J &= \sum_{x=1}^N \left(\vec{S}_x \cdot \vec{S}_{x+1} - \frac{1}{4} \right) = \\ &= \sum_{x=1}^N \left(-\frac{1}{2} L_x R_x - \frac{1}{4} \rho(x)\rho(x+1) \right) \end{aligned} \quad (5.45)$$

and, on the degenerate subspace, one has

$$\langle H_J \rangle = \left\langle \sum_{x=1}^N \left(\vec{S}_x \cdot \vec{S}_{x+1} - \frac{1}{4} \right) \right\rangle = \left\langle \sum_{x=1}^N \left(-\frac{1}{2} L_x R_x \right) \right\rangle \quad . \quad (5.46)$$

Taking into account that products of L_x and R_y at different points have vanishing expectation values on the ground states, and using Eq.(5.46), Eq.(5.43) reads

$$E_0^{(2)} = 4 \langle H_J \rangle \quad . \quad (5.47)$$

The ground state of H_J singles out the correct vacuum, on which to perform the perturbative expansion. In one dimension H_J is exactly diagonalizable [36, 34]. In the spin model a flavor 1 particle on a site can be represented by a spin up, a flavor 2 particle by a spin down. The spectrum of H_J exhibits 2^N eigenstates; among these, the spin singlet with lowest energy is the non degenerate ground state $|g.s. \rangle$.

I shall construct the strong coupling perturbation theory of the two-flavor Schwinger model using $|g.s. \rangle$ as the unperturbed ground state. $|g.s. \rangle$ is invariant under translations by one lattice site, which amounts to invariance under discrete chiral transformations. As a consequence, At variance with the one-flavor model [61], chiral symmetry cannot be spontaneously broken even in the infinite coupling limit.

$|g.s. \rangle$ has zero charge density on each site and zero electric flux on each link

$$\rho(x)|g.s. \rangle = 0 \quad , \quad E_x|g.s. \rangle = 0 \quad (x = 1, \dots, N) \quad . \quad (5.48)$$

$|g.s. \rangle$ is a linear combination of all the possible states with $\frac{N}{2}$ spins up and $\frac{N}{2}$ spins down. The coefficients are not explicitly known for general N . In chapter 3 I exhibited $|g.s. \rangle$ explicitly for finite size systems of 4, 6 and 8 sites. The Heisenberg energy of $|g.s. \rangle$ is known exactly and, in the thermodynamic limit, is [37, 30]

$$H_J|g.s. \rangle = (-N \ln 2)|g.s. \rangle \quad . \quad (5.49)$$

Eq.(5.49) provides the second order correction Eq.(5.47) to the vacuum energy, $E_{g.s.}^{(2)} = -4N \ln 2$.

There exist two kinds of excitations created from $|g.s. \rangle$; one kind involves only spin flipping and has lower energy since no electric flux is created, the other involves fermion transport besides spin flipping and thus has a higher energy. For the latter excitations the energy is proportional to the coupling times the length of the electric flux: the lowest energy is achieved when the fermion is transported by one lattice spacing. Of course only the excitations of the first kind can be mapped into states of the Heisenberg model.

In [30] the antiferromagnetic Heisenberg model excitations have been classified. There it was shown that any excitation may be regarded as the scattering state of quasiparticles of spin-1/2: every physical state contains an even number of quasiparticles and the spectrum exhibits only integer spin states. The two simplest excitations of lowest energy in the thermodynamic limit are a triplet and a singlet [30]; they have a dispersion relation depending on the momenta of the two quasiparticles. For vanishing total momentum (relative to the ground state momentum $P_{g.s.} = 0$ for $\frac{N}{2}$ even, $P_{g.s.} = \pi$ for $\frac{N}{2}$ odd) in the thermodynamic limit they are degenerate with the ground state.

In chapter 3 I showed that even for finite size systems, the excited states can be grouped in families corresponding to the classification given in [30]. I explicitly exhibited all the energy eigenstates for $N = 4$ and $N = 6$. The lowest lying are a triplet and a singlet, respectively; they have a well defined relative (to the ground state) P -parity and G -parity - 1^{-+} for the triplet and 0^{++} for the singlet. Since they share the same quantum numbers these states can be identified, in the limit of vanishing fermion mass, with the soliton-antisoliton excitations found by Coleman in his analysis of the two-flavor Schwinger model. A related analysis about the parity of the lowest lying states in finite size Heisenberg chains, has been given in [77].

Moreover in [30] a whole class – \mathcal{M}_{AF} – of gapless excitations at zero momentum was singled out in the thermodynamic limit; these states are eigenstates of the total momentum and consequently have positive G-parity at zero momentum. The low lying states of the Schwinger model also contain [76] many massless excitations with positive G-parity; they are identified [39, 40] with the excitations belonging to \mathcal{M}_{AF} . The mass of these states in the Schwinger model can be obtained from the differences between the excitation energies at zero momentum and the ground state energy. The energies of the states $|ex. \rangle$ belonging to the class \mathcal{M}_{AF} have the same perturbative expansion of the ground state. Consequently, the states $|ex. \rangle$ at zero momentum up to the second order in the strong coupling expansion have the same energy of the ground state (5.41), $E_{ex}^{(2)} = -4N \ln 2$. To this order the mass gap is zero. Higher order corrections may give a mass gap.

5.2.1 The low lying spectrum of QCD_2

In section (2.3.2) I already explained that QCD_2 with colour group $SU(2)$ and 1 flavor is also mapped onto the spin-1/2 quantum Heisenberg antiferromagnetic chain. This result was originally found by Langmann and Semenoff in [24]. It is worth stressing this fact here, and speculating about the model spectrum.

I claim that the massless excitation spectrum of this non-abelian theory in the strong coupling limit is the same of the massless excitation spectrum of the two-flavor massless Schwinger model. Both the models exhibit an exact correspondence with the infrared limit of the Heisenberg antiferromagnetic chain.

The quark-like excitations of QCD_2 are gapless spin-1/2 kinks or spinons. They always appear in even number so that the only physical excitations have integer spin and an even number of spinons. This phenomenon is not exactly what one would call confinement. These quark-spinons are localizable objects and one can consider their scattering. There are no bound states of spinons in the spin-1/2 quantum antiferromagnetic chain [30]. Spinons exist only in even number and this constraint is the spin model counterpart of the absence of coloured states in QCD_2 . One flavor QCD_2 exhibits only mesons in its spectrum and it is not possible to generate baryons. I can say nothing, at this level of analysis, about the massive excitations of lattice QCD_2 which are created by the non abelian currents of the model acting on $|g.s. \rangle$. These currents involve charge transport on $|g.s. \rangle$ and create electric flux. The non zero electric flux generates the masses of the excitations, with a mechanism similar to that of the two-flavor Schwinger model.

5.3 The meson masses

In this section I determine the masses for the states obtained by fermion transport of one site on the Heisenberg model ground state. My analysis shows that besides the G -odd pseudoscalar isosinglet 0^{--} with mass $m_S = e_L \sqrt{2/\pi}$, there are also a G -even pseudoscalar isotriplet 1^{-+} and a G -odd scalar isotriplet 1^{+-} with masses of the order of m_S or greater. The quantum numbers are relative to those of the ground state $I_{g.s.}^{PG} = 0^{++}$ for $N/2$ even $I_{g.s.}^{PG} = 0^{--}$ for $N/2$ odd.

Two states can be created using the spatial component of the vector $j^1(x)$ Eq.(5.10) and isovector $j_\alpha^1(x)$ Eqs.(5.8,5.9) Schwinger model currents. They are the G -odd pseudoscalar isosinglet $I^{PG} = 0^{--}$ and the G -even pseudoscalar isotriplet $I^{PG} = 1^{-+}$. The lattice operators with the correct quantum numbers creating these states at zero momentum, when

acting on $|g.s. \rangle$, read

$$S = R + L = \sum_{x=1}^N j^1(x) \quad (5.50)$$

$$T_+ = (T_-)^\dagger = R^{(12)} + L^{(12)} = \sum_{x=1}^N j_+^1(x) \quad (5.51)$$

$$T_0 = \frac{1}{\sqrt{2}}(R^{(11)} + L^{(11)} - R^{(22)} - L^{(22)}) = \sum_{x=1}^N j_3^1(x) \quad . \quad (5.52)$$

$R^{(ab)}$ and $L^{(ab)}$ in (5.51,5.52) are the right and left flavor changing hopping operators ($L^{(ab)} = (R^{(ab)})^\dagger$)

$$R^{(ab)} = \sum_{x=1}^N \psi_{a,x+1}^\dagger e^{iA} \psi_{b,x} \quad .$$

The states are given by

$$|S \rangle = |0^{--} \rangle = S|g.s. \rangle \quad (5.53)$$

$$|T_\pm \rangle = |1^{-+}, \pm 1 \rangle = T_\pm |g.s. \rangle \quad (5.54)$$

$$|T_0 \rangle = |1^{-+}, 0 \rangle = T_0 |g.s. \rangle \quad . \quad (5.55)$$

They are normalized as

$$\langle S|S \rangle = \langle g.s.|S^\dagger S|g.s. \rangle = -4 \langle g.s.|H_J|g.s. \rangle = 4N \ln 2 \quad (5.56)$$

$$\langle T_+|T_+ \rangle = \frac{2}{3}(N + \langle g.s.|H_J|g.s. \rangle) = \frac{2}{3}N(1 - \ln 2) \quad (5.57)$$

and

$$\langle T_0|T_0 \rangle = \langle T_-|T_- \rangle = \langle T_+|T_+ \rangle \quad . \quad (5.58)$$

In Eqs.(5.56,5.57,5.58) $\langle g.s.|g.s. \rangle = 1$.

The isosinglet energy, up to the second order in the strong coupling expansion, is $E_S = E_S^{(0)} + \epsilon^2 E_S^{(2)}$ with

$$E_S^{(0)} = \frac{\langle S|H_0|S \rangle}{\langle S|S \rangle} = 1 \quad , \quad (5.59)$$

$$E_S^{(2)} = \frac{\langle S|H_h^\dagger \Lambda_S H_h|S \rangle}{\langle S|S \rangle} \quad , \quad (5.60)$$

$\Lambda_S = \frac{\Pi_S}{E_S^{(0)} - H_0}$ and $1 - \Pi_S$ a projection operator onto $|S \rangle$. On $|g.s. \rangle$

$$[H_0, (\Pi_S H_h)^n S] = (n+1)(\Pi_S H_h)^n, \quad (n = 0, 1, \dots), \quad (5.61)$$

holds; Eq.(5.60) may then be written in terms of spin correlators as

$$E_S^{(2)} = E_{g.s.}^{(2)} + 4 - \frac{\sum_{x=1}^N \langle g.s.|\vec{S}_x \cdot \vec{S}_{x+2} - \frac{1}{4}|g.s. \rangle}{\langle g.s.|H_J|g.s. \rangle} \quad . \quad (5.62)$$

One immediately recognizes that the excitation spectrum is determined once $\langle g.s.|\vec{S}_x \cdot \vec{S}_{x+2}|g.s. \rangle$ is known. Equations similar to Eq.(5.62) may be established also at a generic order of the strong coupling expansion.

At the zeroth perturbative order the pseudoscalar triplet is degenerate with the isosinglet $E_T^{(0)} = E_S^{(0)} = 1$. Following the same procedure as before one may compute the energy of

the states (5.54) and (5.55) to the second order in the strong coupling expansion. To this order, the energy is given by

$$E_T^{(2)} = E_{g.s.}^{(2)} - \Delta_{DS}(T) - \frac{4 \langle g.s. | H_J | g.s. \rangle + 5 \sum_{x=1}^N \langle g.s. | \vec{S}_x \cdot \vec{S}_{x+2} - \frac{1}{4} | g.s. \rangle}{N + \langle g.s. | H_J | g.s. \rangle} \quad (5.63)$$

where in terms of the vector operator $\vec{V} = \sum_{x=1}^N \vec{S}_x \wedge \vec{S}_{x+1}$, one can write $\Delta_{DS}(T)$ as

$$\Delta_{DS}(T_{\pm}) = 12 \frac{\langle g.s. | (V_1)^2 | g.s. \rangle + \langle g.s. | (V_2)^2 | g.s. \rangle}{N + \langle g.s. | H_J | g.s. \rangle} \quad (5.64)$$

$$\Delta_{DS}(T_0) = 12 \frac{2 \langle g.s. | (V_3)^2 | g.s. \rangle}{N + \langle g.s. | H_J | g.s. \rangle} . \quad (5.65)$$

The VEV of each squared component of \vec{V} on the rotationally invariant singlet $|g.s. \rangle$ give the same contribution *i.e.* $\Delta_{DS}(T_{\pm}) = \Delta_{DS}(T_0)$: the triplet states (as in the continuum theory) have a degenerate mass gap. This is easily verified by direct computation on finite size systems; when the size of the system is finite one may also show that Δ_{DS} is of zeroth order in N .

The excitation masses are given by $m_S = \frac{e_L^2 a}{2} (E_S - E_{g.s.})$ and $m_T = \frac{e_L^2 a}{2} (E_T - E_{g.s.})$. Consequently, the (N -dependent) ground state energy terms appearing in $E_S^{(2)}$ and $E_T^{(2)}$ cancel and what is left are only N independent terms. This is a good check of our computation, being the mass an intensive quantity.

In principle one should expect also excitations created acting on $|g.s. \rangle$ with the chiral currents, in analogy with the one flavor Schwinger model where, as shown in ref. [63], the chiral current creates a two-meson bound state. The chiral currents operators for the two flavor Schwinger model are given by

$$j^5(x) = \bar{\psi}(x) \gamma^5 \psi(x) \quad (5.66)$$

$$j_{\alpha}^5(x) = \bar{\psi}_a(x) \gamma^5 \left(\frac{\sigma}{2} \right)_{ab} \psi_b(x) . \quad (5.67)$$

The corresponding lattice operators at zero momentum are

$$S^5 = R - L = \sum_{x=1}^N j^5(x) \quad (5.68)$$

$$T_{+}^5 = (T_{-}^5)^{\dagger} = R^{(12)} - L^{(12)} = \sum_{x=1}^N j_{+}^5(x) \quad (5.69)$$

$$T_0^5 = \frac{1}{\sqrt{2}} (R^{(11)} - L^{(11)} - R^{(22)} + L^{(22)}) = \sum_{x=1}^N j_3^5(x) . \quad (5.70)$$

$$(5.71)$$

The states created by (5.68,5.69,5.70) when acting on $|g.s. \rangle$, are

$$|S^5 \rangle = |0^{++} \rangle = S^5 |g.s. \rangle \quad (5.72)$$

$$|T_{\pm}^5 \rangle = |1^{+-}, \pm 1 \rangle = T_{\pm}^5 |g.s. \rangle \quad (5.73)$$

$$|T_0^5 \rangle = |1^{+-}, 0 \rangle = T_0^5 |g.s. \rangle . \quad (5.74)$$

They are normalized as

$$\langle S^5 | S^5 \rangle = \langle g.s. | S^{5\dagger} S^5 | g.s. \rangle = -4 \langle g.s. | H_J | g.s. \rangle = 4N \log 2 \quad (5.75)$$

$$\langle T_{+}^5 | T_{+}^5 \rangle = \frac{2}{3} (N + \langle g.s. | H_J | g.s. \rangle) = \frac{2}{3} N (1 - \log 2) \quad (5.76)$$

and

$$\langle T_0^5 | T_0^5 \rangle = \langle T_{-}^5 | T_{-}^5 \rangle = \langle T_{+}^5 | T_{+}^5 \rangle . \quad (5.77)$$

Following the computational scheme used to study $|S\rangle$ and $|T\rangle$, one finds that the state $|S^5\rangle$ is not a particle-like excitation since its energy depends on the volume of the system and this would lead to an extensive mass; consequently, there is no 0^{++} massive singlet in agreement with [73]. For the triplet $|T^5\rangle$ one gets

$$E_{T^5}^{(0)} = 1 \quad (5.78)$$

$$E_{T^5}^{(2)} = E_{g.s.}^{(2)} + \frac{\sum_{x=1}^N \langle g.s. | \vec{S}_x \cdot \vec{S}_{x+2} - \frac{1}{4} | g.s. \rangle - 4 \langle g.s. | H_J | g.s. \rangle}{N + \langle g.s. | H_J | g.s. \rangle} \quad (5.79)$$

Now I can compute the mass spectrum up to the second order in the strong coupling expansion. Using Eq.(3.159), the isosinglet mass reads as

$$\frac{m_S}{e^2 a} = \frac{1}{2} + 1.9509 \epsilon^2 \quad (5.80)$$

For what concerns the isotriplet mass, since the double sum in Eq.(5.63) is given by

$$\Delta_{DS}(T) = 8 \frac{\langle g.s. | \vec{V} \cdot \vec{V} | g.s. \rangle}{N + \langle g.s. | H_J | g.s. \rangle} \quad (5.81)$$

using Eq.(3.180), one gets

$$\frac{m_T}{e_L^2 a} = \frac{1}{2} + 0.0972 \epsilon^2 \quad (5.82)$$

The existence of massive isotriplets was already noticed in [76], and their mass in the continuum theory was numerically computed for various values of the fermion mass. In particular there is a G -parity even isotriplet with mass approximately equal to the mass of the isosinglet 0^{--} .

The mass of the $|T_5^5\rangle$ isotriplet is

$$\frac{m_{T^5}}{e^2 a} = \frac{1}{2} + 4.4069 \epsilon^2 \quad (5.83)$$

Equations (5.80), (5.82) and (5.83) provide the values of m_S , m_T and m_{T^5} for small values of $z = \epsilon^2 = \frac{t^2}{e_L^4 a^4}$ up to the second order in the strong coupling expansion. Whereas (5.82) is only approximate (5.80) and (5.83) are exact at the second order in the ϵ expansion. In section (5.5) I shall extrapolate these masses to the continuum limit using the standard technique of the Padé approximants.

5.4 Chiral condensate

In the following I shall first prove that also on the lattice either the isoscalar $\langle \bar{\psi} \psi \rangle$ or the isovector $\langle \bar{\psi} \sigma^a \psi \rangle$ chiral condensates are zero to every order of perturbation theory. This should be verified by explicit computation since on the lattice the symmetry $SU_L(2) \otimes SU_R(2)$ is already broken by introducing staggered fermions; thus, there is no symmetry to prevent the formation of such chiral condensates. In the continuum theory, instead, the breaking of the $SU_L(2) \otimes SU_R(2)$ down to $SU_V(2)$ is prevented by the Coleman theorem [43].

In the staggered fermion formalism the isoscalar condensate is given by

$$\sum_{a=1}^2 \overline{\psi_a(x)} \psi_a(x) \longrightarrow \frac{(-1)^x}{2a} (\psi_{1,x}^\dagger \psi_{1,x} + \psi_{2,x}^\dagger \psi_{2,x} - 1) \quad ; \quad (5.84)$$

it is obtained by considering the mass operator

$$M = \frac{1}{2Na} \sum_{x=1}^N (-1)^x (\psi_{1,x}^\dagger \psi_{1,x} + \psi_{2,x}^\dagger \psi_{2,x}) \quad (5.85)$$

and evaluating its expectation value on the perturbed states $|p_{g.s.}\rangle$ generated by applying H_h to $|g.s.\rangle$. To the second order in the strong coupling expansion, one has

$$|p_{g.s.}\rangle = |g.s.\rangle + \epsilon |p_{g.s.}^1\rangle + \epsilon^2 |p_{g.s.}^2\rangle + \dots \quad (5.86)$$

where

$$|p_{g.s.}^1\rangle = -H_h |g.s.\rangle \quad (5.87)$$

$$|p_{g.s.}^2\rangle = \frac{\Pi_{g.s.}}{2} H_h H_h |g.s.\rangle \quad (5.88)$$

To the fourth order, (5.85) is given by

$$\chi_{isos.} = \frac{\langle p_{g.s.} | M | p_{g.s.} \rangle}{\langle p_{g.s.} | p_{g.s.} \rangle} = \frac{\langle g.s. | M | g.s. \rangle + \epsilon^2 \langle p_{g.s.}^1 | M | p_{g.s.}^1 \rangle + \epsilon^4 \langle p_{g.s.}^2 | M | p_{g.s.}^2 \rangle + \dots}{\langle g.s. | g.s. \rangle + \epsilon^2 \langle p_{g.s.}^1 | p_{g.s.}^1 \rangle + \epsilon^4 \langle p_{g.s.}^2 | p_{g.s.}^2 \rangle + \dots} \quad (5.89)$$

It is very easy to see that $\chi_{isos.}$ is zero to all orders in the strong coupling expansion. Let us introduce the translation operator

$$\hat{T} = e^{i\hat{p}a} \quad ; \quad (5.90)$$

using

$$\hat{T} M \hat{T}^{-1} = -M \quad (5.91)$$

$$\hat{T} H_h \hat{T}^{-1} = H_h \quad (5.92)$$

and

$$\hat{T} |g.s.\rangle = \pm |g.s.\rangle \quad (5.93)$$

one gets order by order in the strong coupling expansion in Eq.(5.89)

$$\chi_{isos.} = -\chi_{isos.} \quad (5.94)$$

In Eq.(5.93) the $+$ appears when $N/2$ is even and the $-$ when $N/2$ is odd.

The isovector chiral condensate is given by the expectation value of the operator

$$\vec{\Sigma} = \frac{1}{2Na} \sum_{x=1}^N (-1)^x \psi_{a,x}^\dagger \vec{\sigma}_{ab} \psi_{b,x} \quad (5.95)$$

on the perturbed states $|p_{g.s.}\rangle$. Taking into account that

$$\hat{T} \Sigma \hat{T}^{-1} = -\Sigma \quad (5.96)$$

one gets

$$\chi_{isov.} = -\chi_{isov.} \quad ; \quad (5.97)$$

also the isovector chiral condensate is identically zero.

In the continuum there is, as evidenced in section (5.1), only a non-vanishing chiral condensate associated to the anomalous breaking of the $U_A(1)$ symmetry [72, 62]. Since

$$\overline{\psi}_L^a(x) \psi_R^a(x) = \overline{\psi}^a(x) \frac{1 + \gamma_5}{2} \psi^a(x) \quad , \quad (5.98)$$

the pertinent operator is $F = \overline{\psi}_L^{(2)} \overline{\psi}_L^{(1)} \psi_R^{(1)} \psi_R^{(2)}$; its expectation value has been computed in [72][62] and is given by

$$\langle \overline{\psi}_L^{(2)} \overline{\psi}_L^{(1)} \psi_R^{(1)} \psi_R^{(2)} \rangle = \left(\frac{e^\gamma}{4\pi}\right)^2 \frac{2}{\pi} e_c^2 = \left(\frac{e^\gamma}{4\pi}\right)^2 m_S^2 \quad . \quad (5.99)$$

On the lattice one has

$$\overline{\psi}_L^a(x) \psi_R^a(x) \longrightarrow \frac{1}{2a} \frac{1}{2} (\psi_{a,x}^\dagger \psi_{a,x} - \psi_{a,x+1}^\dagger \psi_{a,x+1} + L_x^{(a)} - R_x^{(a)}) \quad . \quad (5.100)$$

The factor $1/2a$ is due to the doubling of the lattice spacing in the antiferromagnetic bipartite lattice. Upon introducing the occupation number operators $n_x^{(a)} = \psi_{a,x}^\dagger \psi_{a,x}$, the umklapp operator F is represented on the lattice by

$$F = -\frac{1}{16a^2 N} \sum_{x=1}^N N \left\{ (n_x^{(1)} - n_{x+1}^{(1)})(n_x^{(2)} - n_{x+1}^{(2)}) + (L_x^{(1)} - R_x^{(1)})(L_x^{(2)} - R_x^{(2)}) \right\} \quad . \quad (5.101)$$

The strong coupling expansion carried up to the second order in $\epsilon = \frac{t}{e_L^2 a^2}$, yields

$$\langle F \rangle = \frac{\langle p_{g.s.} | F | p_{g.s.} \rangle}{\langle p_{g.s.} | p_{g.s.} \rangle} = \frac{\langle g.s. | F | g.s. \rangle + \epsilon^2 \langle p_{g.s.}^1 | F | p_{g.s.}^1 \rangle}{\langle g.s. | g.s. \rangle + \epsilon^2 \langle p_{g.s.}^1 | p_{g.s.}^1 \rangle} \quad (5.102)$$

for the lattice chiral condensate. Since

$$\langle g.s. | g.s. \rangle = 1 \quad (5.103)$$

$$\langle p_{g.s.}^1 | p_{g.s.}^1 \rangle = -4 \langle g.s. | H_J | g.s. \rangle \quad , \quad (5.104)$$

and taking into account that

$$\langle g.s. | F | g.s. \rangle = \frac{1}{8a^2 N} \langle g.s. | H_J | g.s. \rangle \quad (5.105)$$

$$\begin{aligned} \langle p_{g.s.}^1 | F | p_{g.s.}^1 \rangle &= \frac{1}{4a^2 N} (-2 \langle g.s. | (H_J)^2 | g.s. \rangle - \frac{5}{3} \langle g.s. | H_J | g.s. \rangle + \frac{5}{12} N \\ &\quad - \frac{2}{3} \sum_{x=1}^N \langle g.s. | \vec{S}_x \cdot \vec{S}_{x+2} - \frac{1}{4} | g.s. \rangle) \quad , \quad (5.106) \end{aligned}$$

from Eqs.(5.49) and (3.167), one gets

$$\langle F \rangle = \frac{1}{a^2} (0.0866 - 0.4043 \epsilon^2) \quad . \quad (5.107)$$

A nonvanishing value of the lattice chiral condensate is due to the coupling – induced by the lattice gauge field – between the right and left fermions. This is the relic in the lattice of the $U_A(1)$ anomaly in the continuum theory.

5.5 Lattice versus continuum

I now want to compare our lattice results with the exact results of the continuum model; to do this, one should extrapolate the strong-coupling expansion derived under the assumption that the parameter $z = \epsilon^2 = \frac{t^2}{e_L^4 a^4} \ll 1$ to the region in which $z \gg 1$; this corresponds to take the continuum limit since $e_L^4 a^4 \longrightarrow 0$ when $z \longrightarrow \infty$. To make the extrapolation possible, it is customary to make use of Padé approximants, which allow to extrapolate a series expansion beyond the convergence radius. Strong-coupling perturbation theory improved by Padé approximants should then provide results consistent with the continuum theory.

As we shall see the strong-coupling expansion derived in this chapter provides accurate estimates of the meson masses, already at the first order in powers of z .

Let us now evaluate m_S and the lattice light velocity t . I first compute the ratio between the continuum value of the meson mass $m_S = \sqrt{\frac{2}{\pi}}e_c$ and the lattice coupling constant e_L by equating the lattice chiral condensate, Eq.(5.107), to its continuum counterpart Eq.(5.99)

$$\frac{1}{a^2}(0.0866 - 0.4043z) = \left(\frac{e^\gamma}{4\pi}\right)^2 m_S^2 . \quad (5.108)$$

Eq.(5.108) is true only when Padé approximants are used since, as it stands, the left hand side holds only for $z \ll 1$, while the right-hand side provides the value of the chiral condensate to be obtained when $z = \infty$. Using

$$a = \frac{t^{\frac{1}{2}}}{e_L z^{\frac{1}{4}}} , \quad (5.109)$$

one gets from Eq.(5.108)

$$\left(\frac{m_S}{e_L}\right)^2 = \left(\frac{4\pi}{e^\gamma}\right)^2 \frac{z^{\frac{1}{2}}}{t} (0.0866 - 0.4043z) . \quad (5.110)$$

As in Refs.[63, 61], due to the factor $z^{\frac{1}{2}}$, the second power of Eq.(5.110) should be considered in order to construct a non diagonal Padé approximant. Since the strong coupling expansion has been carried out up to second order in z , one is allowed to construct only the $[0, 1]$ Padé approximant for the polynomial written in Eq.(5.110). One gets

$$\left(\frac{m_S}{e_L}\right)^4 = \left(\frac{4\pi}{e^\gamma}\right)^4 \frac{1}{t^2} \frac{0.0074z}{1 + 9.3371z} , \quad (5.111)$$

and, taking the continuum limit $z \rightarrow \infty$, one finds

$$\left(\frac{m_S}{e_L}\right)^4 = \left(\frac{4\pi}{e^\gamma}\right)^4 \frac{0.0008}{t^2} . \quad (5.112)$$

Next I compute the same mass ratio by equating the singlet mass gap given in Eq.(5.80) to its continuum counterpart m_S

$$e_L^2 a \left(\frac{1}{2} + 1.9509z\right) = m_S . \quad (5.113)$$

Again, Eq.(5.113) is true only when Padé approximants are used. Dividing both sides of Eq.(5.113) by e_L and taking into account that

$$e_L a = \frac{t^{\frac{1}{2}}}{z^{\frac{1}{4}}} \quad (5.114)$$

one gets

$$\frac{m_S}{e_L} = \frac{t^{\frac{1}{2}}}{z^{\frac{1}{4}}} \left(\frac{1}{2} + 1.9509z\right) . \quad (5.115)$$

Taking the fourth power and constructing the $[1, 0]$ Padé approximant for the right hand side of Eq.(5.115) one has

$$\left(\frac{m_S}{e_L}\right)^4 = \frac{t^2}{z} \left(\frac{1}{16} + 0.9754z\right) ; \quad (5.116)$$

when $z \rightarrow \infty$, Eq.(5.116) gives

$$\left(\frac{m_S}{e_L}\right)^4 = t^2 0.9754 . \quad (5.117)$$

The numerical value of the hopping parameter t , determined if one equates Eq.(5.117) and Eq.(5.112), is

$$t = \frac{4\pi}{e^\gamma} 0.1692 = 1.1940 \quad (5.118)$$

and lies 19% above the exact value. Putting this value of t in Eq.(5.112) or Eq.(5.117) one gets

$$\frac{m_S}{e_L} = 1.0969 \quad (5.119)$$

which lies 37% above the exact value $\sqrt{\frac{2}{\pi}}$. It is comforting to see that the lattice reproduces in a sensible way the continuum results even if I use just first order (in z) results of the strong coupling perturbation theory.

Using the value of t given in Eq.(5.118) one gets for the isotriplet mass Eq.(5.124)

$$\frac{m_T}{e_L} = 0.5143 \quad . \quad (5.120)$$

By direct computation on an 8 sites chain one gets

$$\frac{m_T}{e_L} = 1.3524 \quad . \quad (5.121)$$

The discrepancy between Eq.(5.120) and Eq.(5.121) is mainly due to the approximation involved in the computation of $\langle g.s. | \vec{V}^2 | g.s. \rangle$. However, it is safe to believe that my lattice computation implies the existence of a massive isotriplet 1^{-+} with a mass between the lower bound (5.120) and the upper bound (5.121). This is in agreement with the results provided for the continuum theory in [76].

Using a similar procedure one may also compute the mass of the triplet 1^{+-} . From Eq.(5.83) one gets

$$\frac{m_{T^s}}{e_L} = 1.3347 \quad . \quad (5.122)$$

This triplet, being G -odd, is a scattering state of a 0^{--} singlet with a 1^{-+} triplet, which are the fundamental excitations of the system. The mass of this 1^{+-} triplet should be larger than the mass of the massive 1^{-+} triplet, which should be a scattering state of massless 1^{-+} triplets.

Putting $t = c = 1$, *i.e.* $e_L a = \frac{1}{z^{\frac{1}{4}}}$ the lattice mass spectrum gets closer to its continuum counterpart; for the isosinglet mass, one gets

$$\frac{m_S}{e} = 0.9938 \quad (5.123)$$

while for the isotriplet one gets

$$\frac{m_T}{e_L} = 0.4695 \quad . \quad (5.124)$$

Eq.(5.123) provides a value of the isosinglet mass lying 24% above the exact answer. Again the triplet mass is reproduced with lesser accuracy due to the random phase approximation used in the computation of the pertinent correlator; a better answer is given however by a direct computation on the 8 sites chain yielding the value 1.2346 for m_T/e_L .

5.6 Summary

In this chapter I used the correspondence between the two-flavor strongly coupled lattice Schwinger model and the antiferromagnetic Heisenberg Hamiltonian [39, 40] to investigate

the spectrum of the gauge model. Using the analysis of the excitations of the finite size chains given in the chapter 3, I showed the equality of the quantum numbers of the states of the Heisenberg model and the low lying excitations of the two-flavor Schwinger model. I provided also the spectrum of the massive excitations of the gauge model; in order to extract numerical values for the masses, I explicitly computed the pertinent spin-spin correlators of the Heisenberg chain in chapter 3. Although the spectrum is determined only up to the second order in the strong coupling expansion the agreement with the continuum theory is satisfactory.

The massless and the massive excitations of the gauge model are created from the spin chain ground state with two very different mechanisms: massless excitations involve only spin flipping while massive excitations are created by fermion transport besides spin flipping and do not belong to the spin chain spectrum. As in the continuum theory, due to the Coleman theorem [73], the massless excitations are not Goldstone bosons, but may be regarded as the gapless quantum excitations of the spin-1/2 antiferromagnetic Heisenberg chain [48].

In computing the chiral condensate I showed that, also in the lattice theory, the expectation value of the umklapp operator F is different from zero, while both $\langle \bar{\psi}\psi \rangle$ and $\langle \bar{\psi}\sigma^a\psi \rangle$ are zero to every order in the strong coupling expansion. This implies that both on the lattice and the continuum the $SU(2)$ flavor symmetry is preserved whereas the $U_A(1)$ axial symmetry is broken. The umklapp operator F is the order parameter for this symmetry, but being quadri-linear in the fermi fields, is invariant, in the continuum, under chiral rotation of $\pi/2$ and on the lattice under the corresponding discrete axial symmetry (5.30) (translation by one lattice site). This shows that the discrete axial symmetry is not broken in both cases. Our lattice computation enhance this result since the ground state of the strongly coupled two-flavor Schwinger model is translationally invariant.

The pattern of symmetry breaking of the continuum is exactly reproduced even if the Coleman theorem does not apply on the lattice and the anomalous symmetry breaking is impossible due to the Nielsen-Ninomiya [27] theorem. At variance with the strongly coupled one-flavor lattice Schwinger model, the anomaly is not realized in the lattice theory via the spontaneous breaking of a residual chiral symmetry [61], but, rather, by explicit breaking of the chiral symmetry due to staggered fermions. The non-vanishing of $\langle F \rangle$ may be regarded as the only relic, in the strongly coupled lattice theory, of the anomaly of the continuum two-flavor Schwinger model. It is due to the coupling induced by the gauge field, between the right and left-movers on the lattice.

Chapter 6

The multicolor lattice Schwinger models

In this chapter I study the \mathcal{N} -flavor lattice Schwinger models in the hamiltonian formalism using staggered fermions. I illustrated in chapter 5 how the presence of a nontrivial $SU(2)$ -flavor symmetry makes the spectrum much richer than the one-flavor model spectrum and changes drastically the chiral symmetry breaking pattern.

The \mathcal{N} -flavor Schwinger models have many features in common with four dimensional QCD : at the classical level they have a symmetry group $U_L(\mathcal{N}) \otimes U_R(\mathcal{N}) = SU_L(\mathcal{N}) \otimes SU_R(\mathcal{N}) \otimes U_V(1) \otimes U_A(1)$ that is broken down to $SU_L(\mathcal{N}) \otimes SU_R(\mathcal{N}) \otimes U_V(1)$ by the axial anomaly exactly like in QCD [78]. The massless \mathcal{N} -flavor Schwinger models describe no real interactions between their particles as one can infer by writing the model action in a bosonized form. The model exhibits one massive and $\mathcal{N}^2 - 1$ massless pseudoscalar “mesons” [79].

On the lattice I shall prove that – at the second order in the strong coupling expansion – the lattice Schwinger models are effectively described by $SU(\mathcal{N})$ quantum antiferromagnetic spin-1/2 Heisenberg Hamiltonians with spins in a particular fundamental representation of the $SU(\mathcal{N})$ Lie algebra and with nearest neighbours couplings. The features of the model are very different depending on if \mathcal{N} is odd or even. When \mathcal{N} is odd, the ground state energy in the strong coupling limit is proportional to e_L^2 , the square of the electromagnetic coupling constant. In contrast, when \mathcal{N} is even the ground state energy in the strong coupling limit is of order 1. This difference arises from the proper definition of the charge density

$$\rho(x) = \sum_{a=1}^{\mathcal{N}} \psi_{a,x}^\dagger \psi_{a,x} - \frac{\mathcal{N}}{2} \quad (6.1)$$

where the constant $\mathcal{N}/2$ has been subtracted from the charge density operator in order to make it odd under the charge conjugation transformation. As a consequence, when \mathcal{N} is even, $\rho(x)$ admits zero eigenvalues and the ground state does not support any electric flux, while when \mathcal{N} is odd the ground state exhibits a staggered configuration of the charge density and electromagnetic fluxes.

In the continuum the Coleman theorem [43] prevents the formation of either an isoscalar chiral condensate $\langle \bar{\psi}\psi \rangle$ or an isovector chiral condensate $\langle \bar{\psi}T^a\psi \rangle$ – where T^a is an $SU(\mathcal{N})$ generator – for every model with an internal $SU(\mathcal{N})$ -flavor symmetry. We shall see that this feature should be reproduced on the lattice also for this class of models.

6.1 The continuum \mathcal{N} -flavor Schwinger models

The continuum $SU(\mathcal{N})$ -flavor Schwinger models are defined by the action

$$S = \int d^2x \left(\sum_{a=1}^{\mathcal{N}} \bar{\psi}_a (i\gamma_\mu \partial^\mu + \gamma_\mu A^\mu) \psi_a - \frac{1}{4e_c^2} F_{\mu\nu} F^{\mu\nu} \right) \quad (6.2)$$

where the \mathcal{N} fermions have been introduced in a completely symmetric way. Although the theory described by (6.2) strictly parallels what has been shown in chapter 5 for the $SU(2)$ model, I shall now report a detailed analysis both for the sake of clarity and to show that some difference appears between \mathcal{N} even and odd.

The Dirac fields are an \mathcal{N} -plet, *i.e.* transform according to the fundamental representation of the flavor group while the electromagnetic field is an $SU(\mathcal{N})$ singlet. The flavor symmetry of the theory cannot be spontaneously broken for the same reasons as in the $SU(2)$ case. The particles of the theory belong to $SU(\mathcal{N})$ multiplets. The action is invariant under the symmetry

$$SU_L(\mathcal{N}) \otimes SU_R(\mathcal{N}) \otimes U_V(1) \otimes U_A(1) \quad (6.3)$$

The symmetry generators act as follows

$$SU_L(\mathcal{N}) : \psi_a(x) \longrightarrow (e^{i\theta_\alpha T^\alpha P_L})_{ab} \psi_b(x), \quad \bar{\psi}_a(x) \longrightarrow \bar{\psi}_b(x) (e^{-i\theta_\alpha T^\alpha P_R})_{ba} \quad (6.4)$$

$$SU_R(\mathcal{N}) : \psi_a(x) \longrightarrow (e^{i\theta_\alpha T^\alpha P_R})_{ab} \psi_b(x), \quad \bar{\psi}_a(x) \longrightarrow \bar{\psi}_b(x) (e^{-i\theta_\alpha T^\alpha P_L})_{ba} \quad (6.5)$$

$$U_V(1) : \psi_a(x) \longrightarrow (e^{i\theta(x)\mathbf{1}})_{ab} \psi_b(x), \quad \psi_a^\dagger(x) \longrightarrow \psi_b^\dagger(x) (e^{-i\theta(x)\mathbf{1}})_{ba} \quad (6.6)$$

$$U_A(1) : \psi_a(x) \longrightarrow (e^{i\alpha\gamma_5\mathbf{1}})_{ab} \psi_b(x), \quad \psi_a^\dagger(x) \longrightarrow \psi_b^\dagger(x) (e^{-i\alpha\gamma_5\mathbf{1}})_{ba} \quad (6.7)$$

where T^α are the generators of the $SU(\mathcal{N})$ group, θ_α , $\theta(x)$ and α are real coefficients and

$$P_L = \frac{1}{2}(1 - \gamma_5), \quad P_R = \frac{1}{2}(1 + \gamma_5) \quad . \quad (6.8)$$

At the classical level the above symmetries lead to conservation laws for the isovector, vector and axial currents

$$j_\alpha^\mu(x)_R = \bar{\psi}_a(x) \gamma^\mu P_R (T_\alpha)_{ab} \psi_b(x) \quad , \quad (6.9)$$

$$j_\alpha^\mu(x)_L = \bar{\psi}_a(x) \gamma^\mu P_L (T_\alpha)_{ab} \psi_b(x) \quad , \quad (6.10)$$

$$j^\mu(x) = \bar{\psi}_a(x) \gamma^\mu \mathbf{1}_{ab} \psi_b(x) \quad , \quad (6.11)$$

$$j_5^\mu(x) = \bar{\psi}_a(x) \gamma^\mu \gamma_5 \mathbf{1}_{ab} \psi_b(x) \quad . \quad (6.12)$$

At the quantum level the vector and axial currents cannot be simultaneously conserved. If the regularization is gauge invariant, so that the vector current is conserved, then the axial current acquires the anomaly which breaks the symmetry $U_A(1)$ [78]

$$\partial_\mu j_5^\mu(x) = \mathcal{N} \frac{e_c^2}{2\pi} \epsilon_{\mu\nu} F^{\mu\nu}(x) \quad . \quad (6.13)$$

The isoscalar $\langle \bar{\psi}\psi \rangle$ and isovector $\langle \bar{\psi}T^\alpha\psi \rangle$ chiral condensates are zero due to the Coleman theorem [43], in fact they would break not only the $U_A(1)$ symmetry of the action but also the continuum internal symmetry $SU_L(\mathcal{N}) \otimes SU_R(\mathcal{N})$ down to $SU_V(\mathcal{N})$. There is an order parameter just for the breaking of the $U_A(1)$ symmetry [62, 72], the operator

$$\langle \bar{\psi}_L^{(\mathcal{N})} \dots \bar{\psi}_L^{(1)} \psi_R^{(1)} \dots \psi_R^{(\mathcal{N})} \rangle = \left(\frac{e^\gamma}{4\pi}\right)^\mathcal{N} \left(\sqrt{\frac{\mathcal{N}}{\pi}} e_c\right)^\mathcal{N} \quad . \quad (6.14)$$

Under a discrete chiral rotation

$$\psi_L \rightarrow \gamma_5 \psi_L = -\psi_L \quad , \quad \psi_R \rightarrow \gamma_5 \psi_R = \psi_R \quad (6.15)$$

the operator (6.14) of course transforms as

$$\langle \bar{\psi}_L^{(\mathcal{N})} \dots \bar{\psi}_L^{(1)} \psi_R^{(1)} \dots \psi_R^{(\mathcal{N})} \rangle \rightarrow (-1)^\mathcal{N} \langle \bar{\psi}_L^{(\mathcal{N})} \dots \bar{\psi}_L^{(1)} \psi_R^{(1)} \dots \psi_R^{(\mathcal{N})} \rangle \quad (6.16)$$

The umklapp operator is even under (6.15) when \mathcal{N} is even and this implies that notwithstanding the fact that the continuous chiral rotations $U_A(1)$ are broken by the non-zero VEV (6.14), the discrete chiral symmetry (6.15) is unbroken. When \mathcal{N} is odd also the discrete chiral symmetry (6.15) is broken by the non-zero VEV (6.14).

The usual abelian bosonization procedure may again be applied provided that \mathcal{N} Bose fields are introduced [78, 79, 80]

$$: \bar{\psi}_a \gamma^\mu \psi_a := \frac{1}{\sqrt{\pi}} \epsilon^{\mu\nu} \partial_\nu \Phi_a, \quad a = 1, \dots, \mathcal{N} \quad (6.17)$$

The electric charge density and the action read

$$j_0 =: \sum_{a=1}^{\mathcal{N}} \psi_a^\dagger \psi_a := \frac{1}{\sqrt{\pi}} \partial_x \left(\sum_{a=1}^{\mathcal{N}} \Phi_a \right), \quad (6.18)$$

$$S = \int d^2x \left(\frac{1}{2} \sum_{a=1}^{\mathcal{N}} \partial_\mu \Phi_a \partial^\mu \Phi_a + \frac{e_c^2}{2\pi} \left(\sum_{a=1}^{\mathcal{N}} \Phi_a \right)^2 \right) \quad (6.19)$$

The mass matrix is determined by the last term in Eq.(6.19) and must be diagonalized. The field degrees of freedom span the vector space on which the mass matrix is defined. The action must be expressed in terms of an orthonormal basis of field vectors, in order to have a properly normalised kinetic energy term. The original Φ^a in Eq.(6.19) are orthonormal basis vectors, but they are not eigenvectors of the mass matrix. The mass matrix has one non-zero eigenvalue $\frac{e_c^2}{\mathcal{N}\pi}$ with associated eigenvector $\frac{1}{\sqrt{\mathcal{N}}} \sum_{a=1}^{\mathcal{N}} \Phi^a$ and all the other eigenvalues are zero. The remaining eigenvectors can be made orthonormal by the following change of variables

$$\tilde{\Phi}^a = O_b^a \Phi^b \quad (6.20)$$

where the orthogonal matrices O_b^a are [80]

$$O_b^1 = \frac{1}{\sqrt{\mathcal{N}}} (1, 1, \dots, 1), \quad (6.21)$$

$$O_b^2 = \frac{1}{\sqrt{\mathcal{N}(\mathcal{N}-1)}} (1, 1, \dots, -\mathcal{N}+1), \quad (6.22)$$

$$O_b^3 = \frac{1}{\sqrt{(\mathcal{N}-1)(\mathcal{N}-2)}} (1, 1, \dots, -\mathcal{N}+2, 0), \quad (6.23)$$

$$\vdots$$

$$O_b^\mathcal{N} = \frac{1}{\sqrt{2}} (1, -1, 0, \dots, 0). \quad (6.24)$$

In terms of these new fields $\tilde{\Phi}^a$ the action (6.19) reads

$$S = \int d^2x \left(\frac{1}{2} \sum_{a=1}^{\mathcal{N}} \partial_\mu \tilde{\Phi}_a \partial^\mu \tilde{\Phi}^a - \frac{1}{2} \mu^2 (\tilde{\Phi}^1)^2 \right) \quad (6.25)$$

where $\mu^2 = \mathcal{N} \frac{e_c^2}{\pi}$. The action (6.25) describes \mathcal{N} non interacting fields, one massive and $\mathcal{N}-1$ massless. The multiflavor Schwinger model can also be studied in the framework of non abelian bosonization [73], where the relationship between isovector currents and bosonic excitations appears in a more symmetrical form [75].

The Hamiltonian, gauge constraint and non-vanishing (anti-)commutators of the continuum \mathcal{N} -flavor Schwinger models are

$$H = \int dx \left[\frac{e^2}{2} E^2(x) + \sum_{a=1}^{\mathcal{N}} \psi_a^\dagger(x) \alpha (i\partial_x + eA(x)) \psi_a(x) \right] \quad (6.26)$$

$$\partial_x E(x) + \sum_{a=1}^{\mathcal{N}} \psi_a^\dagger(x) \psi_a(x) \sim 0 \quad (6.27)$$

$$[A(x), E(y)] = i\delta(x-y), \quad \left\{ \psi_a(x), \psi_b^\dagger(y) \right\} = \delta_{ab} \delta(x-y) \quad (6.28)$$

6.2 The lattice \mathcal{N} -flavor Schwinger models

On the lattice the Hamiltonian, constraint and (anti-) commutators reducing to (6.26,6.27,6.28) in the naive continuum limit are

$$\begin{aligned} H_S &= \frac{e_L^2 a}{2} \sum_{x=1}^N E_x^2 - \frac{it}{2a} \sum_{x=1}^N \sum_{a=1}^{\mathcal{N}} (\psi_{a,x+1}^\dagger e^{iA_x} \psi_{a,x} - \psi_{a,x}^\dagger e^{-iA_x} \psi_{a,x+1}) \\ E_x - E_{x-1} &+ \sum_{a=1}^{\mathcal{N}} \psi_{a,x}^\dagger \psi_{a,x} - \frac{\mathcal{N}}{2} \sim 0, \\ [A_x, E_y] &= i\delta_{x,y}, \quad \left\{ \psi_{a,x}, \psi_{b,y}^\dagger \right\} = \delta_{ab} \delta_{xy} \end{aligned} \quad (6.29)$$

The fermion fields are defined on the sites, $x = 1, \dots, N$, gauge and the electric fields, A_x and E_x , on the links $[x; x+1]$, N is an even integer and, when N is finite it is convenient to impose periodic boundary conditions. When N is finite, the continuum limit is the \mathcal{N} -flavor Schwinger model on a circle [68]. The coefficient t of the hopping term in (6.29) plays the role of the lattice light speed. In the naive continuum limit, $e_L = e_c$ and $t = 1$.

The lattice \mathcal{N} -flavor Schwinger model is equivalent to a one dimensional quantum Coulomb gas on the lattice with \mathcal{N} kinds of particles. To see this one can fix the gauge, $A_x = A$ (Coulomb gauge). Eliminating the non-constant electric field and using the gauge constraint, one obtains the effective Hamiltonian

$$\begin{aligned} H_S &= H_u + H_p \equiv \left[\frac{e_L^2}{2N} E^2 + \frac{e_L^2 a}{2} \sum_{x,y} \rho(x) V(x-y) \rho(y) \right] + \\ &+ \left[-\frac{it}{2a} \sum_x \sum_{a=1}^{\mathcal{N}} (\psi_{a,x+1}^\dagger e^{iA} \psi_{a,x} - \psi_{a,x}^\dagger e^{-iA} \psi_{a,x+1}) \right], \end{aligned} \quad (6.30)$$

where $\rho(x)$ is given in Eq.(6.1) and the Coulomb potential $V(x-y)$ is given in Eq.(4.22). The constant electric field is normalized so that $[A, E] = i$. The constant modes of the gauge field decouple in the thermodynamic limit $N \rightarrow \infty$. In the thermodynamic limit the Schwinger Hamiltonian (6.30), rescaled by the factor $e_L^2 a/2$, reads

$$H = H_0 + \epsilon H_h \quad (6.31)$$

with

$$H_0 = \sum_{x>y} \left[\frac{(x-y)^2}{N} - (x-y) \right] \rho(x) \rho(y), \quad (6.32)$$

$$H_h = -i(R - L) \quad (6.33)$$

and $\epsilon = t/e_L^2 a^2$. In Eq.(6.33) the right R and left L hopping operators are defined ($L = R^\dagger$) as

$$R = \sum_{x=1}^N R_x = \sum_{x=1}^N \sum_{a=1}^{\mathcal{N}} R_x^{(a)} = \sum_{x=1}^N \sum_{a=1}^{\mathcal{N}} \psi_{a,x+1}^\dagger e^{iA} \psi_{a,x}. \quad (6.34)$$

On a periodic chain the commutation relation

$$[R, L] = 0 \quad (6.35)$$

is satisfied.

When \mathcal{N} is even the ground state of the Hamiltonian (6.32) is the state $|g.s. \rangle$ with $\rho(x) = 0$ on every site, *i.e.* with every site half-filled

$$\prod_{a=1}^{\mathcal{N}} \psi_{ax}^\dagger \psi_{ax} |g.s. \rangle = \frac{\mathcal{N}}{2} |g.s. \rangle \quad (6.36)$$

It is easy to understand that $\rho(x) = 0$ on every site in the ground state by observing that the Coulomb Hamiltonian (6.32) is a non-negative operator and that the states with zero charge density are zero eigenvalues of (6.32). $|g.s. \rangle$ is an highly degenerate state; in fact at each site x the quantum configuration is

$$\prod_{a=1}^{\frac{\mathcal{N}}{2}} \psi_{ax}^\dagger |0 \rangle \quad (6.37)$$

The state (6.37) is antisymmetric in the indices $a = 1, \dots, \frac{\mathcal{N}}{2}$; *i.e.* it takes on any orientation of the vector in the representation of the flavor symmetry group $SU(\mathcal{N})$ with Young tableau given in fig.(6.1). The energy of $|g.s. \rangle$ is of order 1, since it is non zero only at the second

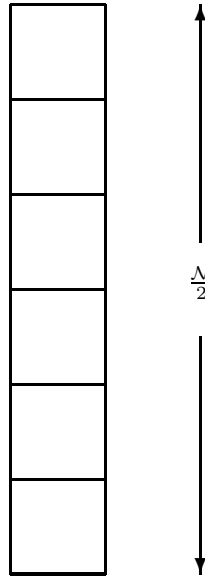


Figure 6.1: The representation of $SU(\mathcal{N})$ at each site when \mathcal{N} is even

order in the strong coupling expansion.

When \mathcal{N} is odd the ground states of the Hamiltonian (6.32) are characterized by the staggered charge distribution

$$\rho(x) = \pm \frac{1}{2} (-1)^x \quad (6.38)$$

since (6.38) minimizes the Coulomb Hamiltonian (6.32); one can have $\rho(x) = +1/2$ on the even sublattice and $\rho(x) = -1/2$ on the odd sublattice or viceversa. The electric fields generated by the charge distribution (6.38) are

$$E_x = \pm \frac{1}{4} (-1)^x \quad (6.39)$$

Since now

$$H_0|g.s. \rangle = \frac{1}{16}|g.s. \rangle \quad (6.40)$$

the ground state energy is of order ϵ_L^2 . The states $|g.s. \rangle$ are highly degenerate since they can take up any orientation in the vector space which carries the representation of the $SU(\mathcal{N})$ group with the Young tableaux given in fig.(6.2).

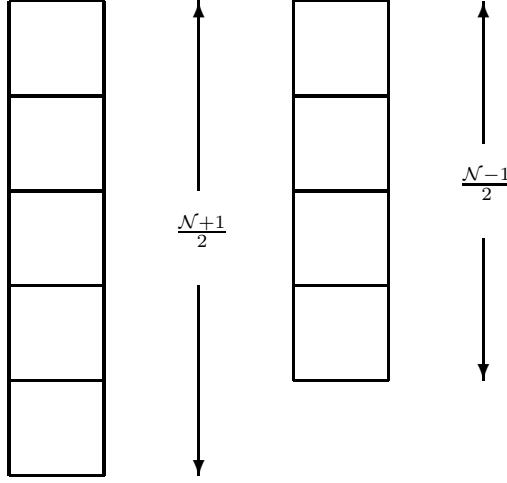


Figure 6.2: The representation of $SU(\mathcal{N})$ at each site of the even sublattice and odd sublattice when \mathcal{N} is odd

Either when \mathcal{N} is even or when \mathcal{N} is odd the ground state degeneracy is resolved at the second order in the strong coupling expansion. First order perturbations to the vacuum energy vanish. The vacuum energy at order ϵ^2 reads

$$E_0^{(2)} = \langle H_h^\dagger \frac{\Pi}{E_0^{(0)} - H_0} H_h \rangle \quad (6.41)$$

where the expectation values are defined on the degenerate subspace of ground states and Π is a projection operator projecting orthogonal to the states of the degenerate subspace. Due to the commutation relation

$$[H_0, H_h] = \frac{N-1}{N} H_h - 2 \sum_{x,y} [V(x-y) - V(x-y-1)] (L_y + R_y) \rho(x) \quad (6.42)$$

Eq.(6.41) can be rewritten as

$$E_0^{(2)} = -2 \langle RL \rangle \quad (6.43)$$

On the ground state the combination RL can be written in terms of the Heisenberg Hamiltonian of a generalized $SU(\mathcal{N})$ antiferromagnet. By introducing as in chapter 5 the Schwinger spin operators

$$\vec{S}_x = \psi_{ax}^\dagger T_{ab}^\alpha \psi_{bx} \quad (6.44)$$

where T^α are now the generators of the $SU(\mathcal{N})$ group, the $SU(\mathcal{N})$ Heisenberg Hamiltonian reads

$$H_J = \sum_{x=1}^N \left(\vec{S}_x \cdot \vec{S}_{x+1} - \frac{\mathcal{N}}{8} + \frac{1}{2\mathcal{N}} \rho(x) \rho(x+1) \right) = -\frac{1}{2} \sum_{x=1}^N L_x R_x \quad (6.45)$$

When \mathcal{N} is even, on the degenerate ground states one has

$$\langle H_J \rangle = \left\langle \sum_{x=1}^N \left(\vec{S}_x \cdot \vec{S}_{x+1} - \frac{\mathcal{N}}{4} \right) \right\rangle = \left\langle -\frac{1}{2} \sum_{x=1}^N L_x R_x \right\rangle \quad (6.46)$$

while when \mathcal{N} is odd one has

$$\langle H_J \rangle = \left\langle \sum_{x=1}^N (\vec{S}_x \cdot \vec{S}_{x+1} - \frac{\mathcal{N}^2 + 1}{8\mathcal{N}}) \right\rangle = \left\langle -\frac{1}{2} \sum_{x=1}^N L_x R_x \right\rangle . \quad (6.47)$$

Taking into account that the products of L_x and R_y at different points have vanishing expectation values on the ground states and using Eq.(6.46) or Eq.(6.47), Eq.(6.43) reads

$$E_0^{(2)} = 4 \langle H_J \rangle . \quad (6.48)$$

The problem of determining the correct ground state, on which to perform the perturbative expansion, is then reduced again to the diagonalization of the $SU(\mathcal{N})$ Heisenberg spin-1/2 Hamiltonian (6.45). As I already pointed out in chapter 3, generalized $SU(\mathcal{N})$ antiferromagnetic chains have not been yet analysed in the literature in such a detailed way as the $SU(2)$ chains. Consequently, the study of the lattice $SU(\mathcal{N})$ flavor lattice Schwinger models become extremely complicated for $\mathcal{N} > 2$. Nonetheless, the computational scheme that I developed for the $U(1)$ - and $SU(2)$ -flavor models in chapters 4 and 5, should work for a generic $SU(\mathcal{N})$ -flavor model.

The ground state of the gauge models is very different when \mathcal{N} is even or \mathcal{N} is odd. When \mathcal{N} is even, the ground state $|G.S. \rangle$ of the spin Hamiltonian (6.45) is non-degenerate and translationally invariant, and since it is the ground state of the gauge model in the infinite coupling limit, there is no spontaneous breaking of the chiral symmetry for any $SU(2\mathcal{N})$ -flavor lattice Schwinger model. In contrast, when \mathcal{N} is odd, the ground state $|G.S. \rangle$ of the spin Hamiltonian (6.45) is degenerate of order two and is not translationally invariant and consequently any $SU(2\mathcal{N}+1)$ -flavor lattice Schwinger model exhibits spontaneous symmetry breaking of the discrete axial symmetry. By translating of one lattice spacing $|G.S. \rangle$ one gets the other one. The \mathcal{N} -flavor lattice Schwinger models excitations are also generated from $|G.S. \rangle$ by two very different mechanisms, that I already described for the two-flavor model in chapter 5. There are excitations involving only flavor changes of the fermions without changing the charge density $\rho(x)$ which correspond to spin flips in the $SU(2)$ invariant model. These excitations are massless. At variance massive excitations involve fermion transport besides flavor changes and are created by applying to $|G.S. \rangle$ the lattice currents of the Schwinger models which vary the on site value of $\rho(x)$.

Very different is the case of the massive multiflavor Schwinger models [81]. When \mathcal{N} is odd, the presence of a non-zero fermionic mass m removes the degeneracy and selects one of the two $|G.S. \rangle$ as the non degenerate ground state. When \mathcal{N} is even the ground state remains translationally invariant in the strong coupling limit $e_L^2 \gg m$. In the weak coupling limit $m \gg e_L^2$ the discrete chiral symmetry is broken for every \mathcal{N} .

Summary and conclusions

In this thesis I showed explicitly that the strong coupling limit of the multiflavor lattice Schwinger models is effectively described by quantum spin-1/2 generalized $SU(\mathcal{N})$ antiferromagnetic Heisenberg chains. Exploiting the mapping existing between these gauge and spin models, exact results about antiferromagnetic chains have been used to analyse the chiral symmetry breaking on the lattice. In particular an interesting question has been how the effects of the axial anomaly appear in the lattice regularization. Since [27] fermion theories on a lattice have an equal number of species of left- and right-handed Weyl particles in the continuum limit, there is no axial anomaly in a lattice theory.

I studied in detail the $U(1)$ -flavor and $SU(2)$ -flavor models, archetypes for all $SU(2\mathcal{N} + 1)$ and $SU(2\mathcal{N})$ models. The results are very different depending on if the number of flavors is even or odd. The $SU(2\mathcal{N})$ -flavor Schwinger models exhibit non-degenerate and translationally invariant ground states in the strong coupling limit and their energy is of order 1. At variance, the $SU(2\mathcal{N} + 1)$ models have two degenerate ground states, break the symmetry of translation by one lattice spacing and their energy is of order e_L^2 . The difference between \mathcal{N} even and odd arises, since, also on the lattice, the charge density operator must be odd under charge conjugation; therefore the constant $\mathcal{N}/2$ should be subtracted from the charge density operator (6.1). As a consequence, when the \mathcal{N} is odd, the ground state supports electric fluxes while this becomes impossible when \mathcal{N} is even.

In the one-flavor model I proved that the discrete axial symmetry is spontaneously broken on the lattice, reproducing the effects due to the axial anomaly in the continuum. In the infinite coupling limit the ground state of the gauge model is the ground state of an antiferromagnetic Ising chain with long range spin-spin Coulomb interactions. The Schwinger model excitations are created by acting on the ground state with the latticized currents. The excitation masses are determined in the strong coupling expansion by computing the excitation energies up to the fourth order in the strong coupling expansion. Using suitable Padé approximants, I extrapolated to the continuum the lattice results and I found that the lattice answers are in very good agreement with the continuum theory.

In the two-flavor Schwinger model, I demonstrated that in the strong coupling limit the gauge model is effectively described by the spin-1/2 antiferromagnetic Heisenberg Hamiltonian and the ground state of the gauge model in the infinite coupling limit is the ground state of the spin chain. Since the antiferromagnetic Heisenberg model is exactly solvable in one-dimension, it is very interesting to exhibit a gauge theory with the same low lying excitation spectrum.

The antiferromagnetic spin chain admits spin-1/2 quarklike spinon excitations but has physical states with integer spin and an even number of spinons. Spinons behave like $U(1)$

quarks and they can be identified in conventional materials and models by high-energy spectroscopy and inconsistencies in sum rules [25]. The two-flavor Schwinger model strictly parallels this scenario. The fundamental particles are spin-1/2 fermions but the spectrum exhibits only integer spin bosonic excitations [28]. I proved that the spinons have the same quantum numbers of the gauge model excitations. While spinons are the gapless excitations created from the spin chain ground state by spin flipping, the massive excitations of the gauge model are created from the spin chain ground state by fermion transport besides spin flipping and do not belong to the antiferromagnetic Heisenberg spectrum. The lattice mass spectrum, properly extrapolated to the continuum by using Padé approximants, reproduces in a satisfactory way the continuum results. The pattern of chiral symmetry breaking of the continuum model is exactly reproduced on the lattice, even if the Coleman theorem does not apply and the anomalous symmetry breaking is impossible [27]. In fact, both the isoscalar $\langle \bar{\psi}\psi \rangle$ and the isovector $\langle \bar{\psi}\sigma^a\psi \rangle$ chiral condensates are zero to every order in the strong coupling expansion, while the expectation value of the umklapp operator F is different from zero.

The multiflavor Schwinger models are the gauge theories associated to the quantum spin-1/2 antiferromagnetic Heisenberg chains. It would be interesting to extend my analysis to QCD_2 with different flavor and color groups. The number of colors \mathcal{N}_C determines the representation of the antiferromagnetic chain, since the spin is $S = \mathcal{N}_C/2$. Varying \mathcal{N}_C one changes the spin S . In particular, by considering the $SU(2)$ -flavor case, *i.e.* QCD_2 with two kinds of quarks, one finds that in the strong coupling limit the gauge model is effectively described by the antiferromagnetic Heisenberg chain with spin- S representation. Since half-integer spin chains are expected to exhibit gapless excitations, while integer spin chains have a gap [48], it would be an interesting problem to investigate if also QCD_2 exhibits a gapless or gapped spectrum depending on if \mathcal{N}_C is odd or even. Two dimensional QCD affords an excellent opportunity to study various dynamical questions of gauge theories, since many of its qualitative features are also valid in four dimensions. QCD_2 still resists analytic solutions for general $SU(\mathcal{N}_C)$ colour groups, except in the planar limit $\mathcal{N}_C \rightarrow \infty$ [82, 83]. In fact, 't Hooft [82] analysed the QCD_2 spectrum in the continuum exploiting a perturbation expansion with respect to $1/\mathcal{N}_C$ and showed that the $\mathcal{N}_C \rightarrow \infty$ limit, keeping $g\mathcal{N}_C$ constant (g is the strong interactions coupling constant), corresponds to taking only the planar Feynman diagrams with no fermion loops [83]. The $\mathcal{N}_C \rightarrow \infty$ limit of two flavor QCD_2 should be compared with the $S \rightarrow \infty$ of the antiferromagnetic Heisenberg chain. The study of the spin chain in the large S limit can be performed using the spin-wave theory and it would be fascinating to single out “gluon” and “hadron” degrees of freedom in the antiferromagnetic chain.

Padé approximants

For the sake of clarity and to make the thesis self-contained, I define here what are Padé approximants [29, 84]. Although the method of Padé approximant has a long history, dating back more than one century, it is only in the 1960s that the procedure has become a part of the “bag of tricks” of the working physicist [29]. When a power series representation of a function diverges, it indicates the presence of singularities. The divergence of the series reflects the inability of a polynomial to approximate a function adequately near a singularity. The basic idea of summation theory is to represent $f(z)$, the function in question, by a convergent expression. In Euler summation this expression is the limit of a convergent series, while in Borel summation this expression is the limit of a convergent integral. The difficulty with Euler and Borel summation is that all of the terms of the divergent series must be known exactly before the “sum” can be found even approximately. In realistic perturbation problems only a few terms of a perturbative series can be calculated as we have seen in chapters 4 and 5. Therefore, it is needed a summation algorithm, which requires as input only a finite number of terms of the divergent series. The Padé summation is a method having such a property.

The idea of Padé summation is to replace a power series such as $\sum_{n=0}^{\infty} a_n z^n$ by a sequence of rational functions of the form

$$P_M^N(z) = \frac{\sum_{n=0}^N A_n z^n}{\sum_{n=0}^M B_n z^n} \quad (6.49)$$

where one can choose $B_0 = 1$ without loss of generality. As it stands from Eq.(6.49) $P_M^N(z)$ is the ratio of a polynomial of degree N and one of degree M . The $M + N + 1$ coefficients $A_0, A_1, \dots, A_n, B_1, B_2, \dots, B_M$ are determined in such a way that the first $M + N + 1$ terms in the Taylor series expansion of $P_M^N(z)$ match the first $M + N + 1$ terms of the power series $\sum_{n=0}^{\infty} a_n z^n$. The rational functions $P_M^N(z)$ are called Padé approximants. Constructing Padé approximants $P_M^N(z)$ is very useful; in fact, if $\sum_{n=0}^{\infty} a_n z^n$ is a power series representation of a function $f(z)$, then in many instances $P_M^N(z) \rightarrow f(z)$ as $M, N \rightarrow \infty$, even if $\sum_{n=0}^{\infty} a_n z^n$ is a divergent series. The sequence of Padé approximants (6.49) with $M = N$ is called the diagonal sequence. Let us sketch the computation of $P_1^0(z)$. One has to expand $P_1^0(z)$ in a Taylor series

$$P_1^0(z) = \frac{A_0}{1 + B_1 z} = A_0 - A_0 B_1 z + O(z^2) \quad (z \rightarrow 0) \quad (6.50)$$

and comparing the series (6.50) with the first two terms in the power series representation of $f(z) = \sum_{n=0}^{\infty} a_n z^n$ one gets two equations: $a_0 = A_0$, $a_1 = -A_0 B_1$ from which

$$P_1^0 = \frac{a_0}{1 - \frac{a_1}{a_0} z} \quad (6.51)$$

As it clear from this very simple example, to construct a Padé approximant $P_M^N(z)$ one does not need the full power series representation of a function, but just the first $M + N + 1$ terms.

Since Padé approximants involve only algebraic operations, they are more convenient for computational purposes than Borel summation, which requires one to integrate on an infinite range the analytic continuation of a function defined by a power series. Padé approximants often work quite well, even beyond their proven range of applicability. For an analysis of the convergence theory of Padé approximants, see Ref. [84].

Bibliography

- [1] See for instance P. W. Anderson, *Basic Notions of Condensed Matter Physics*, Frontiers in Physics, Addison Wesley Pub. Company 1983; C. Itzykson and J.-B. Zuber, *Quantum Field Theory*, McGraw-Hill, Inc. 1985, and references therein.
- [2] K. G. Wilson, Phys. Rev. **D2**, 1438 (1970); Phys. Rev. **B4**, 3174 (1971); Phys. Rev. Lett. **28**, 548 (1972); K. G. Wilson and M. E. Fisher, Phys. Rev. Lett. **28**, 240 (1972); K. G. Wilson and J. Kogut, Phys. Rep. **12 C**, 75 (1974).
- [3] K. G. Wilson, Phys. Rev. **D10**, 2445 (1974).
- [4] L. D. Landau and E. M. Lifshitz, *Statistical Physics*, Pergamon Press, Oxford, 1969; A. Z. Patashinskii and V. L. Pokrovskii, *Fluctuation Theory of Phase Transitions*, Pergamon Press, Oxford, 1979.
- [5] G. 't Hooft, unpublished (1972); H. D. Politzer, Phys. Rev. Lett. **30**, 1346 (1973); D. J. Gross and F. Wilczek, Phys. Rev. Lett. **30**, 1343 (1973); Phys. Rev. **D8**, 3633 (1973).
- [6] See for instance B. W. Lee, *Chiral Dynamics*, Gordon and Breach Science Pub. 1972.
- [7] P. Fomin, V. Gusynin, V. Miransky and Yu. Sitenko, Riv. Nuov. Cim. **6**, 1 (1983); V. Miransky, Nuovo Cimento **90A**, 149 (1985).
- [8] See for instance J. B. Kogut, Rev. Mod. Phys. **55**, 775 (1983) and references therein.
- [9] K. G. Wilson, "New Phenomena in Subnuclear Physics", Erice, ed. A. Zichichi (New York, Plenum, 1975).
- [10] T. Banks, J. Kogut and L. Susskind, Phys. Rev. **D13**, 1043 (1976); L. Susskind, Phys. Rev. **D16**, 3031 (1977).
- [11] T. Banks, S. Raby, L. Susskind, J. Kogut, D. R. T. Jones, P. N. Scharbach and D. K. Sinclair, Phys. Rev. **D15**, 1111 (1977).
- [12] C. Borgs, Comm. Math. Phys. **116**, 343 (1988); E. Seiler, *Gauge theories as a problem of constructive quantum field theory and statistical mechanics*, Lecture Notes in Physics Vol. **159**, Berlin, Heidelberg, New York: Springer 1982.
- [13] J. Kogut and L. Susskind, Phys. Rev. **D11**, 395 (1975).
- [14] J. Smit, Nucl. Phys. **B175**, 307 (1980).
- [15] See for a review E. Fradkin, *Field Theories and Condensed Matter Systems*, Addison Wesley Pub. Company, 1991.
- [16] I. Affleck and J. B. Marston, Phys. Rev. **B37**, 3773 (1988); J. B. Marston, Phys. Rev. Lett. **61**, 1914 (1988).
- [17] I. Affleck, Z. Zou, T. Hsu and P. W. Anderson, Phys. Rev. **B38**, 745 (1988).
- [18] P. Wiegmann, Prog. Theor. Phys. Suppl. **107**, 243 (1992).

- [19] C. Mudry and E. Fradkin, Phys. Rev. **B49**, 5200 (1994); Phys. Rev. **B50**, 11409 (1994).
- [20] D. H. Kim and P. A. Lee, cond-mat/9810130.
- [21] D. Hofstaeder, Phys. Rev. **B14**, 2239 (1976).
- [22] G. W. Semenoff and L. C. Wijewardhana, Phys. Rev. **D45**, 1342 (1992).
- [23] D. Schmeltzer and A. R. Bishop, Phys. Rev. **B41**, 9603 (1990); M. C. Diamantini and P. Sodano, Phys. Rev. **B45**, 5737 (1992).
- [24] G. W. Semenoff, Mod. Phys. Lett. **A7**, 2811 (1992); E. Langmann and G. W. Semenoff, Phys. Lett. **B297**, 175 (1992); M. C. Diamantini, E. Langmann, G. W. Semenoff and P. Sodano, Nucl. Phys. **B405**, 595 (1993).
- [25] R. B. Laughlin, cond-mat/9802180; Phys. Rev. Lett. **79**, 1726 (1997).
- [26] S. L. Adler and W. A. Bardeen, Phys. Rev. **182**, 1517 (1969); J. S. Bell and R. Jackiw, Nuovo Cimento **A60**, 47 (1969).
- [27] H. B. Nielsen and M. Ninomiya, Nucl. Phys. **B185**, 20 (1981); **B193**, 173 (1981); Phys. Lett. **B105**, 219 (1981); **B130**, 389 (1983).
- [28] J. Schwinger, Phys. Rev. **125**, 397 (1962); Phys. Rev. **128**, 2425 (1962).
- [29] G. A. Baker, Jr., *Essential of Padé approximants* (Academic, New York, 1975).
- [30] L. D. Faddeev and L. A. Takhtadzhyan, Phys. Lett. **A85**, 375 (1981); L. D. Faddeev and L. A. Takhtadzhyan, Zapiski Nauchnykh Seminarov LOMI, **109**, 134 (1981), english translation in J. Sov. Math. **24**, 241 (1984).
- [31] J. B. Kogut, Rev. Mod. Phys. **51**, 659 (1979); M. Creutz, *Quarks , Gluons and Lattices*, Cambridge University press, 1983; I. Montvay and G. Münster, *Quantum Fields on a Lattice*, Cambridge University press, 1994; H. J. Rothe, *Lattice Gauge Theories: An Introduction*, World Scientific, 1997; R. Gupta, *Introduction to Lattice QCD*, Les Houches Lectures 1998, hep-lat/9807028; G. Grignani and G. W. Semenoff, *Introduction to some common topics in gauge theory and spin systems*, in *Field Theories for Low Dimensional Condensed Matter Systems: Spin Systems and Strongly Correlated Electrons*, ed. by R. B. Laughlin, G. Morandi, P. Sodano, A. Tagliacozzo, V. Tognetti, Spinger Verlag in press.
- [32] F. Wegner, J. Math. Phys. **12**, 2259 (1971).
- [33] H. Kluberg-Stern, A. Morel, O. Napoly and R. Petersson, Nucl. Phys. **B220**, 447 (1983).
- [34] E. H. Lieb and D. C. Mattis, *Mathematical Physics in one dimension*, New York Academic Press (1961); D. C. Mattis, *The Theory of Magnetism*, Harper & Row 1965; W. J. Caspers, *Spin Systems*, World Scientific 1989; I. Affleck, J. Phys. Cond. Mat. **1**, 3047 (1989); I. Affleck, *Field Theory Methods and Quantum Critical Phenomena*, in *Fields, Strings and Critical Phenomena*, ed. by E. Brezin and J. Zinn-Justin, North Holland (1989); D. C. Mattis, *The Many-Body Problem*, World Scientific 1993; V. E. Korepin, N. M. Bogoliubov and A. G. Izergin, *Quantum Inverse Scattering Method and Correlation Functions*, Cambridge University press 1993; A. Auerbach, *Interacting Electrons and Quantum Magnetism*, Springer Verlag 1994; A. M. Tsvelik, *Quantum Field Theory in Condensed Matter Physics*, Cambridge University press 1995; L. D. Faddeev, Int. J. Mod. Phys. **A10**, 1845 (1995), hep-th/9605187; R. B. Laughlin, D. Giuliano, R. Caracciolo and Olivia L. White, *Quantum Number Fractionalization in Antiferromagnets*, in *Field Theories for Low Dimensional Condensed Matter Systems: Spin Systems and Strongly Correlated Electrons*, ed. by R. B. Laughlin, G. Morandi, P. Sodano, A. Tagliacozzo, V. Tognetti, Spinger Verlag in press; A. Auerbach, F. Berruto and L. Capriotti, *Quantum Magnetism Approach to Strongly Correlated Electrons*, in *Field Theories for Low Dimensional Condensed Matter Systems: Spin Systems and Strongly Correlated Electrons*, ed. by R. B. Laughlin, G. Morandi, P. Sodano, A. Tagliacozzo, V. Tognetti, Spinger Verlag in press.

- [35] P. W. Anderson, Phys. Rev. **B86**, 694 (1952); R. Kubo, Phys. Rev. **87**, 568 (1952).
- [36] H. Bethe, Z. Physik **71**, 205 (1931).
- [37] L. Hulthén, Arkiv. Mat. Astron. Fysik **26A** (11), 1 (1938).
- [38] R. B. Laughlin, unpublished (1995).
- [39] F. Berruto, G. Grignani, G. W. Semenoff and P. Sodano, Phys. Rev. **D59**, 034504 (1999).
- [40] F. Berruto, G. Grignani, G. W. Semenoff and P. Sodano, hep-th/9901142, submitted to Annals of Physics.
- [41] F. D. M. Haldane, Phys. Rev. Lett. **60**, 635 (1988); *ibid.* **66**, 1529 (1991); B. S. Shastry, Phys. Rev. Lett. **60**, 639 (1988).
- [42] M. Takahashi, J. Phys. **C10**, 1289 (1977); cond-mat/9708087.
- [43] N. D. Mermin, H. Wagner, Phys. Rev. Lett. **22**, 1133 (1966); S. Coleman, Commun. Math. Phys. **31**, 259 (1973).
- [44] F. Calogero, J. Math. Phys. **10**, 2197 (1969); B. Sutherland, Phys. Rev. **A4**, 2019 (1971); *ibid.* **5**, 1537 (1972).
- [45] See for example J. C. Talstra, *Integrability and Applications of the Exactly-Solvable Haldane-Shastry Quantum Spin Chain*, Ph. D. Thesis, Princeton University, cond-mat/9509178 and references therein.
- [46] V. Kalmeyer and R. B. Laughlin, Phys. Rev. Lett. **59**, 2095 (1987); Phys. Rev. **B39**, 163 (1989).
- [47] R. B. Laughlin, Ann. Phys. (N. Y.) **159**, 220 (1985).
- [48] F. D. M. Haldane, Phys. Rev. Lett. **50**, 1153 (1983).
- [49] See for example *The Hubbard Model*, ed. by A. Montorsi, World Scientific 1992.
- [50] S. Coleman, Ann. Phys. (N.Y.) **101**, 239 (1976).
- [51] J. des Cloizeaux and J. J. Pearson, Phys. Rev. **128**, 2131 (1962).
- [52] V. E. Korepin, A. G. Izergin, F. H. L. Essler and D. B. Uglov, Phys. Lett. **A190**, 182 (1994).
- [53] S. Lukyanov, cond-mat/9712314.
- [54] I. Affleck, J. Phys. **A31**, 4573 (1998).
- [55] S. V. Tyablikov, Ukrain. Math. Zh. **11**, 287 (1959); D. N. Zubarev, Soviet Physics-Uspokhi **3**, 320 (1960).
- [56] H. Q. Lin and D. K. Campbell, J. Appl. Phys. **69**, 5947 (1991).
- [57] B. Sutherland, Phys. Rev. **B12**, 3795 (1975); P. P. Kulish and Yu. Reshetikhin, Sov. Phys. JETP **53**, 108 (1981); A. Doikou and R. I. Nepomechie, hep-th/9803118.
- [58] I. Affleck, Phys. Rev. Lett. **54**, 966 (1985); N. Read and S. Sachdev, Phys. Rev. Lett. **62**, 1694 (1989); N. Read and S. Sachdev, Nucl. Phys. **B316**, 609 (1989); N. Read and S. Sachdev, Phys. Rev. **B42**, 4568 (1990).
- [59] I. Affleck and E. H. Lieb, Lett. Math. Phys. **12**, 57 (1986).
- [60] E. Lieb, T. Schultz and D. Mattis, Ann. Phys. **16**, 407 (1961).
- [61] F. Berruto, G. Grignani, G. W. Semenoff and P. Sodano, Phys. Rev. **D57**, 5070 (1998).

- [62] J. E. Hetrick and Y. Hosotani, Phys. Rev. **D38**, 2621 (1988); J. E. Hetrick, Y. Hosotani and S. Iso, Phys. Lett. **B350**, 92 (1995); Y. Hosotani, R. Rodriguez, J. E. Hetrick and S. Iso, hep-th/9606129; Y. Hosotani, hep-th/9606167.
- [63] T. Banks, L. Susskind and J. Kogut, Phys. Rev. **D13**, 1043 (1976); A. Carrol, J. Kogut, D. K. Sinclair and L. Susskind, Phys. Rev. **D13**, 2270 (1976).
- [64] J. Lowenstein and J. A. Swieca, Ann. Phys. (N.Y.) **68**, 172 (1971).
- [65] S. Chandrasekharan, hep-lat/9809084.
- [66] S. Coleman, R. Jackiw and L. Susskind, Ann. Phys. (N.Y.) **93**, 167 (1975).
- [67] C. J. Hamer, Z. Weihong and J. Oitmaa, Phys. Rev. **D56**, 55 (1997).
- [68] N. S. Manton, Ann. Phys. (N. Y.) **159**, 220 (1985).
- [69] Y. Nambu, Prog. Theor. Phys. **116**, 1474 (1950).
- [70] J. P. Steinhardt, Phys. Rev. **D16**, 1782 (1977).
- [71] Y. Hosotani, J. Phys. **A30**, L757 (1997); hep-th/9809066.
- [72] C. Gattringer and E. Seiler, Ann. Phys. **233**, 97 (1994).
- [73] S. Coleman, Ann. Phys. (N.Y.) **101**, 239 (1976).
- [74] E. Witten, Comm. Math. Phys. **92**, 455 (1984).
- [75] D. Gepner, Nucl. Phys. **B252**, 481 (1985).
- [76] K. Harada, T. Sugihara, M. Taniguchi and M. Yahiro, Phys. Rev. **D49**, 4226 (1994).
- [77] S. Eggert and I. Affleck, Phys. Rev. **B46**, 10866 (1992).
- [78] See for example E. Abdalla, M. C. B. Abdalla and K. D. Rothe, *Nonperturbative Methods in 2Dimensional Quantum Field Theory*, World Scientific 1991.
- [79] C. Gattringer, *QED₂ and the U(1) Problem*, Dissertation University of Graz 1995, hep-th/9503137.
- [80] M. Sadzikowski and P. Wegrzyn, Mod. Phys. Lett. **A11**, 1947 (1996).
- [81] J. P. Steinhardt, *Lattice Theory of SU(N) Flavor Quantum Electrodynamics in (1+1)-dimensions*, Ph.D. Thesis, Harvard University (1978).
- [82] G. 't Hooft, Nucl. Phys. **B75**, 461 (1974).
- [83] G. 't Hooft, Nucl. Phys. **B72**, 461 (1974).
- [84] C. M. Bender and S. A. Orszag, *Advanced mathematical methods for scientists and engineers*, McGraw-Hill Publ. Comp. 1978.

List of Figures

2.1	The dispersion relation $S(k)$ for a free scalar field. The solid line, k^2 , is for the continuum theory, the dashed line is for the lattice theory.	10
2.2	Spectrum of the free, continuum Dirac fermion in 1 + 1 dimensions.	10
2.3	Spectrum of the naively latticized Dirac fermion in 1 + 1 dimensions.	11
2.4	Link variables.	16
2.5	A plaquette.	17
2.6	Young tableaux representations allowed at a given site.	25
2.7	Young tableau with \mathcal{N}_C columns and $\mathcal{N}/2$ rows.	26
2.8	Dispersion relations for 1 + 1 dimensional lattice Weyl fermions. Each curve is closed since end points are identified.	
2.9	Around a degeneracy point all the curves of the type $\langle a \omega_i(\vec{p})\rangle$ are oriented away on one level and towards on the other.	
3.1	Strings for $L = 0, \frac{1}{2}, 1, \frac{3}{2}$	47
3.2	Four sites chain spectrum	53
3.3	Six sites chain spectrum	56
6.1	The representation of $SU(\mathcal{N})$ at each site when \mathcal{N} is even	102
6.2	The representation of $SU(\mathcal{N})$ at each site of the even sublattice and odd sublattice when \mathcal{N} is odd	103

List of Tables

3.1	$I_o(r)$ and $I_e(r)$	39
3.2	Spin-wave theory spin-spin correlation functions	40
3.3	Triplet internal quantum numbers	52
3.4	Triplet internal quantum numbers	54
3.5	Four holes triplet internal quantum numbers	54
3.6	Singlet internal quantum numbers	55
3.7	Spin-spin correlation functions	59